Mask proteins are co-factors of Yorkie/YAP in the Hippo signaling pathway

Clara M. Sidor

University College London

and

Cancer Research UK London Research Institute

PhD Supervisor: Dr Barry J. Thompson

A thesis submitted for the degree of

Doctor of Philosophy

University College London

September 2011

Declaration

I, Clara M. Sidor, confirm that the work presented in this thesis is my own. Where information has been derived from other sources, I confirm that this has been indicated in the thesis.

Abstract

Mask proteins are cofactors of Yki/YAP in the Hippo signaling pathway

One of the key questions in developmental biology is how tissue growth is controlled to give rise to organs of specific sizes and shapes. Although some genes and pathways involved in the genetic and environmental control of tissue growth have been uncovered, the understanding of this process remains incomplete. In order to find new regulators of growth we carried out an in vivo RNAi screen in the *Drosophila* wing. I participated in the validation of candidate genes from the screen and identified the *mask* gene as an essential regulator of tissue growth acting in the Hippo signaling pathway. This pathway acts via the Yorkie (Yki)/Yes-associated protein (YAP) transcriptional co-activator to control tissue growth in both *Drosophila* and mammals. Yki/YAP translocates from the cytoplasm to the nucleus to activate target genes, a process that is negatively regulated by the Warts kinase, one of the core components of the Hippo pathway. I found that Mask is an essential positive regulator of Yki acting downstream of Warts. Mask is required for normal tissue growth, for the expression of Yki target genes and for the overgrowth phenotype caused by Yki overexpression. Mask binds to Yki and the two proteins translocate from the cytoplasm to the nucleus together in response to various stimuli. My results show that Mask acts in the nucleus to promote Yki target gene activation. Finally, Mask's function appears to be conserved in humans, as two human homologues of Mask (hMask1 and hMask2) translocate with YAP to the cytoplasm upon cell contact inhibition, and we demonstrate that one of these homologues promotes YAP's transactivation function.

Acknowledgements

First I would like to express my gratitude to Barry, for being such a motivating supervisor, so passionate about science, for giving me the opportunity to work in this stimulating scientific environment and for being always there to support me during my PhD while giving me independence over my work. I would like to thank deeply the "old" members of the lab, whom I have spent most of my days with for the past four years (!). Thanks to all members of the lab for the great atmosphere and friendship. Ruth, who participated in my project, for a lot of help and for tea and evening discussions in the lab, Neil, for the ginger and science (fi) coffee breaks, Eliana, for nice teas and for heating my hands, Georgina for teaching me how to use a timer and for getting me into yoga, and the "kids", Mariana and Graham, who have been a really supportive graduate student team. I would like to thank Nic Tapon and people from the Tapon lab for great scientific and non-scientific interactions. Thanks to Yanlan, Eunice, Paulo, Yianxiang, thanks to Gaspar for interesting discussions and help, thanks to Alice, my PhD student example, thanks to the two German biochemists Michael and Tobi, thanks to Rachael, the gut expert. Thanks to all the people who helped me along the way, including my family and friends. In particular Lisa, Solenn, Erik and Alessandra, and my old university friends Delphine, Amandine, Elise, Chloé and Kamal who have been great motivating friends during all my studies. My gratitude also goes to Dr Stéphane Ronsseray for his support, and to Prof Denise Busson and Prof Guy Echalier who brought me into fly research when I was an undergraduate student.

This work was funded by Cancer Research UK.

Table of Contents

Table of figures

List of tables

Abbreviations

ANK	Ankyrin
ANKHD1	ankyrin repeat and KH domain containing 1
ANKR	Ankyrin repeats
ANKRD17	ankyrin repeat domain 17
aPKC	atypical Protein Kinase C
App	Approximated
Crb	Crumbs
Csw	Corkscrew
Cyclin E	CycE
D	Dachs
Dco	Disc overgrown
DER	*Drosophila* epidermal growth factor receptor
DIAP1	*Drosophila* inhibitor of apoptosis 1
Dpp	Decapentaplegic
Ds	Dachsous
ee	entero-endocrine cell
EB	enteroblast
EC	enterocyte
EGFR	Epidermal growth factor receptor
ELAV	embryonic lethal abnormal visual system
En	Engrailed
Ex	Expanded
Ey	Eyeless
Fj	Four-jointed
Ft	Fat
GMR	glass multimer reporter
Hep	Hemipterous
Hh	Hedgehog
Hpo	Hippo
HRE	Hippo responsive element
Hth	Homothorax
IR	inverted repeat
ISC	intestinal stem cell

JNK	c-Jun N-terminal kinase
Jub	Ajuba
LATS	Large tumor supressor
Lft	Lowfat
Lgl	Lethal giant larvae
MAPK	mitogen-activated protein kinase
Mask	Multiple ankyrin repeats and single KH domain
Mats	Mob as a tumor suppressor
Mer	Merlin
Mop	Myopic
MST	Mammalian STE20-like protein kinase
RASSF	Ras association domain family
RTK	receptor tyrosine kinase
Sav	Salvador
Sd	Scalloped
Sev	Sevenless
Stg	String
STRIPAK	Striatin-interacting phosphatase and kinase
TAZ	Tafazzin
Tsh	Tea shirt
UAS	upstream activation sequence
Vg	Vestigial
Wbp2	WW domain binding protein 2
Wg	Wingless
Wts	Warts
Yki	Yorkie
Zyx	Zyxin

Chapter 1. Introduction

Evolution has given rise to a great diversity of animal forms, each adapted to different environmental niches. Animal tissues come in an astonishing variety of sizes and shapes, and the question of how tissue size is controlled has fascinated developmental biologists for decades. First, I am going to introduce the question of size control in animal development. I will then focus on the growth effectors acting downstream of the developmental signaling pathways controlling tissue size, in particular on the recently discovered Hippo signaling pathway, which controls cell survival and cell proliferation in all animals.

1.1 Growth control in animals

Vertebrate skeletons are a very good illustration of how diversity in forms can arise. Most bones of the vertebrate skeleton have homologues in all vertebrates, but they exhibit simple variations in size and proportions that have evolved to adapt to different environments and functions. For instance, the human arm is remarkably homologous to the bat's anterior limb (Fig 1.1 A). The most striking difference, scale aside, is the change in proportions of bones that has allowed formation of the human arm and hand, adapted to manipulation, and formation of the bat wing, adapted to flight. An examination of our closer relatives such as the chimpanzee or the gorilla also illustrates how body size and proportions can evolve from a common ancestor and produce different body shapes (Fig 1.1 B). Within a species, nutrition has a profound effect on body size. From flies to human, deprivation in nutrients during development lead to an adult of a smaller size (Fig 1.1 C). This nutrient dependent growth control mechanism is mediated by the Insulin/TOR signaling pathway (Parker, 2011). Thus, organ size is determined by intrinsic genetic mechanisms that determine the proportions of the body, and can be modulated by extrinsic signals in response to environmental conditions.

The developmental mechanisms that control body and organ size are still poorly understood. One of the most fascinating questions is how organs "know" which size they should grow to. Evidence for an intrinsic organ size control mechanism comes from transplantation experiments. In rats and mice, it was found that infant organs

(kidney, heart or thymus) transplanted to adult animals grow to their correct adult size (Dittmer et al., 1974; METCALF, 1963; Silber, 1976). The same is true of *Drosophila* wing imaginal discs, which are the larval precursors of the adult wing. Immature wing imaginal discs from young larvae transplanted into adult hosts grow to their normal final size (Bryant and Simpson, 1984). Thus, there is a conserved intrinsic mechanism that allows organs to sense their mass and grow to their correct size. Some organs are also capable of monitoring their size after their development is complete. For instance, the rat liver is able to regenerate to its full size after ablation of 2/3 of its volume, and the human liver is also capable of regeneration (Michalopoulos and DeFrances, 1997).

The size of an organ depends on the number and size of its cells. However, organs do not control their size by counting their cell number and measuring single cells size. Various experiments have shown that organ size is sensed in a more global way, as a measure of their total volume. One particularly striking piece of evidence comes from spontaneous variations in ploidy found in salamanders. Salamanders are diploid, but at a low frequency, some individuals are born triploid and even more rarely with higher degrees of polyploidy. Cells from polyploid animals contain more DNA and are bigger than cells from diploids, but this increase in cell size is compensated by a reduction in cell number that results in a normal body size (Fankhauser, 1941). In the *Drosophila* wing disc, increases or decreases in cell proliferation rates caused by alterations in the expression of cell cycle genes are compensated by decreases or increases in cell size, leaving the organ final size relatively unchanged (Neufeld et al., 1998; Weigmann et al., 1997).

A

radius: homologies of the forelimb among vertebrates. [Art]. *Encyclopædia Britannica Online*. Retrieved 29 March 2012, from http://www.britannica.com/EBchecked/media/101873/Bones-of-the-forelimb-of-select-vertebrates-showing-homologies-as

C

B

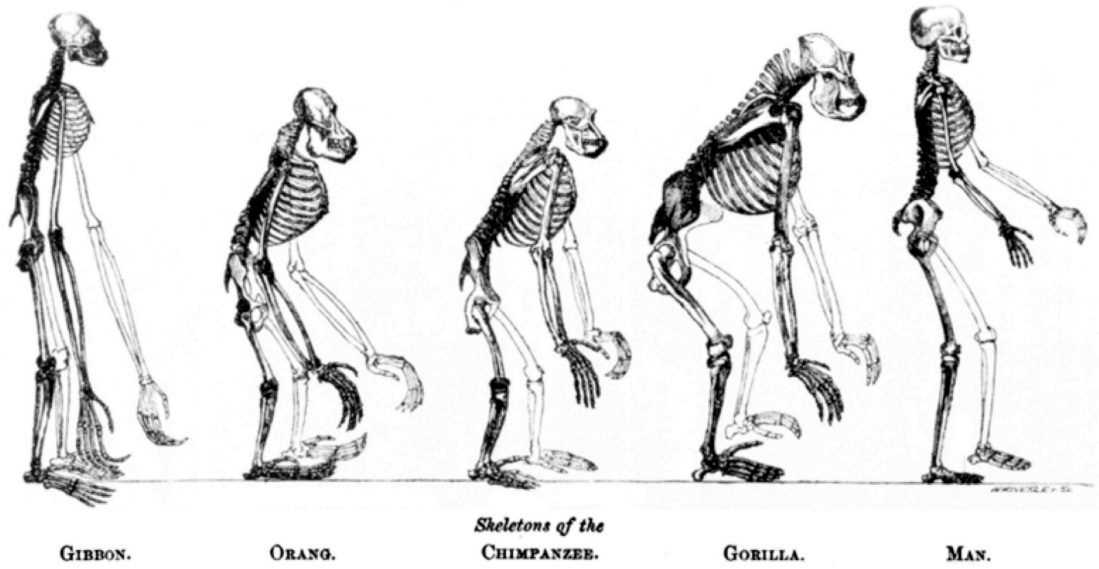

Figure 1.1: Intrinsic and extrinsic control of size, the influence of genes and environment.
(A) human and bat anterior limbs, Source: Encyclopaedia Britanica (B) Illustration from T. H. Huxley's book *Man's place in Nature*. From left to right: Gibbon, Orang-outang, Chimpanzee, Gorilla and Man skeletons. They are all at the same scale apart from the Gibbon which is drawn twice its natural size. (C) *Drosophila melanogaster* adult flies; top: control fly; bottom: fly starved during its development.

Long before the molecular mechanisms of organ size control started to be unravelled, classical regeneration experiments in various organisms led to the hypothesis that cells within an organ perceive positional information and activate genes in function of their position. Regeneration experiments performed by Bohn in the 1960's have shown that when the distal part of a cockroach tibia is grafted on a host limb that has been sectioned more proximally, cells at the boundary are confronted with cells they are normally not adjacent with and proliferate, regenerating the missing parts (Bohn, 1967; Fig 1.2). Positional information is encoded by gradients of secreted molecules called morphogens that diffuse from their source of production and induce different target genes in function of their concentration, thereby controlling tissue patterning and tissue growth (Lawrence, 2001).

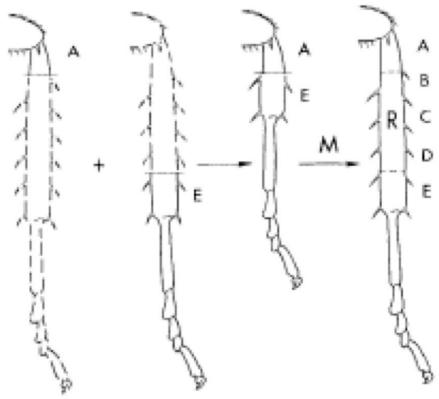

Figure 1.2: Regeneration in the cockroach limb
Graft of the distal part (position E) of a cockroach tibia to a more proximal position (position A) in a host leads to intercalary proliferation and regeneration of the missing parts (B-C-D) (Illustration from French et al., 1976).

The first morphogen to be identified in animals, the transcription factor *bicoid*, was discovered in *Drosophila* early embryos where it forms a concentration gradient essential for anteroposterior patterning (Driever and Nüsslein-Volhard, 1988). Since then, more morphogens have been discovered, and their essential roles in tissue growth and patterning in animals have been brought to light. Most of the understanding of the mechanisms of tissue growth control originates from studies in *Drosophila*, which has proven to be a very good model to study growth.

1.2 *Drosophila* as a model to study growth

All animal embryos face two key challenges. First, before they develop specialised organs for nutrient intake, they cannot grow. Second, cell proliferation is incompatible with highly differentiated cells as it disrupts cell architecture and metabolism. Thus proliferation is usually limited to early stages of embryonic development prior to differentiation, and different species use different strategies to allow later growth, such as uncoupling of cell growth and cell division or maintaining pools of stem cells (P. H. O'Farrel, Cell growth, Chapter 1). *Drosophila* development remarkably overcomes these two constraints (Fig 1.3 A). The fertilized egg contains enough nutrients deposited by the mother to fully develop into a larva with a mouth and a digestive system. Larval development is divided into 3 larval stages separated by moults, and lasts 4 days during which the larva feeds and grows by two-hundred-fold. Most of the larval growth occurs by increases in cell size without cell divisions, via cell growth and endo-replicative cycles. *Drosophila* adult structures derive from undifferentiated epithelial structures called imaginal discs (Fig 1.3 B) that are specified early in the embryo and acquire their identity in response to positional cues. Imaginal discs undergo extensive cell proliferation throughout larval development without differentiating. In response to a hormonal signal, larvae crawl out of the source of food to pupariate. At pupariation, imaginal discs stop cell proliferation and differentiate: using nutrients accumulated by the larva during the feeding period, they undergo metamorphosis to form the adult fly. Among all the imaginal discs, the wing disc has been extensively used as a model to study tissue growth: easy to dissect, it grows by more than a thousand-fold during its development, following a very precise sequence of signaling events that coordinate tissue patterning and tissue growth.

1.2.1 Wing disc development: coordination of patterning and growth

The wing imaginal disc derives from an epithelial monolayer that invaginates from the embryonic ectoderm between parasegments 4 and 5. It grows from approximately 20 cells to 50 000 cells during the three larval stages until metamorphosis, when it generates the adult wing and half of the notum. The wing disc is composed of 3 regions (Fig 1.3 B): the blade region, the hinge region, and a region that gives rise to half of the notum. The centre of the blade region is the presumptive distal part of the wing. The wing fate is specified by expression of the *wingless* gene while expression of

the EGFR (Epidermal Growth Factor Receptor) ligand Vein specifies the notum, and the 2 domains are established through mutual antagonistic regulation between *wingless* signaling and EGFR signaling (Ng et al., 1996; Simcox et al., 1996; Wang et al., 2000).

Early in development, the action of selector genes subdivides the wing disc into fields of cells called compartments, separated by two straight boundaries of lineage restriction: the antero-posterior (AP) boundary and the dorso-ventral (DV) boundary (Vincent, 1998). Cells from each compartment have distinct adhesive properties and do not mix with each other. Growth and patterning of the wing disc are tightly linked and are coordinated by signals emanating from the AP and DV boundaries (Fig 1.4) (Klein, 2001).

The wing disc inherits expression of the *engrailed (en)* selector gene from the embryonic parasegment boundary it arises from, which specifies posterior fate and the antero-posterior boundary. *en* activates the expression of hedgehog (hh) ligand, which acts as a short-range morphogen and activates the expression of *decapentaplegic* (*dpp*) (Basler and Struhl, 1994). Cells from the posterior compartment are not receptive to hh signaling. Thus, hh triggers the expression of *dpp* in a narrow stripe in the anterior compartment along the antero-posterior boundary. Dpp is a protein of the BMP/TGFβ family that acts as a long-range morphogen to promote patterning and differentiation of the wing in a medial-to-lateral direction, inducing the expression of target genes such as *spalt* (*sal*) and *optomotor-blind* (*omb*) in a concentration dependant manner (Affolter and Basler, 2007; Schwank and Basler, 2010). Activation of target genes at different positions in the wing field by *hh* and *dpp* signaling leads to the formation of wing veins L2 to L5 (Fig 1.3 B) at specific positions in the wing blade, in a process involving EGFR signaling (Crozatier et al., 2004; Sturtevant and Bier, 1995). In addition, the Dpp gradient promotes uniform tissue growth (Affolter and Basler, 2007).

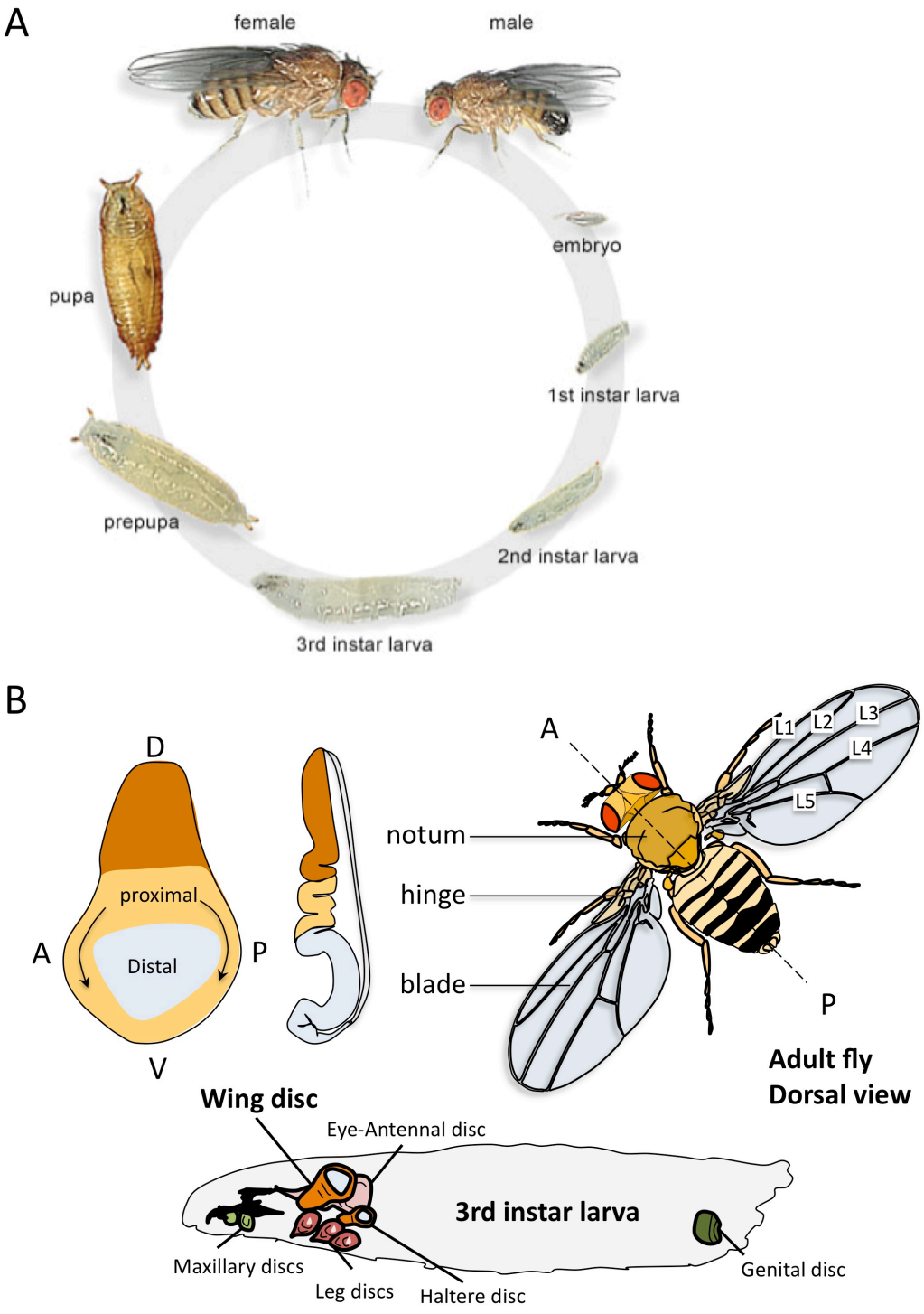

Figure 1.3: *Drosophila* development
(A) *Drosophila* life cycle. Source: http://flymove.uni-muenster.de; (B) Imaginal discs of the *Drosophila* third instar larva. The wing disc gives rise to the adult wing, the wing disc pouch gives rise to the wing blade, its centre being the future distal part of the wing, and the wing disc proximal region gives rise to the hinge and half the notum (figure from Pedro Gaspar, modified with his permission).

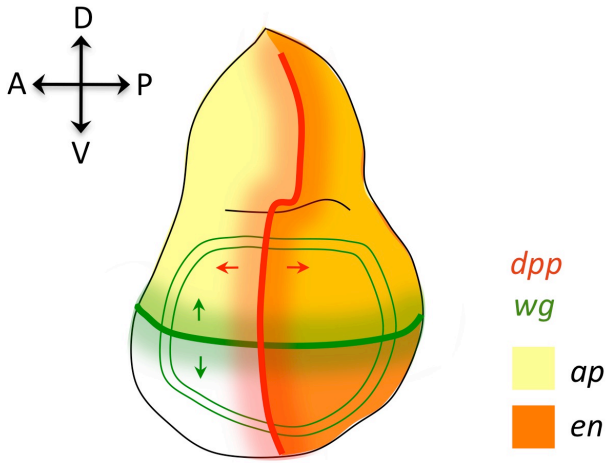

Figure 1.4: Wg and Dpp morphogen gradients in the wing imaginal disc
The action of the *apterous* (*ap*) and *engrailed* (*en*) selector genes sets the antero-posterior and dorso-ventral boundaries expressing the *decapentaplegic* (*dpp*) and *wingless* (*wg*) morphogens that diffuse from their source to control patterning and growth of the wing.

Shortly after hatching of the larva, Vein activates expression in the dorsal compartment of the selector gene *apterous* (*ap*) (Wang et al., 2000), a transcription factor which specifies dorsal fate and the dorso-ventral boundary (Blair et al., 1994; Diaz-Benjumea and Cohen, 1993). *ap* activates the expression of Notch pathway components. Notch signaling is activated specifically at the dorso-ventral boundary and initiates the expression of target genes such as *wingless* (*wg*) and *vestigial* in a narrow stripe along the DV boundary. Wg behaves as a long-range morphogen, diffusing from its source along the antero-posterior axis and acting as an organizer to promote tissue growth in the proximo distal axis (Diaz-Benjumea and Cohen, 1995). Vestigial (Vg) is a transcriptional co-activator that specifies the wing blade with its binding partner, the transcription factor Scalloped (Sd) (Halder et al., 1998). Vg domain of expression is expanded by a regulatory mechanism involving the combined activity of Vg itself, Dpp, which diffuses from the AP boundary, and Wg, which diffuses from the DV boundary (Zecca and Struhl, 2007a; Zecca and Struhl, 2007b). Wg is also expressed in two concentric rings in the proximal region of the wing disc, the future wing hinge. The wing hinge is specified by the expression of two transcription factors and binding partners: Homothorax (Hth) and Teashirt (Tsh). *hth/tsh* and *vg* mutually antagonise each other and their expression is restricted to the hinge region and to the blade region respectively (Azpiazu and Morata, 2000; Casares and Mann, 2000).

Thus, a hierarchy of selector genes specifies compartments of the wing disc and set up the AP and DV organizers expressing the long-range morphogens Dpp and Wg respectively. Dpp and Wg then promote wing growth and patterning in a coordinated manner.

1.2.2 Tissue growth effectors

The link between developmental programs and regulators of tissue growth is still poorly understood. Clearly, wing growth proceeds by cell proliferation, so developmental signals and transcription factors must control the cell proliferation machinery. In *Drosophila*, the rate-limiting G1-S cell cycle regulator is Cyclin E (CycE), which acts with Cdk2, and the rate limiting G2-M cell cycle regulator is cdc25/String (Stg), an activator of cyclinB/Cdk1 complexes. In the wing disc, overexpression of CycE and Cdc25/String or the E2F1/Dp transcription factor complex, which activates the transcription of cell cycle genes including CycE and Stg, leads to an increase in the rate of cell division (Neufeld et al., 1998). Interestingly, this increase in cell division does not result in overgrowth, but in a tissue of a relatively normal size containing an increased number of cells smaller than normal. On the contrary, slowing or arresting the cell cycle by using *Cdc2* mutations or overexpressing RBF, an E2F1 inhibitor, results in a tissue composed of fewer but bigger cells (Fig 1.5) (Neufeld et al., 1998; Weigmann et al., 1997). Thus, in order to control tissue growth, developmental signals need to regulate both cell growth and cell division rates. In addition, these experiments show that the developmental program does not measure cell number but rather absolute tissue size.

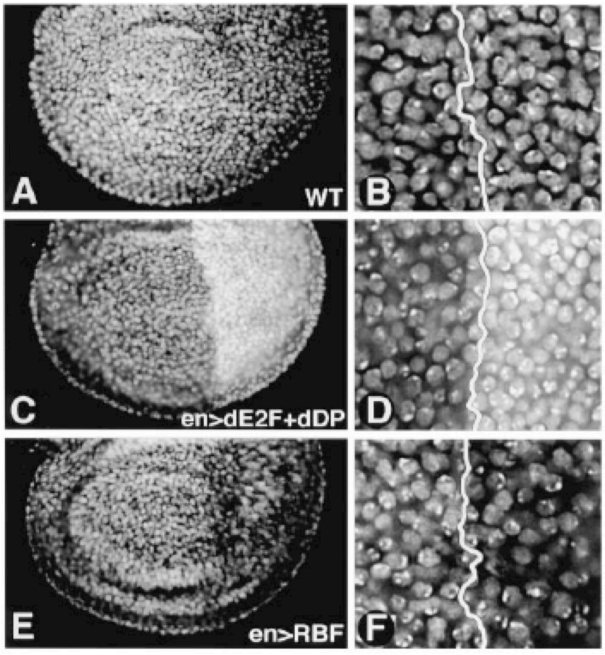

Figure 1.5: Uncoupling of cell growth and cell division in the *Drosophila* wing disc
Nuclear staining in *Drosophila* wing discs. A-B: control wing disc; C-D: Over-expression of E2F/DP in the posterior compartment accelerates the cell cycle progression thereby increasing the number of cells as shown by the increase in nuclei density. E-F: Over-expression of RBF delays cell cycle progression, resulting in a reduction in cell number and an increase in cell size, as shown by the reduced density of nuclei.
Figure from (Neufeld et al., 1998)

Control of cell growth

In order to increase its volume, a cell needs to increase the amount of proteins it produces. Thus, regulation of protein synthesis rates is critical for cell growth. Genes essential for cell growth include genes related to protein synthesis like the ribosomal proteins Minutes, translation and elongation factors, and factors involved in ribosome biogenesis. One particularly interesting one is the transcription factor *dmyc*, a potent dose dependent regulator of cell growth (Bellosta and Gallant, 2010). It activates the transcription of several genes involved in protein synthesis and *dmyc* overexpression results in abnormally large cells. Moreover, *dmyc* expression is not ubiquitous but follows a pattern. Therefore, it is probably a key effector targeted by developmental signaling pathways to control growth. Cell growth is also controlled by the Insulin/TOR signaling pathway. In response to nutrient intake, insulin-like peptides (dILPs) are secreted by the gut and neurosecretory cells in the brain, and activate the Insulin Receptor (InR) in different tissues. The InR activates a signaling cascade that leads to the activation of ribosome biogenesis (Hietakangas and Cohen, 2009). Thus, Insulin signaling allows tissues to coordinate their growth in function of nutritional conditions. Loss of InR in the wing disc phenocopies starvation and results in small cells. Interestingly, patterning and cell proliferation scale with this input, resulting in smaller organs of the right proportions (Parker, 2011). Other endocrine factors affect cell

growth such as ecdysone, Juvenile Hormone (JH) and Imaginal disc growth factors (IDGFs).

Control of cell proliferation: the sum of cell growth and cell division

Different factors have been shown to control cell proliferation including Cyclin D/Cdk4, which promotes both cell growth and cell cycle progression (Datar et al., 2000), and the *bantam* microRNA, which promotes cell proliferation and inhibits apoptosis (Hipfner et al., 2002). *bantam* was shown to downregulate the apoptotic gene *hid* (Brennecke et al., 2003) and the *myc* negative regulator *mei-P26* (Herranz et al., 2010), but is also predicted to target more genes controlling cell proliferation. Interestingly, *bantam* expression is higher in proliferating tissues, indicating it may be controlled by pathways regulating cell proliferation. Indeed, *bantam* microRNA was identified as a target of the Hippo growth control pathway (Thompson and Cohen, 2006). In addition to those downstream regulators, mutagenic screens have uncovered several tumor suppressor genes essential to control cell proliferation (Watson et al., 1994), and have led to the discovery of a key cell proliferation control pathway: the Hippo signaling pathway, which I will describe in the next section.

1.3 The Hippo signaling pathway

In the last decade, new light has been shed on growth control from the discovery of the Hippo signaling pathway (Halder and Johnson, 2011; Harvey and Tapon, 2007; Zhao et al., 2010a). All developmental signaling pathways known to affect tissue growth also affect other processes such as patterning and differentiation. The Hippo signaling pathway is a unique pathway in that it is mainly dedicated to tissue growth control. Moreover, it is the first pathway that was shown to regulate both cell proliferation and cell survival. This conserved pathway was discovered in *Drosophila* where its core components, such as the upstream kinase Hippo (Hpo) and the downstream kinase Warts (Wts) are strong tumour suppressors. Mutations in any of those components lead to massive tissue overgrowth (Fig 1.6). Thus, Hippo signaling is required during development to restrict tissue growth and allow organs to reach their correct size.

1.3.1 Core components

The key effector of Hippo signaling is the transcriptional co-activator Yorkie (Yki), which activates the expression of target genes that promote cell proliferation and cell survival such as *cyclin E (cycE)* and *Drosophila inhibitor of apoptosis 1* (*DIAP1*) (Huang et al., 2005). Yki is a dose dependent regulator of tissue growth: mutations in *yki* result in strong undergrowth, while overexpression of *yki* triggers massive overproliferation (Fig 1.7 A-C'). Yki is regulated by a cascade of phosphorylations involving the upstream kinase Hpo, a member of the Ste20 (sterile20)-like family of serine/threonine kinases, and the downstream kinase Wts, an NDR (nuclear Dbf2-related) serine/threonine kinase (Fig 1.8) (Harvey et al., 2003; Jia et al., 2003; Justice et al., 1995; Pantalacci et al., 2003; Udan et al., 2003; Wu et al., 2003; Xu et al., 1995).

Activation of the kinase cascade is not well understood, but requires phosphorylation of one of Hpo tyrosine residues (Tyrosine 195) in its activation loop (Colombani et al., 2006; Polesello et al., 2006), possibly via auto-phosphorylation or phosphorylation by an unknown kinase (Genevet and Tapon, 2011; Pantalacci et al., 2003). Activated Hpo binds to and phosphorylates its co-factor Salvador (Sav), which stimulates Hpo to phosphorylate the downstream kinase Wts (Kango-Singh et al., 2002; Tapon et al., 2002; Wu et al., 2003). In addition to phosphorylating Wts, Hpo phosphorylates the Wts co-factor Mob as a tumor suppressor (Mats), promoting its association with Wts. Phosphorylation of Wts by Hpo and association with its co-factor Mats activates Wts catalytic domain (Lai et al., 2005). This complex cascade of phosphorylations thus leads to the activation of Wts, which in turn phosphorylates its target Yki on 3 conserved serine residues (serines 111, 168 and 250)(Huang et al., 2005; Oh and Irvine, 2009). Yki phosphorylation on S168 promotes its binding to 14-3-3 proteins which sequester Yki in the cytoplasm, preventing it from activating its target genes (Dong et al., 2007). Mutations in all components of the kinase cascade in imaginal discs lead to massive overgrowth due to an important increase in cell proliferation and reduced levels of apoptosis.

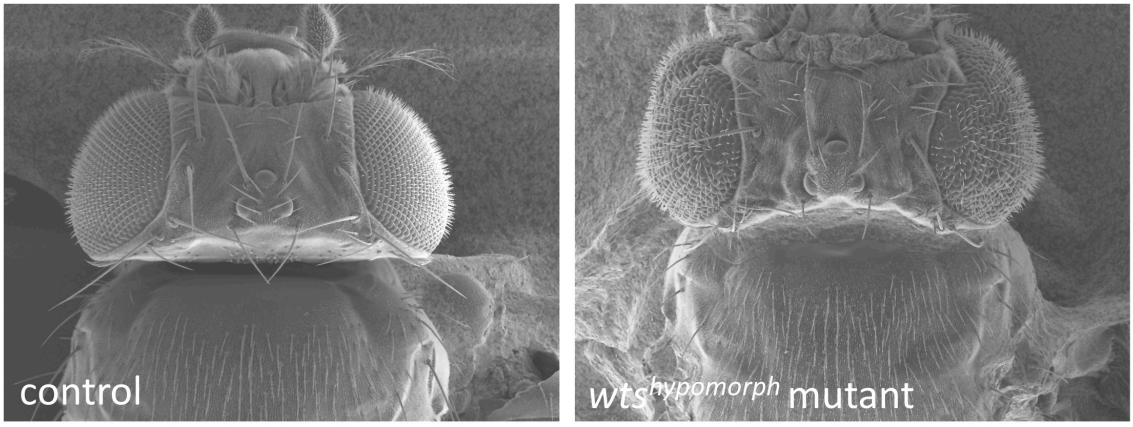

Figure 1.6: Loss of Wts leads to a strong overgrowth phenotype
Scanning Electron Micrographs of adult flies: top view of a wild type *Drosophila* head (left), and a *Drosophila* head with overgrown *wts* homozygous mutant eyes (right).

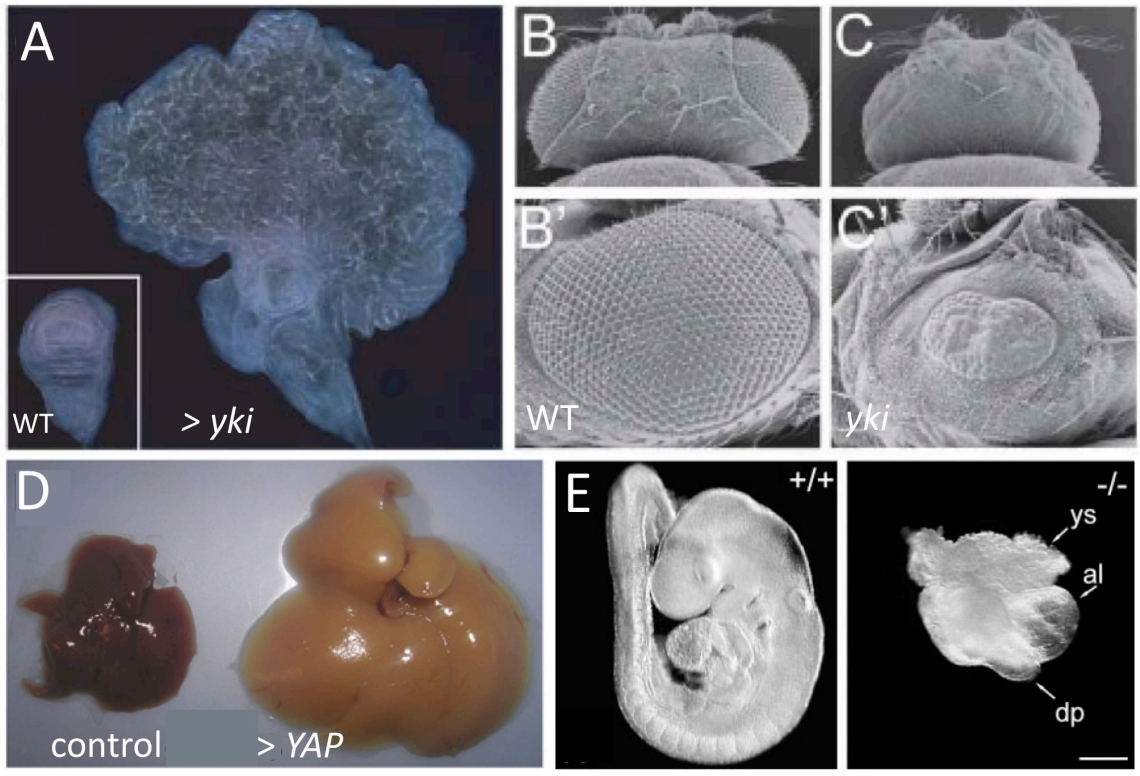

Figure 1.7: Yki is a conserved dose dependent regulator of tissue growth
(A) Over-expression of Yki in the *Drosophila* wing disc leads to dramatic overgrowth compared to a wild type wing disc (bottom left). Image from (Huang et al., 2005). (B-C') Scanning Electron Micrographs from (Huang et al., 2005): eyes lacking *yki* (C, top view ; C', lateral view) are dramatically undergrown compared to wild type (B, top view ; B', lateral view). (D) Over-expression of Yki homologue YAP in the mouse liver leads to a massive tissue overgrowth (right) compared to control (left). Image from (Dong et al., 2007). (E) YAP homozygous mutant mice embryos (right) are much smaller than their wild type siblings (left). Images from (Morin-Kensicki et al., 2006).

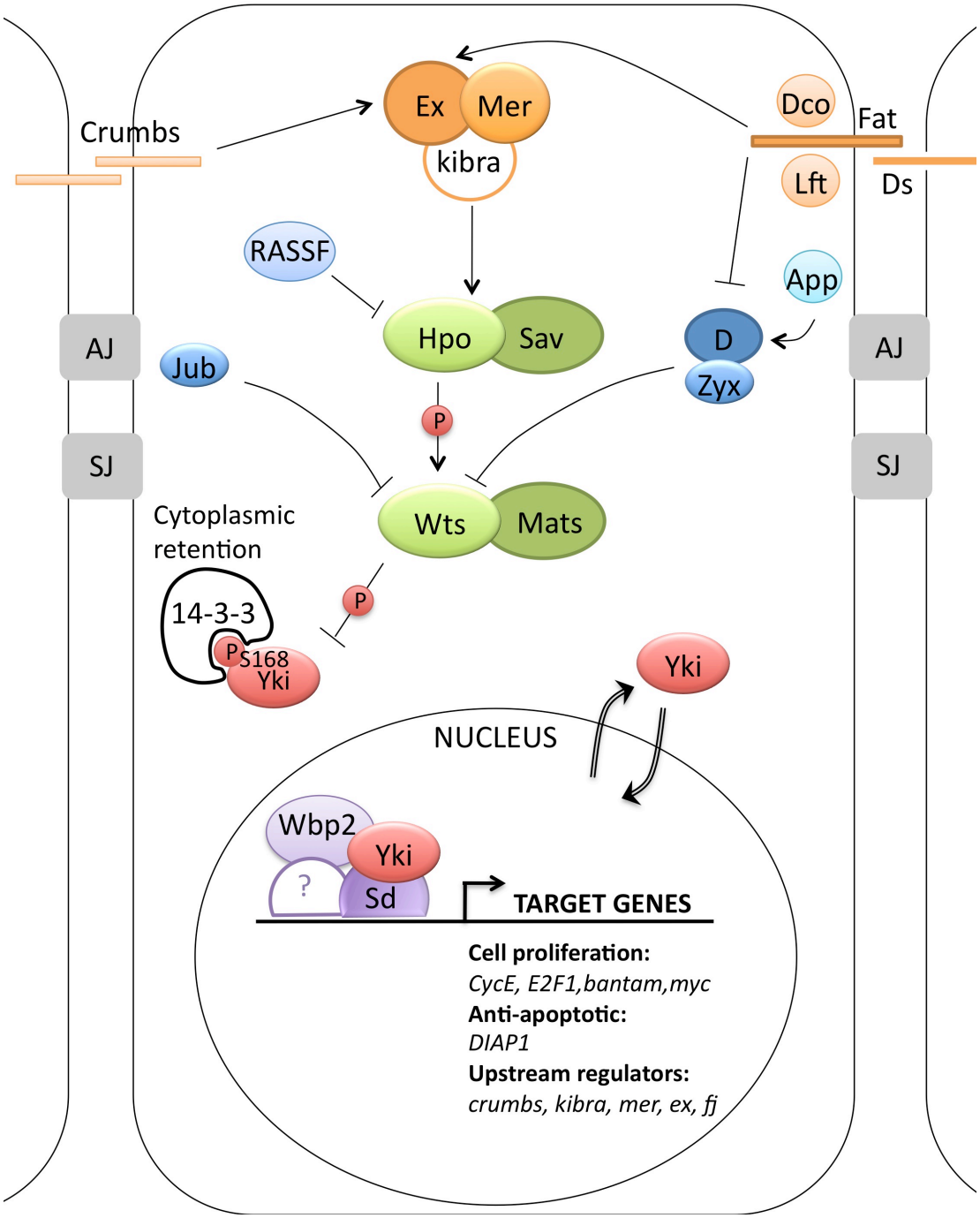

Figure 1.8: Schematics of the Hippo signaling pathway in *Drosophila*
Plasma membrane and nucleus are outlined in black with adherens junctions (AJ) and septate junctions (SJ) represented by grey boxes. The kinase cascade is represented in green, Yki in red, and Yki nuclear partners in purple. Positive regulators of the kinase cascade are represented in orange, negative regulators are represented in blue.

All the core components of the Hpo pathway are conserved in mammals. MST1/2 (Hpo homologues), SAV1 (Sav homologue), LATS1/2 (Wts homologues), and MOBKL1A/B (Mats homologues), form a kinase cascade like their *Drosophila* counterparts and phosphorylate YAP and TAZ (Yki homologues), promoting their cytoplasmic retention by 14-3-3 proteins (Zeng and Hong, 2008; Zhao et al., 2007). One additional mechanism has been described: in mammals, phosphorylation of YAP and TAZ by LATS1/2 not only promotes their binding to 14-3-3 but also promotes their subsequent phosphorylation by another kinase, promoting their binding to $SCF^{\beta TRCP}$ E3 ubiquitin ligase which triggers their degradation (Dong et al., 2007; Liu et al., 2010; Zhao et al., 2010b). Hippo pathway function in organ size control is conserved in mammals. YAP is essential for growth of mice embryos and YAP overexpression or conditional knock-outs of MST or NF2 in mice liver leads to massive tissue overgrowth and tumourigenesis (Fig 1.7 D, E) (Camargo et al., 2007; Dong et al., 2007; Song et al., 2010; Zhang et al., 2010). In addition, YAP is found strongly expressed and nuclear in many human tumours (Dong et al., 2007; Steinhardt et al., 2008), and levels of expression of other components of the pathway are affected in several human cancers (Pan, 2010).

Although the core components of the Hippo signalling pathway are known and their biochemical interactions and functions have been well-characterised, upstream activation of the pathway as well as its downstream effects are poorly understood. Some of the upstream components have been identified in genetic interaction experiments but their exact biochemical mechanisms are not known. These components will be described in the following paragraphs.

1.3.2 Kibra/Expanded/Merlin complex

One key upstream regulatory component of Hippo signaling is the Kibra/Expanded/Merlin (Kibra/Ex/Mer) complex. Mutations in these components lead to moderate overgrowth phenotypes. Mer and Ex both contain a FERM domain: an F-actin binding domain found in proteins that link the actin cytoskeleton and the plasma membrane such as 4.1, ezrin, radixin and moesin, after which the FERM domain was named (Chishti et al., 1998). Mer and Ex both localise at the cell cortex and colocalise with Kibra at the sub-apical region of epithelial cells (Genevet et al., 2010; McCartney et al., 2000). Kibra, Mer and Ex bind to each other and act genetically upstream of

Hpo. The Kibra/Ex/Mer complex binds directly Hpo and Sav – via multiple interactions between Ex and Hpo, Mer and Sav, and Kibra and Sav – and promotes Hpo activity through an unknown mechanism (Baumgartner et al., 2010; Genevet et al., 2010; Hamaratoglu et al., 2006; McCartney et al., 2000; Yu et al., 2010). Mutants of *kibra, ex* or *mer* present tissue specific differences in phenotype severity, reflecting tissue specific requirements (Genevet et al., 2010; Pellock et al., 2007). Although single mutants for *ex*, *mer* and *kibra* show weak overgrowth phenotypes, double mutant combinations of *ex*, *mer* and *kibra* present more severe phenotypes, similar to those of *hpo*, *sav*, *mats* and *wts* mutants (Hamaratoglu et al., 2006; Yu et al., 2010). Thus, *kibra, ex* and *mer* act semi-redundantly to promote Hippo signaling.

Human KIBRA, NF2/Merlin (Merlin human homolog) and Willin/FRMD6 (Expanded human homolog) all stimulate Hippo signaling and affect YAP activity in human cell lines: their function in Hippo signaling is conserved (Angus et al., 2011; Xiao et al., 2011; Yu et al., 2010; Zhang et al., 2010). FRMD6 binding to KIBRA and NF2 has not been investigated, but KIBRA and NF2 bind to each other, indicating they may act in a complex like their *Drosophila* homologues (Zhang et al., 2010).

1.3.3 Phosphorylation independent regulation of Yki

Yki contains 2 WW domains in its C terminal part, which can associate with PPXY motifs in other proteins to mediate direct binding. In addition to regulating Yki through Hippo signaling, Ex directly binds Yki via an interaction between its PPXY motifs and Yki WW domains. This binding can lead to Yki cytoplasmic retention in a phosphorylation independent manner (Badouel et al., 2009; Oh et al., 2009). Hpo and Wts contain PPXY motifs too and they are also able to sequester Yki in the cytoplasm by binding its WW domains. Expression of Hpo or Wts is able to suppress the nuclear localisation of a non-phosphorylatable form of Yki in the eye disc, showing that Hpo and Wts can regulate Yki in a phosphorylation independent manner. However, these experiments have been carried out in non-physiological conditions as they involved overexpression of Ex, Hpo or Wts. The physiological significance of this phosphorylation independent effect on the regulation of Yki localisation has not been proven. A similar mode of regulation was suggested in human cells with Angiomotin family proteins. These junctional proteins directly bind YAP and TAZ, promoting their junctional localisation and preventing their nuclear localisation (Zhao et al., 2011). Another phosphorylation independent

mechanism, yet not clearly understood, is the negative regulation of Yki by the endosomal protein Myopic (Mop). Mop binds Yki WW domains through its PPXY motif and appears to affect Yki association with specific endosomal compartments (Gilbert et al., 2011).

1.3.4 Fat/Hippo signaling

The first transmembrane protein found to regulate Hippo signaling was the protocadherin Fat (Ft), which localises at the subapical-region of cells (Bennett and Harvey, 2006; Cho et al., 2006; Silva et al., 2006; Willecke et al., 2006). *Drosophila fat* mutant tissues present strong overgrowth phenotypes and perturbations in bristle orientation (Bryant et al., 1988; Mahoney et al., 1991). Fat is a well-known regulator of planar cell polarity (PCP), which is the mechanism that orients cellular structures such as hairs within the plane of a tissue (Axelrod, 2009). PCP is regulated by molecular complexes that localise in a planar polarised manner within cells. *fat* mutant overgrowth phenotypes, but not planar cell polarity (PCP) defects, can be rescued by *wts* overexpression. Thus, Fat regulates the establishment of PCP and restricts tissue growth via two independent pathways (Feng and Irvine, 2007). Fat regulates tissue growth by feeding into the Hippo pathway at 2 levels. First, it promotes the membrane localisation of Ex, thereby promoting Hpo activation (Bennett and Harvey, 2006; Silva et al., 2006; Willecke et al., 2006). In addition, Fat negatively regulates the unconventional myosin Dachs (D) (Cho and Irvine, 2004). In the wing disc, Dachs is present in the cytoplasm but localises preferentially at the apical cell cortex, where Wts is presumably activated by the Kibra/Ex/Mer complex (Mao et al., 2006), and this membrane localisation requires the palmitoyltransferase Approximated (App) (Matakatsu and Blair, 2008). Dachs binds to the LIM domain containing protein Zyxin (Zyx), an adherens junction localised protein, and promotes its binding to Wts, which leads to Wts degradation through an unknown mechanism (Cho et al., 2006; Rauskolb et al., 2011). In *fat* mutant cells, Dachs accumulates at the membrane, whereas in cells overexpressing *fat*, Dachs is mostly cytoplasmic. Thus, Fat antagonises Dachs by inhibiting its membrane localisation (Cho et al., 2006). The level of Fat at the membrane is regulated by the protein Lowfat (Lft), which interacts with Fat intracellular domain (Mao et al., 2009). Fat activation is regulated by its ligand, the protocadherin Dachsous (Ds), and by the serine/threonine kinase Disc overgrown (Dco)

which activates Fat by promoting its intracellular domain phosphorylation in a Ds dependent manner (Clark et al., 1995; Feng and Irvine, 2009; Sopko et al., 2009; Willecke et al., 2008). Fat and Ds form trans-heterodimers and their interaction is modulated by the Golgi kinase Four-jointed (Fj) which phosphorylates their cadherin domains: Fat phosphorylation by Fj increases Fat affinity for Ds, while Ds phosphorylation by Fj decreases Ds affinity for Fat (Brittle et al., 2010; Ishikawa et al., 2008; Simon et al., 2010).

Dachsous and Four-jointed are expressed in two opposite gradients along the proximo-distal axis of *Drosophila* imaginal discs: with Ds higher expression in the proximal region, and Fj higher expression in the distal region (Brodsky and Steller, 1996; Clark et al., 1995; Villano and Katz, 1995). These gradients modulate the amount of Ds binding to Fat and result in the enrichment of Ds-bound (active) Fat at the proximal side of the cells thereby restricting Dachs membrane localisation to the distal side (Mao et al., 2006). This planar polarisation of Fat activity is involved in the establishment of PCP. In addition to regulating PCP, graded expression of *fj* and *ds* leads to partial inactivation of Fat signaling thereby restricting Hippo signaling and promoting tissue growth. Restriction of Dachs activity to the distal side of cells was also shown to be important for controlling shape in the wing by promoting the orientation of cell divisions along the proximo-distal axis (Mao et al., 2011b). Interestingly, *fj* and *ds* expression is influenced by Dpp and Wg signaling, providing a potential link between upstream developmental signals and coordination of planar cell polarity, tissue shape, and tissue growth control by Hippo signaling (Lawrence et al., 2008; Rogulja et al., 2008; Zecca and Struhl, 2010).

Fat and Ds homologues are Fat4 and Dchs1. Mutant mice for these 2 genes present PCP and organ shape defects but no obvious defects in organ size (Mao et al., 2011a; Saburi et al., 2008), indicating that other homologues may accomplish Fat/Ds signaling function in growth control, or that there may be some redundancy among paralogues.

1.3.5 Lgl, aPKC and Crumbs

Recently, the regulators of apico-basal polarity Lgl (Lethal giant larvae), aPKC (atypical Protein Kinase C) and Crumbs have been linked to Hippo signaling. The apical determinant aPKC inhibits Hippo signaling by reducing Hpo apical localisation and

promoting Hpo colocalisation with its negative regulator RASSF. The protein RASSF is an inhibitor of Hpo that competes with Sav for binding to Hpo, and recruits the protein phosphatase 2A (PP2A) complex STRIPAK (Striatin-interacting phosphatase and kinase), which de-phosphorylates and thus inactivates Hpo (Polesello et al., 2006; Ribeiro et al., 2010). aPKC function is antagonised by the basal determinant Lgl, which promotes Hippo signaling (Grzeschik et al., 2010). Crumbs (Crb) is a transmembrane protein that localises at the sub-apical region of epithelial cells and regulates apico-basal polarity in embryonic epithelia but not in imaginal discs. In imaginal discs, loss of *crb* causes overgrowth and Yki dependent Hippo pathway target genes up-regulation (Chen et al., 2010; Ling et al., 2010; Richardson and Pichaud, 2010; Robinson et al., 2010). Crb binds Ex through its FERM binding domain and promotes Ex apical localisation (Chen et al., 2010; Ling et al., 2010; Robinson et al., 2010). Clones of cells mutant for *crb* loose Ex apical localisation. Interestingly, adjacent cells also loose apical localisation of Crb and Ex specifically at the junction with *crb* mutant cells, possibly because Crb needs to trans-homodimerise to be stable at the membrane (Chen et al., 2010). Thus, Crb may be involved in cell-cell contact inhibition (cf paragraph 1.3.6). Crb homologue CRB3 was also shown to affect Hippo signaling in cell cultures and mouse embryos (Varelas et al., 2010).

1.3.6 Hippo signaling: from the cell cortex to the nucleus

In recent years, a new view of Hippo signaling has emerged. Many components of Hippo signaling are localised apically, at cell junctions, or associated with the actin cytoskeleton. Localisation of the Hpo kinase cassette at the apical cortex appears to be important for efficient activation of the pathway, and it has been proposed that Hippo signaling senses molecular and mechanical cues from neighbouring cells at the apical cell cortex and at cell-cell junctions, and responds by changes in gene expression through regulation of Yki/YAP/TAZ (reviewed by (Genevet and Tapon, 2011)). In mammalian cell lines, Hippo signaling is involved in contact inhibition of cell proliferation (Ota and Sasaki, 2008; Zhao et al., 2007). Contact inhibition is a phenomenon by which cells stop proliferating once they have reached confluence. This property is characteristic of differentiated cells in normal tissues and loss of contact inhibition leads to tumour formation (Fagotto and Gumbiner, 1996). At low cell density, YAP localises predominantly in the nucleus and drives cell proliferation with its partner TEAD

(Ota and Sasaki, 2008; Zhao et al., 2007). By contrast, at high cell density, YAP is phosphorylated by LATS1/2 and translocates to the cytoplasm (Zhao et al., 2007). Although the mechanism of Hippo signaling activation upon cell contact inhibition remains elusive, the link between cell adhesion molecules mediating cell contact inhibition and Hippo signaling is starting to be unravelled. Recently, Hippo pathway dependent cell contact inhibition was shown to be regulated by the adherens junction proteins E-cadherin, α-catenin and β-catenin (Kim et al., 2011), and by the tight junction Crumbs complex, which includes Angiomotin family proteins (Varelas et al., 2010; Zhao et al., 2011). Interestingly, in *Drosophila*, 2 adherens junction proteins have been shown to affect Hippo signaling: Zyxin, described above, and Ajuba, which negatively regulates Wts kinase activity by an unknown mechanism (Das Thakur et al., 2010; Rauskolb et al., 2011). Considering the role of junction proteins in cell contact inhibition in human cells, and considering the role of *zyxin* and *ajuba* in controlling cell proliferation, these proteins could be involved in cell contact inhibition in *Drosophila* tissues.

Another important role for Hippo signaling was recently discovered in mechanotransduction (Dupont et al., 2011; Wada et al., 2011). Mechanotransduction is the translation of a mechanical stimulus, such as cell compression or cell stretching, into a biological response such as cell proliferation or differentiation. Both Dupont et al and Wada et al show that YAP/TAZ localisation responds to the degree of cell spreading: YAP/TAZ are more nuclear in isolated cells that occupy a large area than in isolated cells that are more compact. They also show that spread cells produce more actin stress fibers than compact cells and that experimental induction of stress fibre formation promotes YAP/TAZ nuclear translocation. Moreover, Dupont et al show that inhibition of ROCK and non-muscle myosin – which are required to generate cytoskeletal tension – prevents YAP/TAZ nuclear localisation. Therefore, nuclear translocation of YAP/TAZ upon cell spreading is dependent on tensile forces generated by actin stress fibres. The involvement of upstream Hippo pathway components is unclear, and the molecular mechanism of this regulation is not elucidated, but the role of F-actin on Hippo pathway regulation was also shown in *Drosophila*, where experimental induction of actin stress fibres in wing imaginal discs leads to strong overgrowth, Yki nuclear translocation and upregulation of Hippo pathway target genes in a Yki dependent manner (Fernández et al., 2011; Sansores-Garcia et al., 2011).

1.3.7 Yki regulation, partners and targets

From multiple upstream inputs, Hippo signaling converges on the transcriptional co-activator Yki. Mutations in *yki* completely suppress the overgrowth phenotype of *hpo*, *wts* or *sav* mutant clones and *yki* overexpression in the wing or eye causes strong tissue overgrowth (Huang et al., 2005). Known Yki target genes include the cell proliferation genes *cycE* (Huang et al., 2005), *E2F1* (Goulev et al., 2008), *bantam* microRNA (Nolo et al., 2006; Thompson and Cohen, 2006), and *myc* (Neto-Silva et al., 2010), the anti-apoptotic gene *DIAP1 (Huang et al., 2005)*, and upstream Hippo pathway regulators *kibra, ex, mer, fj* and *crb* (Cho et al., 2006; Genevet et al., 2009; Genevet et al., 2010; Hamaratoglu et al., 2006), providing a negative feedback mechanism. Direct association of Yki to target gene promoters has been shown for *bantam* (Peng et al., 2009), *myc* (Neto-Silva et al., 2010) and *DIAP1* (Wu et al., 2008). In some developmental contexts, Hippo signaling also affects the expression of signaling molecules such as the Wnt signaling ligand *wg* (in the wing disc inner ring of *wg* expression), the Notch ligands *delta* (in the adult gut) and *serrate* (in the leg disc) and the JAK-STAT ligands *unpaired (upd) 1/2/3* (in the adult gut) (Cho et al., 2006; Shaw et al., 2010).

Very little is known about the mechanism of activation of Hippo pathway target genes. Yki does not contain a DNA binding domain and must therefore associate with transcription factors to activate its target genes. The first transcription factor identified as a crucial partner for Yki was the TEF/TEAD family protein Scalloped, which binds a conserved domain in Yki N-terminal region (Goulev et al., 2008; Wu et al., 2008; Zhang et al., 2008). The role of Sd in Yki target gene activation is conserved in mammals, where TEAD transcription factors bind YAP/TAZ and are required for the expression of YAP/TAZ target genes (Zhang et al., 2009a; Zhao et al., 2008). In *Drosophila*, Sd recruits Yki to the DNA, and in addition promotes Yki nuclear localisation both in cell culture and in *Drosophila* tissues. In the wing and eye imaginal discs, mutations in *sd* suppress the overgrowth phenotype and target gene upregulation caused by *yki* overexpression. Thus, Sd is required for Yki to promote target gene expression and growth. However, there is plenty of evidence that Yki needs to interact with other DNA binding factors to activate its target genes. Indeed, *yki* is required for normal growth in all of the imaginal tissues (Huang et al., 2005) but *sd* is not

ubiquitously expressed and seems specifically required for cell proliferation in the wing (Campbell et al., 1992). Whereas *yki* mutant clones are strongly undergrown in all imaginal tissues, *sd* mutant clones are small in the wing blade region but grow normally in the eye disc (Peng et al., 2009; Wu et al., 2008). Two non-mutually exclusive hypothesis explain the discrepancy between *yki* and *sd* phenotypes:

1. *Default repression*: Sd may act as a transcriptional activator in the presence of Yki, and as a transcriptional repressor in the absence of Yki. Thus, target genes in *sd* mutant clones would lack Yki activation but also Sd repression, which would produce an intermediate phenotype. Consistent with this hypothesis is the fact that overexpression of Sd alone in the wing or in the eye causes tissue undergrowth, whereas overexpression of Sd with Yki strongly enhances Yki overgrowth phenotype (Wu et al., 2008).

2. *Binding of Yki to other transcription factors:* as Sd is not expressed ubiquitously, Yki needs other transcription factors to bind DNA and ensure target gene activation in tissues where Sd is not expressed such as the anterior eye disc (Campbell et al., 1992). Indeed, the transcription factor Homothorax (Hth) was identified as a Yki partner in that tissue (Peng et al., 2009). Specification of the eye occurs as a wave of differentiation, or morphogenetic furrow (MF), sweeps across the eye disc epithelium from the posterior to the anterior. Cells anterior to the MF proliferate to provide a sufficient number of progenitor cells to form a functional eye, while cells posterior to the MF stop proliferating and start to differentiate to produce photoreceptors. Later during eye development, a second mitotic wave occurs in undifferentiated cells posterior to the MF. Homothorax (Hth) and its binding partner Teashirt (Tsh) are expressed anterior to the MF, where they inhibit premature differentiation. Yki associates with Hth/Tsh at *bantam* promoter and activates *bantam* expression, thereby promoting cell proliferation. Interestingly, Sd is expressed posterior to the morphogenetic furrow (Campbell et al., 1992), and may therefore be involved in Yki target gene activation posterior to the furrow.

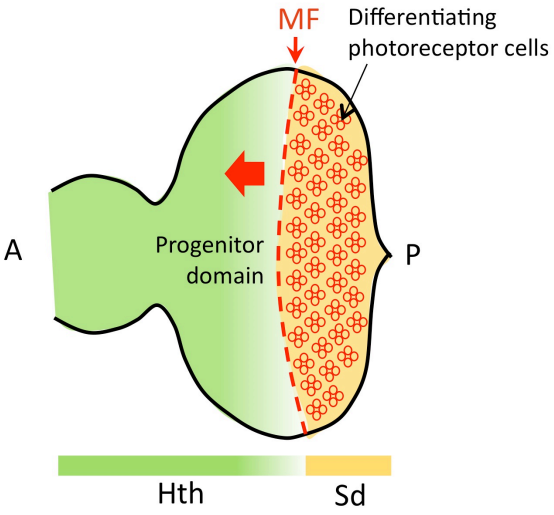

Figure 1.9: Schematics of the differentiating eye imaginal disc
The morphogenetic furrow (MF) sweeps the eye disc from posterior (P) to anterior (A). Progenitor cells proliferate until they are met by the MF. Cells posterior to the furrow stop proliferating and differentiate into photoreceptor cells. Hth domain of expression is represented in green, Sd domain of expression is represented in yellow.

Yki can also cooperate with other transcription factors that bind to the same promoters to drive target gene expression. Indeed, Wu et al have identified a Hippo pathway Responsive Element (HRE), a minimal sequence of 26 base pair upstream of *DIAP1* that is necessary and sufficient for *DIAP1* induction upon Yki activation. HRE contains a 7-nucleotide Sd binding motif, but the other 19 nucleotides are as essential as the Sd binding motif for target gene expression, indicating that there are other factors binding to the HRE, necessary for Yki activity.

Recently, Yki was shown to bind the *bantam* regulatory region with Mad, the transcription factor regulated by Dpp signaling, and to promote *bantam* expression (Oh and Irvine, 2011). Thus, although they control different sets of genes, Mad and Yki cooperate to activate a common set of target genes. This link between Hippo and TGFβ signaling is conserved in mammals where YAP and TAZ associate with different Smad transcription factors, although the precise role of these interactions in growth control by Hippo signaling remains to be determined (Alarcón et al., 2009; Ferrigno et al., 2002; Varelas et al., 2008). Cooperativity was also described between Yki and E2F1, which share a common set of target genes (Nicolay et al., 2011).

In addition to cooperating with different transcription factors, Yki recruits transcriptional co-activators. For instance, the Yki WW domains are important for Yki repression, but are also essential for Yki's transactivator function in the nucleus. Recently, the conserved protein Wbp2 was found to bind to Yki's WW domains and to promote Yki target gene expression when overexpressed in both *Drosophila* and human

cells (Chan et al., 2011; Chen et al., 1997; Zhang et al., 2011b). However, identification of more Yki partners is needed in order to better understand how Yki activates its target genes to promote tissue growth in different developmental contexts.

Chapter 2. Materials and methods

2.1 *Drosophila* genetics

2.1.1 GAL4/UAS system

The GAL4/UAS system is a powerful genetic tool used to label specific cells or tissues or to overexpress genes in a particular tissue to study their phenotypes (Brand and Perrimon, 1993). GAL4 is a yeast transcription factor that binds to a specific UAS (Upstream Activation Sequence) to activate its target genes. Expression of GAL4 in *Drosophila* cells has no effect as GAL4 specifically binds the UAS. A gene *X* can be cloned under the control of a UAS promoter and used to generate transgenic flies carrying a *UAS.X* sequence. This *UAS.X* transgenic line can be crossed to a transgenic line carrying a *GAL4* construct under the control of a tissue specific promoter, producing flies carrying both constructs, therefore expressing gene *X* in that particular tissue (Fig 2.1). Several tissue-specific GAL4 lines are available, such as *hedgehog.GAL4 (hh.GAL4)* and *MS1096.GAL4* used to express UAS transgenes in the posterior compartment of the wing and in the whole wing respectively, or *eyeless.GAL4 (ey.GAL4)* and *GMR.GAL4*, used to express UAS transgenes in the eye.

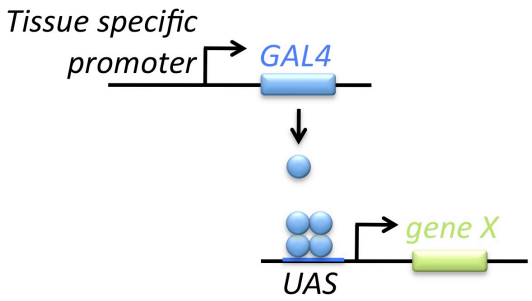

Figure 2.1: The GAL4/UAS system

2.1.2 Generation of mitotic clones

Mosaic tissues were generated using the FLP/FRT and the MARCM system with a heat shock promoter (hs) to drive the expression of the FLP recombinase. Clones were induced by heat shocking larvae at 84 hr (± 12 hr) of development and larvae were dissected at the third instar stage.

The FLP/FRT system is used to generate mitotic clones of homozygous mutant cells in a heterozygous mutant tissue (Harrison and Perrimon, 1993). This genetic tool makes use of the yeast site-specific FLP recombinase, under the control of a heat shock-inducible promoter (*hs*), which catalyses recombination between FRT sequences (FLP Recombination Target). The system is described in Figure 2.2.

A variant of the system is to use a tissue-specific promoter to induce FLP expression. For instance the *ey.FLP* transgene allows generation of clones in the eye. In this case, a w^+ transgene can be used instead of the GFP to mark clones in adult eyes (in a *white* mutant background). Another variant is the FRT Minute system. When clones of cells with reduced viability are induced in a tissue, they are outcompeted by surrounding cells by a process called cell competition, proliferating very poorly and undergoing apoptosis. Thus, it is sometimes difficult to recover mutant clones for certain genes that strongly affect cell viability. The FRT Minute system allows recovery of bigger mutant clones for such genes. In addition to the GFP reporter, the chromosome arm carrying the wild type allele for the gene of interest also carries a mutation in a dose dependent regulator of growth, such as *minute* genes, which is homozygous lethal and gives a comparative advantage to the homozygous mutant clones that do not carry the *minute* mutation over heterozygous *minute* mutant cells. Using the *FRT Minute* system in combination with *ey.FLP* allows the generation of whole mutant eyes instead of mosaic eyes that would normally be obtained by using the classic ey.FLP/FRT system.

The MARCM system is another elegant variant of the FLP/FRT system (Lee and Luo, 1999). By contrast to the classical FLP/FRT system that marks mutant cells by the absence of GFP, the MARCM system allows positive labelling of mutant cells by GFP expression. This system is described in Figure 2.3.

Clone size quantification: clone size was measured using the ImageJ software. Clone area was measured with a selection tool. For each genotype, the areas of 25-30 clones were measured and averaged. Graphs were generated in Microsoft Excel.

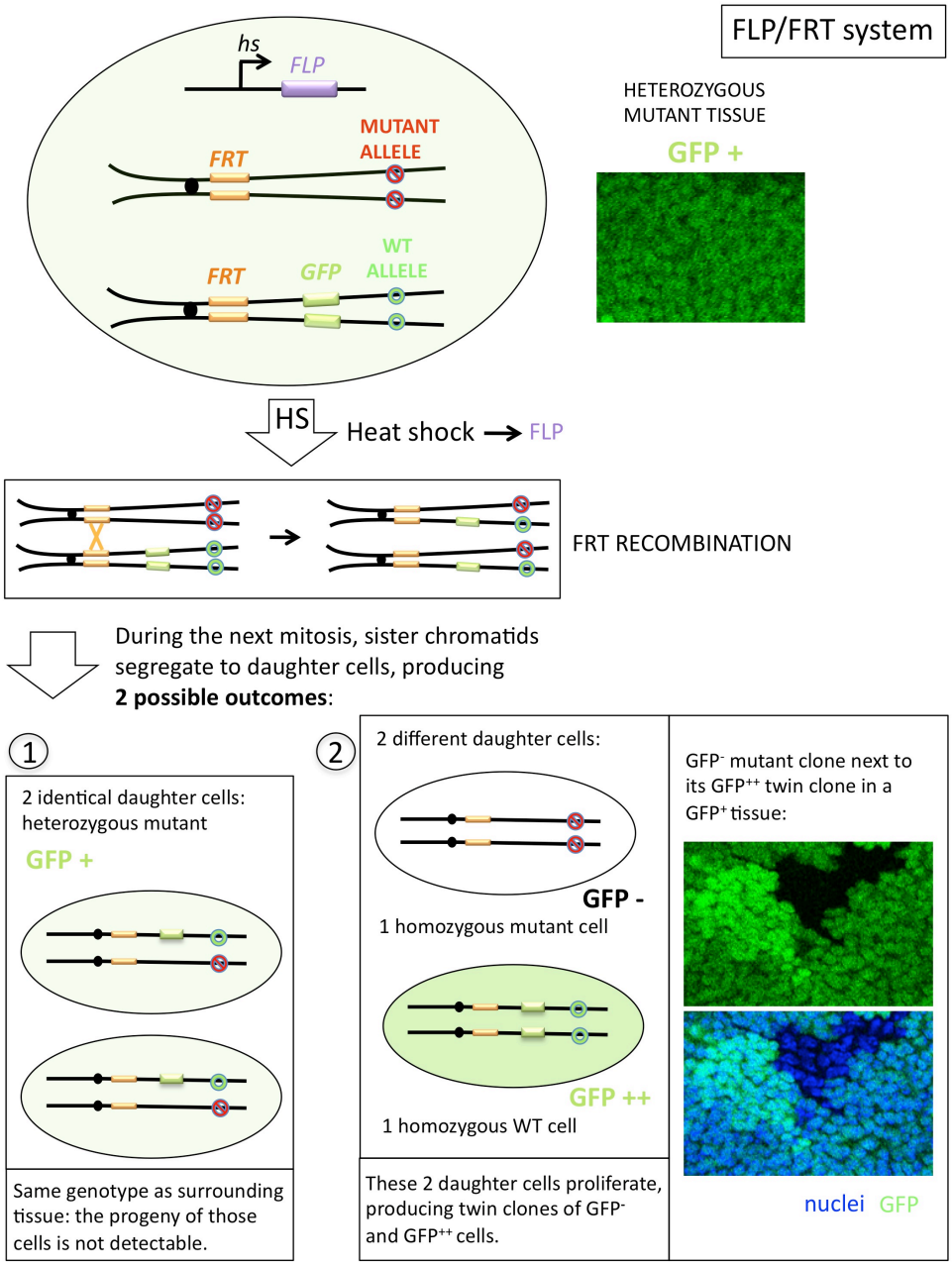

Figure 2.2: The FLP/FRT system

The pair of chromosomes containing the gene of interest *x* carries FRT transgenes near the centromeric region, on the same arm as gene *x*. One homologue of the pair contains a mutant allele x^{MUTANT}, while the other chromosome bears the wild type allele x^{WT} and a *GFP* reporter gene under the control of a ubiquitous promoter. Upon heat-shock, FLP is expressed and catalyses the recombination of FRT sequences between the 2 homologous chromosomes, producing 2 chimeric chromosomes, each carrying the 2 different alleles of gene *x* on its sister chromatids. During the next mitosis, sister chromatids segregate to daughter cells, producing 2 possible outcomes:
1- One chromatid of each genotype moves to each daughter cell, resulting in two genetically identical daughter cells heterozygous mutant for gene *x*, and expressing 1 dose of GFP like other tissue cells. 2- the 2 chromatids that carry the x^{WT} allele and the GFP transgene segregate in one daughter cell, producing a wild type cell expressing 2 doses of GFP; the 2 chromatids carrying x^{MUTANT} allele segregate in the other daughter cell, resulting in a wild-type cell that does not express the GFP. These two daughter cells proliferate, forming twin clones of cells.

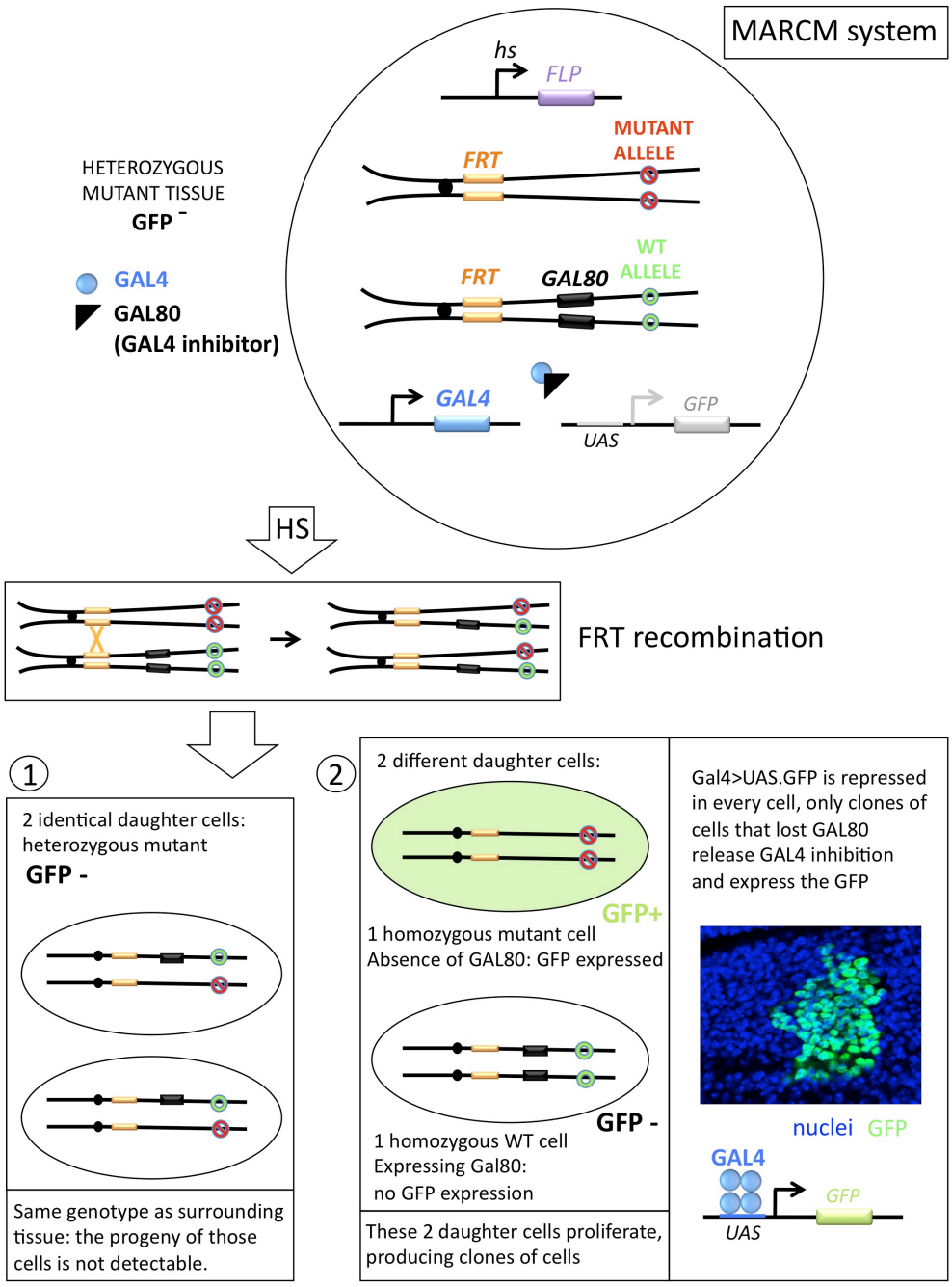

Figure 2.3: The MARCM system
The MARCM system uses the same principle as the FLP/FRT system (Fig 2.2) but differs by 2 points:
1. A *GAL4* transgene is ubiquitously expressed and all cells contain a *UAS.GFP* transgene.
2. The *FRT* WT chromosome arm carries a *GAL80* transgene instead of the *GFP* reporter. *GAL80* is an inhibitor that binds *GAL4* and prevents *GAL4* transactivation activity.
Thus, all cells from the body express both *GAL4* and *GAL80*, and are therefore unable to express the *UAS.GFP* transgene. Only clones of homozygous mutant cells, which do not carry the *GAL80* transgene, can express the *GFP*.

2.1.3 *Drosophila* strains and genotypes

Mask RNAi lines: VDRC GD 33394 , NIG-Fly 6313R2, NIG-Fly 6313R3 ; Wts RNAi line: VDRC GD 9928 ; Raf RNAi line: VDRC GD 2090

Second hairpin RNAi lines ordered from NIG-fly are listed in Table 2 (Appendix)

FRT82B mask $^{10.22}$, *FRT82B mask $^{6.3}$* and *FRT82B mask $^{7.29}$* were gifts from Michael Simon (Smith et al., 2002). UAS.YkiV5, UAS.YkiV5^{S168A} and UAS.YkiV5$^{S111A-S168A-S250A}$ lines were gifts from K. Irvine (Oh and Irvine, 2009). All other fly strains are described in Flybase (Tweedie et al., 2009).

Genotypes were as follows:

Figure 4.1 A: *MS1096.GAL4/+*

Figure 4.1 B: *MS1096.GAL4/+ ;; UAS.mask-IR$^{(VDRC\ GD\ 33394)}$/+*

Figure 4.1 C: *ey.GAL4, GMR.GAL4/+*

Figure 4.1 D: *ey.GAL4, GMR.GAL4/+ ; UAS.mask-IR $^{(NIG\text{-}fly\ 6313R2)}$ /+*

Figure 4.3 A: *yw, ey.flp/+ ;; FRT82B/FRT82B Minute w+*

Figure 4.3 B: *yw ey.flp/+ ;; FRT82B mask$^{10.22}$/FRT82B Minute w+*

Figure 4.3 C: *yw, hs.flp/+ ;; FRT82B/FRT82B GFP*

Figures 4.3 D and 4.4: *yw, hs.flp/+ ;; FRT82B mask$^{10.22}$/FRT82B GFP*

Figure 4.5 A, C: *w ;; hh.GAL4/+*

Figure 4.5 B, D: *w ;; hh.GAL4/P{EPgy2}EY01848*

Figure 4.6 A: *w ;; hh.GAL4, UAS.DIAP1/+*

Figure 4.6 B: *w ;; hh.GAL4, UAS.DIAP1/ UAS.mask-IR $^{(NIG\text{-}fly\ 6313R2)}$*

Figure 4.6 C: *w ;; raf-IR$^{(VDRC\ GD\ 2090)}$ /+ ; hh.GAL4, UAS.DIAP1/+*

Figure 4.6 D, D': *ey.GAL4, GMR.GAL4/+*

Figure 4.6 E, E': *ey.GAL4, GMR.GAL4/+ ; UAS.mask-IR$^{(NIG\text{-}fly\ 6313R2)}$ /+*

Figure 4.6 F: *yw, ey.flp/+ ;; FRT82B mask$^{10.22}$/FRT82B GFP*

Figure 4.7 A: *MS1096.GAL4/+*

Figure 4.7 B: *MS1096.GAL4/+ ;; UAS.wts-IR$^{(VDRC\ GD\ 9928\ )}$/+*

Figure 4.7 C: *ey.GAL4, GMR.GAL4/+*

Figure 4.7 D, E: *ey.GAL4, GMR.GAL4/+ ; UAS.wts-IR$^{(VDRC\ GD\ 9928\ )}$/+*

Figure 4.8 A,B: *w ; fj.lacZ/+ ; hh.GAL4/+*

Figure 4.8 C: *w ; ex.LacZ /+ ; hh.GAL4, UAS.GFP/+*

Figure 4.8 D: *w ; en.GAL4, UAS.GFP /+ ; DIAP1.lacZ/+*

Figure 4.8 E,F: *w ; fj.lacZ/mask-IR$^{(NIG\text{-}fly\ 6313R3)}$; hh.GAL4/+*

Figure 4.8 G: *w ; ex.LacZ / mask-IR$^{(NIG\text{-}fly\ 6313R3)}$; hh.GAL4, UAS.GFP/+*

Figure 4.8 H: *w ; en.GAL4, UAS.GFP /mask-IR$^{(NIG\text{-}fly\ 6313R3)}$; DIAP1.lacZ/+*

Figure 4.9 A, A': *yw, tub.GAL4, hs.flp, UAS nucGFP-myc/+ ; fj.lacZ/+* ;
FRT82B mask$^{10.22}$/FRT82B CD21 y+ GAL80

Figure 4.9 B, B': *yw, tub.GAL4, hs.flp, UAS nucGFP-myc/+* ; *ex.lacZ/+ ;*
FRT82B mask$^{10.22}$/FRT82B CD21 y+ GAL80

Figure 4.9 C, C': *yw, tub.GAL4, hs.flp, UAS nucGFP-myc/+ ; DIAP.lacZ,*
FRT82B mask$^{10.22}$/FRT82B CD21 y+ GAL80

Figure 4.12: *w ; MyoIAGal4/+ ; tubGal80ts, UAS.GFP/+ (adult flies were shifted to restrictive temperature (29°C) to drive the UAS.GFP expression)*

Figure 4.13 A: *yw, tub.GAL4, hs.flp, UAS nucGFP-myc/+ ;; FRT82B/*
FRT82B CD21 y+ GAL80

Figure 4.13 B: *yw, tub.GAL4, hs.flp, UAS nucGFP-myc/+ ;; UAS.YkiV5, FRT82B/*
FRT82B CD21 y+ GAL80

Figure 4.13 C: *yw, tub.GAL4, hs.flp, UAS nucGFP-myc/+ ;; FRT82B mask$^{10.22}$/*
FRT82B CD21 y+ GAL80

Figure 4.13 D: *yw, tub.GAL4, hs.flp, UAS nucGFP-myc/+ ;; UAS.YkiV5,*
FRT82B mask$^{10.22}$/FRT82B CD21 y+ GAL80

Figure 4.14: (control) *w ; FRT82B mask$^{6.3\ or 7.29}$/ FRT82B.* (mask) *w ;*
FRT82B mask$^{6.3}$/ FRT82B mask$^{7.29}$

Figure 4.15 A: *yw, ey.flp/+* ;; *FRT82B/FRT82B Minute w+*

Figure 4.15 B: *yw ey.flp/+* ;; *FRT82B mask$^{10.22}$/FRT82B Minute w+*

Figure 4.15 C: *yw ey.flp/+* ;; *FRT82B wts^{X1}/FRT82B Minute w+*

Figure 4.15 D: *yw ey.flp/+* ;; *FRT82B mask$^{10.22}$, wts^{x1}/FRT82B Minute w+*

Figure 4.15 E: *yw, tub.GAL4, hs.flp, UAS nucGFP-myc/+ ;; FRT82B/*
FRT82B CD21 y+ GAL80

Figure 4.15 F: *yw, tub.GAL4, hs.flp, UAS nucGFP-myc/+ ;; FRT82B mask$^{10.22}$/*
FRT82B CD21 y+ GAL80

Figure 4.15 G: *yw, tub.GAL4, hs.flp, UAS nucGFP-myc/+ ; FRT82B wts^{x1}/*
FRT82B CD21 y+ GAL80

Figure 4.15 H: *yw, tub.GAL4, hs.flp, UAS nucGFP-myc/+ ;; FRT82B mask$^{10.22}$, wts^{x1}/*
FRT82B CD21 y+ GAL80 ;

Figure 4.16 A: *yw, tub.GAL4, hs.flp, UAS nucGFP-myc/+ ;; FRT82B/*

FRT82B CD21 y+ GAL80

Figure 4.16 B and 4.17 E, E': *yw, tub.GAL4, hs.flp, UAS nucGFP-myc/+ ;; UAS.YkiV5, FRT82B/ FRT82B CD21 y+ GAL80*

Figure 4.16 C: *yw, tub.GAL4, hs.flp, UAS nucGFP-myc/+ ;; UAS.Yki^{S168A}V5, FRT82B/ FRT82B CD21 y+ GAL80*

Figure 4.16 D: *yw, tub.GAL4, hs.flp, UAS nucGFP-myc/+ ;; UAS.Yki $^{S111A-S168A-S250A}$V5, FRT82B/ FRT82B CD21 y+ GAL80*

Figure 4.16 E: *yw, tub.GAL4, hs.flp, UAS nucGFP-myc/+ ;; FRT82B mask$^{10.22}$/ FRT82B CD21 y+ GAL80*

Figure 4.16 F and 4.17 F, F': *yw, tub.GAL4, hs.flp, UAS nucGFP-myc/+ ;; UAS.YkiV5, FRT82B mask$^{10.22}$/FRT82B CD21 y+ GAL80*

Figure 4.16 G: *yw, tub.GAL4, hs.flp, UAS nucGFP-myc/+ ;; UAS.Yki ^{S168A}V5, FRT82B mask$^{10.22}$/FRT82B CD21 y+ GAL80*

Figure 4.16 H: *yw, tub.GAL4, hs.flp, UAS nucGFP-myc/+ ;; UAS.Yki$^{S111A-S168A-S250A}$V5, FRT82B mask$^{10.22}$/FRT82B CD21 y+ GAL80*

Figure 4.18 A, A': *yw, tub.GAL4, hs.flp, UAS nucGFP-myc* ; *ex.lacZ/+ ; FRT82B wts^{x1}/ FRT82B CD21 y+ GAL80*

Figure 4.18 B, B': *yw, tub.GAL4, hs.flp, UAS nucGFP-myc* ; *ex.lacZ/+ ; FRT82B mask$^{10.22}$, wts^{x1}/FRT82B CD21 y+ GAL80*

Figure 4.18 C, C': *yw, tub.GAL4, hs.flp, UAS nucGFP-myc* ; *fj.lacZ/+ ; FRT82B mask$^{10.22}$, wts^{x1}/FRT82B CD21 y+ GAL80*

Figure 4.19 A, A': *yw, tub.GAL4, hs.flp, UAS nucGFP-myc* ; *fj.lacZ/+ ; FRT82B wts^{x1}/ FRT82B CD21 y+ GAL80*

Figure 4.19 B, B': *yw, tub.GAL4, hs.flp, UAS nucGFP-myc* ; *fj.lacZ/+ ; FRT82B mask$^{10.22}$, wts^{x1}/FRT82B CD21 y+ GAL80*

Figure 4.19 C, C': *yw, tub.GAL4, hs.flp, UAS nucGFP-myc* ; *ex.lacZ/+ ; FRT82B wts^{x1}/ FRT82B CD21 y+ GAL80*

Figure 4.19 D, D': *yw, tub.GAL4, hs.flp, UAS nucGFP-myc* ; *ex.lacZ/+ ; FRT82B mask$^{10.22}$, wts^{x1}/FRT82B CD21 y+ GAL80*

Figure 4.20: *yw, hs.flp/+ ;; FRT82B wts ^{X1}/FRT82B GFP*

Appendix:

Figure A.1 A: *yw, tub.GAL4, hs.flp, UAS nucGFP-myc/+ ;; UAS.YkiV5, FRT82B/ FRT82B CD21 y+ GAL80*

Figure A.1 B: *yw, tub.GAL4, hs.flp, UAS nucGFP-myc/+ ;; UAS.Yki^{S168A}V5, FRT82B/ FRT82B CD21 y+ GAL80*

Figure A.1 C: *yw, tub.GAL4, hs.flp, UAS nucGFP-myc/+ ;; UAS.Yki $^{S111A-S168A-S250A}$V5, FRT82B/ FRT82B CD21 y+ GAL80*

Figure A.1 D: *yw, tub.GAL4, hs.flp, UAS nucGFP-myc/+ ;; UAS.YkiV5, FRT82B mask$^{10.22}$/FRT82B CD21 y+ GAL80*

Figure A.1 E: *yw, tub.GAL4, hs.flp, UAS nucGFP-myc/+ ;; UAS.Yki ^{S168A}V5, FRT82B mask$^{10.22}$/FRT82B CD21 y+ GAL80*

Figure A.1 F: *yw, tub.GAL4, hs.flp, UAS nucGFP-myc/+ ;; UAS.Yki$^{S111A-S168A-S250A}$V5, FRT82B mask$^{10.22}$/FRT82B CD21 y+ GAL80*

2.2 Histology

2.2.1 Wing mounting

Flies were placed in 100% ethanol over night (flies can be stored in ethanol and dissected later). Wings were dissected away from the body in 70% ethanol, then rinsed in distilled water, and mounted on a slide in a drop of Hoyer's solution.
Samples were imaged on an "axioplan 2 imaging" Zeiss upright microscope and images processed using Adobe Photoshop software.

Hoyer's solution:

Gum arabic (acacia)	30g
Glycerol	16ml
Chloral hydrate	200g
Distilled water	50ml

2.2.2 Photographs of adult eyes

Flies were positioned appropriately in a petri dish with a latex bottom filled with ethanol, and pined down with an insect needle. Samples were imaged on a Leica MZ16 F Stereomicroscope and images processed using Adobe Photoshop software.

2.2.3 Scanning Electron Microscopy (SEM) of adult eyes

Processing and imaging of the samples was carried out by Hannah Armer from the Cancer Research UK Electron Microscopy Unit.

Samples were fixed in 2.5% gluteraldehyde plus 4% paraformaldehyde in phosphate buffer for one hour. Samples were post-fixed in osmium tetroxide and dehydrated step-wise to 100% ethanol. Samples were transferred to 100% acetone and critical point dried.
For SEM: Samples were mounted on SEM stubs, sputter coated with platinum and viewed in a JEOL FESEM 6700.

2.2.4 *Drosophila* adult eye sections

Fixation and embedding for microscopy: The head was dissected away from the body, and one of the eyes was gently cut away with a razor blade to expose the inside of the head and other eye. Putting pressure on the head was avoided when cutting as it may deform the eye. The dissected head was placed into 2% glutaraldehyde in 0.1M phosphate buffer (pH 7.2) in an eppendorf tube and placed on ice for 15-30 min. The head was then processed according to the following protocol (under a hood with gloves):

1. Add an equal volume of 2% osmium tetraoxide (OsO_4: volatile and extremely toxic) in phosphate buffer. Incubate on ice for 30 min.
2. Remove the glutaraldehyde/OsO_4 mixture and wash the tube by filling the tube completely with phosphate buffer. Dispose of the waste glutaraldehyde and OsO_4 in a bottle containing corn oil in excess. The deactivated solution can then be safely removed. Add fresh 2% OsO_4 in phosphate buffer to the tissue and incubate on ice for 1-2 hours.
3. Discard the OsO4 and dehydrate the tissue by successive 10 min incubations in the following ethanol solutions: 30%, 50%, 70%, 90%, 100%. Repeat the final 100% EtOH incubation.
4. Replace the final ethanol treatment with propylene oxide and incubate for 10 min (use hood and gloves). Repeat the propylene oxide wash twice. In the mean time, soft durcupan resin (Fluka) is placed in a heat block at 50 °C to melt.
5. Add an equal volume of durcupan to the last propylene wash and thoroughly mix. Handle resin with non-latex gloves as it is carcinogenic when unpolymerised. Incubate for 2 hours.
6. Replace the resin/propylene oxide mixture with pure resin and incubate over night at room temperature.

7. Using a needle, transfer a fixed head to a mould filled with melted resin (silicon rubber flat embedding mould). Orient the head so that the eye is close to the edge and facing the cutting surface, anterior facing up. Make sure that the head is flat and resting at the bottom of the mould. Bake the resin at 70 °C overnight. Bake any resin before discarding.

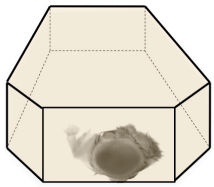

Sectioning and staining specimen

The resin block was trimmed around the eye with a razor blade so that the tip of the resin block formed a pyramid with the eye on top. Excess resin covering the eye surface was trimmed away.

2.5 µM thick sections were cut using a microtome (DIATOME) and transferred in a drop of distilled water on a slide. The slide was then placed on a heating block at 80 °C until the water had evaporated and stained with a drop of toluidine blue for 30 seconds, then rinsed with distilled water, dried, and mounted under a coverslip with a drop of Neutral mounting medium.

2.2.5 Human oesophageal epithelia staining

Adult human tissue processing, embedding and antibody stainings were performed by the Cancer Research UK Experimental HistoPathology laboratory. The tissues were processed, embedded and sectioned at 4 µm. Sections were de-waxed in xylene, dehydrated by passage through graded alcohols to water. If required for antigen retrieval, sections were microwaved in citrate buffer pH6 for 15 minutes and then transferred to PBS. Endogenous peroxidase was blocked using 1.6% hydrogen peroxide in PBS for 10 minutes followed by washing in distilled water. Normal serum diluted to 10% in 1% BSA was used to block non-specific staining in the tissue for 30 minutes. Slides were incubated with Primary antibody (X) diluted to X in 1% BSA for 1 hour at room temperature. Sections were washed in PBS prior to applying secondary antibody – biotinylated X anti X 1:X for 45 min at room temperature. Sections were then washed

in PBS and then incubated in ABC (Vector Laboratories PK-6100) for 30 minutes. Following washing in PBS, DAB solution was applied for 2-5 minutes with development of the colour reaction being monitored microscopically. Slides were washed in tap water, stained with a light haematoxylin, dehydrated, cleared and then mounted.

2.2.6 Immunostaining of *Drosophila* tissues

2.2.6.1 Imaginal discs

Wing or eye imaginal discs were dissected in ice cold PBS and processed as follows:

1. Fix 30 minutes in PBS + 4% formaldehyde
2. Rinse 1x in PBT then wash and permeabilise 2x 10 min in PBT
3. Block 45 min in BBT
4. Incubate over night at 4 °C in BBT and primary antibody
5. Wash 4x30min in BBT
6. Incubate in BBT and secondary antibody for 2 hours at room temperature
7. Wash 4x 15 min in PBT, first wash with 1 µg/ml DAPI (4',6-diamidino-2-phenylindole dihydrochloride, Molecular Probes) to stain DNA.
8. Mount in Fluoromount G (Southern Biotechnology) with gum in corners of the coverslip to avoid squashing the discs.

Samples were imaged on a Leica SP5 confocal and images processed using Adobe Photoshop software.

Solutions:

PBS (Phosphate buffered saline):

NaCl 8 g/L, KCl 0.25 g/L, Na_2HPO_4 1.43 g/L, KH_2HPO_4 0.25 g/L, in distilled water.

PBT(Phosphate buffered saline with Triton): PBS + 0.1 % TritonX-100 (the percentage of Triton can be modified in some particular experiments)

BBT: PBS + 0.1 % TritonX-100 +0.1% BSA (Bovine Serum Albumine, Sigma)

2.2.6.2 Adult gut dissection

Adult flies were dissected in PBS on ice. The abdomen was opened and the gut was detached carefully, without stretching. Most of the Malpighian tubules were removed to prevent tangling. Guts were placed in an eppendorf and processed the following way:

1. 30 min fixation in 4% paraformaldehyde in 0.5X PBS
2. Wash 4 x 5 min in 0.1% PBT
3. 30 min permeabilisation in 0.3% PBT
4. Pre-block 1 hour at room temperature in 10% BSA 0.1%PBT
5. Primary antibody in 5% BSA 0.1%PBT overnight at 4°C
6. Wash 4 x 5min in 0.1% PBT
7. Pre-block 1 hour at room temperature in 10% BSA 0.1% PBT
8. Secondary AB 3-4 hours at room temperature
9. Wash 1x 5min in 0.1% PBT and DAPI to stain DNA
10. Wash 1 x 5 min 0.1% PBT
11. Wash 1x in PBS
12. Mount in Fluoromount G (Southern Biotechnology) with gum in corners of coverslip to avoid squashing the guts.

2.3 *Drosophila* cell cultures

2.3.1 Media

Drosophila S2 cells were grown in *Drosophila* Schneider medium (Invitrogen) containing 10% FBS, 50 µg/ml penicillin, and 50 µg/ml streptomycin.

Drosophila S2R+ cells were grown in Shields and Sang *M3* insect medium (Sigma) containing 10% FBS, 1 % Glutamax (Invitrogen), 50 µg/ml penicillin, and 50 µg/ml streptomycin.

2.3.2 Transfection

Cells were plated in 6 well plates (1.5 mL medium/well)

Cells were transfected using the Effectene transfection reagent with the following protocol (for 1 well):

1. Mix 200 ng of each construct to be transfected in 100 µl of EC buffer, vortex 1s
2. Add Effectene enhancer (10 µl/200ng DNA), vortex 1 s and incubate 2 min
3. Add Effectene reagent (5 µl/200ng DNA), vortex 5-10 s, incubate 10 min at RT
4. Pipette 400 µl from the well to transfect and add it to the Effectene/DNA mix, then pipette the mix gently back in the well.

2.3.3 Fixation and antibody staining of cultured *Drosophila* S2R+ cells

Cells were cultured in 12-well plates on a 13mm sterile coverslip at a density of 3-5.10^5 cells per well.

Cells were fixed and stained according to the following protocol:

1. Rinse cells once with PBS
2. Fix with 4% formaldehyde in PBS for 10 minutes
3. Wash/permeabilise 3x 15 min in PBT (0.1% Triton in PBS)
4. Block 15 min in PBS + 5% BSA
5. Primary antibody incubation in PBS + 5% BSA overnight at 4°C
6. Wash 3 x 15 min in PBT
7. Secondary antibody incubation for 2 hours at room temperature
8. Wash 3 x 15 min in PBT with a 5 min DAPI staining between 2 washes
9. Seize the coverslip with forceps, gently dry the sides on a thin tissue, without touching the surface with the cells, and place the coverslip face down on a drop of Fuoromount G (Southern Biotechnology) on a slide.

Primary antibodies were used two folds less concentrated than in fly tissue immunostainings. Secondary antibodies used at a 1:2000 dilution.

2.4 Human cell cultures

2.4.1 Medium

Cells were cultured in Dulbecco's modified Eagle medium (DMEM) supplemented with10% FBS, 1 % L-Gutamin, 50 µg/ml penicillin, and 50 µg/ml streptomycin.

2.4.2 Cell lines

MCF10A is a non-transformed cell line derived from a human fibrocystic mammary tissue.

HEK293 is a transformed cell line derived from human embryonic kidney cells.

2.4.3 Immunostainings

Cells were cultured in 12-well plates on a 13mm sterile coverslip. Cells were fixed and stained according to the following protocol:

1. Rinse cells once with PBS
2. Fix with 4% paraformaldehyde in PBS for 10 minutes
3. Wash/permeabilise 3x 15 min in PBT (0.1% Triton in PBS)
4. Block 15 min in PBS + 5% BSA
5. Primary antibody incubation in PBS + 5% BSA, overnight at 4°C
6. Wash 3 x 15 min in PBT
7. Secondary antibody incubation in PBS + 5% BSA for 1-2 hours at room temperature
8. Wash 3 x 15 min in PBT with a 5 min DAPI staining between 2 washes
9. Seize the coverslip with forceps, gently dry the sides on a thin tissue, without touching the surface with the cells, and place the coverslip face down on a drop of Fluoromount G (Southern Biotechnology) on a slide.

2.5 Antibodies

Drosophila immunostainings:

Mouse anti-β-galactosidase (Promega) 1:500

Rabbit anti-β-galactosidase (Cappel) 1:200

Rabbit anti-Mask (Michael Simon) 1:500 (1:100 for intestine)

Rat anti-Yki 69 (Nic Tapon) 1:500 (1:100 for intestine)

Mouse anti-V5 1:100 (Abcam)

Rat anti-ELAV 1:300 (DHSB)

Human cells immunostainings:

Goat anti-Mask1/ANKHD1 (Santa-Cruz) 1:100

Mouse anti-Mask2/ANKRD17 (Sigma) 1:100

Goat anti-Mask2/ANKRD17 (Santa-Cruz) 1:100

Rabbit anti-YAP (Santa-Cruz) 1:200

Secondary antibodies:

Alexa-fluor secondary antibodies (Invitrogen) 1:500

The following antibodies were used in western blot analysis:

Rabbit anti-P^{S168}-Yki (N. Tapon) 1/1000

Rabbit anti-GFP (Torrey Pines) 1/5000

Rabbit anti-FLAG (Sigma) 1/250

Rabbit anti-Mask1/ANKHD1 (Sigma) 1:500

Rabbit anti-Mask2/ANKRD17 (Novus) 1: 2000

Mouse anti-Tubulin DM1A (Sigma) 1:1000

Rabbit anti-YAP (Santa-Cruz) 1:500

Mouse anti-Tubulin DM1A (Sigma) 1:1000

Secondary antibodies:

Anti-rabbit Peroxidase conjugated goat antibody (Thermo scientific) 1:10,000

Anti-mouse Peroxidase conjugated goat antibody (Thermo scientific) 1:10,000

2.6 Molecular biology

2.6.1 *Drosophila* genomic DNA preparation

One fly was ground with a pellet pestle in an eppendorf tube containing 40 µl of squishing buffer (10 mM Tris-HCl ; 1 mM EDTA ; 25 mM NaCl ; 200 g/ml Proteinase K freshly added). The mix was incubated at 37 °C for 30 min, then at 95 °C for 5 min to inactivate the proteinase K.

2.6.2 DNA ethanol precipitation

DNA precipitation of a DNA solution of a given volume was carried out according to the following protocol:

1. Add 1/10 volume of 3M Sodium Acetate (pH5.5) to the DNA solution
2. Add 3 volumes of ethanol (100%)
3. Mix briefly and incubate on dry ice for 5 min
4. Spin at 13 000 rpm for 10 min on a bench centrifuge (15.7 rcf)
5. Discard supernatant (carefully so that DNA pellet is undisturbed)
6. Wash pellet with 70% ethanol
7. Spin 5 min at 13 000 rpm
8. Carefully discard the supernatant without touching the pellet
9. Spin 2 min at 13 000
10. Remove as much as possible of the remaining ethanol using a fine tip and leave the tube open for 5-10 min to allow the pellet to dry
11. Resuspend the pellet in distilled water or buffer

2.6.3 Cloning of second Inverted Repeats for candidate gene validation

For each candidate gene, PCR primers were designed to amplify a 300 base pair region with no predicted off targets using E-RNAi application (Horn and Boutros, 2010). For a given candidate gene, 3 primers were used to carry out 2 PCRs on *Drosophila* genomic DNA:

1- forward primer (F): with a BglII restriction site added at the 5' end.

2- reverse primers: both primers have the same sequence but differ by the restriction sites added at their 5' end: XbaI (RX) and EcoRI (RE).

CG12818 second hairpin primers:

F: 5' GAGAGAAGATCTCCTTCAATACCCCACAAGGA 3'

RX: 5' GAGAGATCTAGACTAGAGCATATTTTGCTTTGCTAAC 3'

RE: 5' GAGAGAGAATTCCTAGAGCATATTTTGCTTTGCTAAC 3'

CG32133 second hairpin primers:

F: 5' GAGAGAAGATCTAAATGGCGTCCAGCACTC 3'

RX: 5' GAGAGATCTAGATTTCGTCCACCACGATTTTT 3'

RE: 5' GAGAGAGAATTCTTTCGTCCACCACGATTTTT 3'

Two PCR reactions were set up with the Invitrogen Taq polymerase using (i) the BglII forward primer and EcoRI reverse primer, and (ii) BglII forward primer and XbaI reverse primer. PCR products were purified, digested and ligated in a pMF3 vector. Because of the restriction sites design, the 2 PCR products are ligated in the vector as an inverted repeat (Fig 2.4).

Reaction:	Final concentration
Genomic DNA (100 ng)	
10x buffer (no Mg++)	1X
50mM $MgCl_2$	1.5 mM
10mM dNTPs (2.5mM each)	0.2 mM each
primers (10 µM each)	0.5 µM each
Taq DNA Polymerase (5u/ml)	0.025 U/µl
Distilled water	

PCR Programme (Bio-Rad DNA Engine):

94°C x 3 min

94°C x 30s, 55°C x 30s, 72°C x 1min – 40x cycles

72°C x 10 min

PCRs were checked on a 1% agarose gel and purified using the Qiaquick PCR purification kit. DNA concentrations were measured with a nanodrop.

Digests

1 µg of each PCR product was digested with BglII + EcoRI, or BglII + XbaI restrictions enzymes from NEB, according to manufacturer's instructions.

Vector Preparation

1 µg of pMF3 vector (pDG264) was digested with EcoRI and Xba I restriction enzyme, then treated with phosphatase (Roche CIP) and gel purified on a 1% agarose gel with the Qiaquick Gel Purification Kit (28704). The DNA was then concentrated by ethanol precipitation.

Ligation reaction

A ligation reaction was set up to clone the 2 digested PCR inserts into the digested vector:

10 ng Vector prep.

10 ng BglII-EcoRI insert

10 ng BglII-XbaI insert

T4 DNA ligase buffer(final concentration 1X)

0.4 U T4 DNA ligase (NEB, 400 U/ml)

Distilled Water

Incubate 16°C x 2h or overnight

5 µl from the ligation reaction were transformed into SURE cells (Stratagene 200238), following the manufacturer's instructions. Mini and Maxi DNA preps were carried out using QIAGEN kits. Presence of the constructs was tested by diagnostic digests and PCRs. Maxi-preps were sent to the BESTGENE company for microinjections and generation of transgenic *Drosophila* lines.

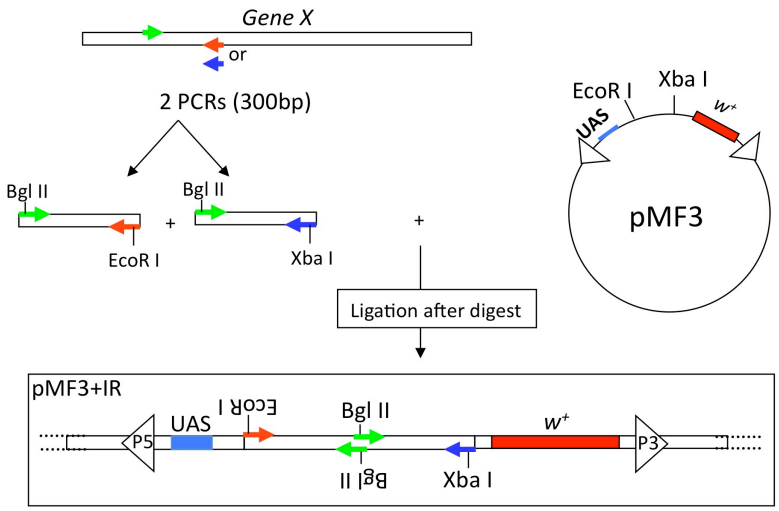

Figure 2.4: Second hairpin cloning schematics

2.6.4 *Drosophila* cDNA synthesis

RNA extraction was carried out using the QIAGEN RNeasy Protect Mini Kit: 30 flies were placed in an eppendorf tube on ice. 600 µl of Buffer RLT was added to the flies and they were finely grinded using a pellet pestle. The lysate was then centrifuged at full speed for 3 minutes and the supernatant was processed according to the kit's instructions. Residues of DNA were eliminated by DNAse treatment using the Promega RQ1 DNAse kit. cDNA synthesis was carried out using Stratagene First strand cDNA synthesis kit and oligo (dT) primers.

2.6.5 Cloning of Mask conserved domains

mask conserved domains were first amplified from a *Drosophila* cDNA pool using QIAGEN DNA polymerase (Finnzymes) and PCR products were cloned into a blunt TOPO vector (Invitrogen). The following pairs of primers were used for PCR amplification from cDNA:

ANKRI: 5' CCGAGGTGAGTTCCTTTCTCC 3' and 5' TTGACGCATCTGATTTGGACC 3';
ANKRII: 5' ACCAAACTCCATCTACAGCCTC 3' and 5' GTGCTGCTGTTTATGTTGCTCG 3' ;
ANKRII+KH,
5' ACCAAACTCCATCTACAGCCTC 3' and 5' CTTGATTAGTGCCAAAATGAGCATA 3'

DNA extractions were carried out using the QIAprep spin Miniprep Kit (QIAGEN). The cloned products were sequenced and one correct clone per construct was used for subsequent cloning with the Gateway system (Invitrogen).

Sequencing primers used to check **ANKRI:**

M13F: 5' GTTTTCCCAGTCACGACGTTGTA 3'

CS153R1: 5' CAAATGACCGGCGGATGCAG 3'

CS153F3: 5' GACATCGTCAAACTGCTGCTC 3'

CS165F: 5' CGGTCATCAGTCTGTGGTGG 3'

ANKRII:

CS160F: 5' CGATACGAGGTGGTGGAACT 3'

CS155R: 5' GATTACTGGTTGAGTTGGTTCCAC 3'

CS154EF: 5' GGTGTTGATATCGGTGGAACCAA 3'

CS157R2: 5' GT GCT GCT GTT TAT GTT GCT CG 3'

ANKRII+KH: M13F, CS160F, CS155R, CS154EF, CS157R2

The 3 sequenced constructs were used as a template for PCR using Phusion high fidelity DNA polymerase, according to the manufacter's instructions, with the following Gateway attB pairs of primers:

ANKRI:

5'-GGGGACAAGTTTGTACAAAAAAGCAGGCTATGCCCGAGGTG-3'

5'-GGGGACCACTTTGTACAAGAAAGCTGGGTGTTGACGCATCTGATTTGGACC-3'

ANKRII:

5'-GGGGACAAGTTTGTACAAAAAAGCAGGCTATGACCAAACTCCATCTACAGCCTC-3'

5'-GGGGACCACTTTGTACAAGAAAGCTGGGTGGGTGCTGCTGTTTATGTTGCTCG-3'

ANKRII+KH:

5'-GGGGACAAGTTTGTACAAAAAAGCAGGCTATGACCAAACTCCATCTACAGCCTC-3'

5'-GGGGACCACTTTGTACAAGAAAGCTGGGTGCTTGATTAGTGCCAAAATGAGCATA-3'

attB PCRs products were cloned by BP recombination into a Gateway entry vector (p-ENTR) and the sequenced ORFs were transferred by LR recombination from the entry vector into the gateway expression vector pAWF (ampicillin resistant) for expression of the peptides fused to a triple FLAG affinity tag at the C terminus, following the manufacturer's instructions.

2.6.6 Co-immunoprecipitation (Co-IP) assay

S2 cells were plated in 6 well plates at a density of 2.10^6 cells/well (1,5 mL medium/well) and transfected with 200 ng of each construct, and harvested 48h later. Materials used for the Co-IP include:

Flag M2 resin (Sigma, A2220)

Lysis buffer:	Final concentration
1M Tris pH7.5	50 mM
5M NaCl	150 mM
Triton-X100 (or 25 ml 10% Triton-X)	1 %
0.5M EGTA	1 mM

Complete tablet, Mini, EDTA-free, Roche (use 1 tablet for 10 mL buffer)
PhosSTOP phosphatase Inhibitor Cocktail, Roche (use 1 tablet for 10 mL buffer)
PMSF (100 mM in isopropanol, stored at -20°C): use 10 µl/ml

IP buffer preparation: Before starting the procedure, IP buffer was prepared as follows and kept on ice:
For 10 mL of Lysis buffer were added 1 tablet of Complete proteases inhibitor, 1 tablet of PhosSTOP phosphatase inhibitor, and 100 µl of PMSF.

Protein extraction: 48 h after transfection, S2 cells were detached from the well by pipetting up and down. The cell suspension was transfered into an eppendorf tube and spinned down at 3000 rpm for 2 mins at 4°C in a cold centrifuge (Heraeus Biofuge fresco).
Samples were then processed according to the following steps:

- Wash 1x in ice cold PBS, spin down again at 3000 rpm for 2 mins at 4°C.
- Add 500 µl of ice cold lysis buffer to the cell pellet, incubate 10 mins on ice.
- Spin down at 13000 rpm for 10 mins at 4°C to remove cell debris.
- Transfer supernatant to a new eppendorf. Keep 50 µl as an input control and use the rest (roughly 450 µl) for the immunoprecipitation.

For the rest of the procedure, tubes were maintained on ice and subsequent incubations and washes were carried out in a cold room (4°C).

Protein beads preparation: M2 anti-Flag coupled beads are stored in a glycerol solution and must be washed 4 or 5 times in IP buffer prior to IP. In between washes, beads are centrifuged for 1 min at 2000 rpm in a cold centrifuge.

Immunoprecipitation:

1. Add 40 µl of beads to each sample
2. Incubate at 4°C for 2 hours on a rotating wheel.
3. Wash 3-4x (5 mins on rotating wheel) in 500 µl freshly prepared IP buffer containing the protease and phosphatase inhibitors. For washing steps, spin down at 1000 rpm for 1 min using bench centrifuge (0.1 rcf).
4. After last wash, remove most of the IP buffer, leaving about 15 µl.
5. Add 4 µl reducing agent (10x, NuPAGE) and 15 µl LDS sample buffer (4x, NuPAGE) to each sample and proceed to Western blot analysis (Alternatively, add only the sample buffer and store the samples at -20°C, add the reducing agent later, prior to Western blot analysis).

2.6.7 Larvae preparation for western blot analysis

Larvae (between 10 and 30) were placed in an eppendorf containing 90 µl of LDS sample buffer (NuPAGE) and 10 µl reducing agent, and were finely ground with a pellet pestle. Samples were heated at 70°C for 10 min to denature the proteins and centrifuged for 5 min at maximum speed using a bench centrifuge (15.7 rcf). The supernatant was then used for Western blot analysis.

2.6.8 Western blot analysis

Using Invitrogen NuPage® electrophoresis system

Reagents (denaturing electrophoresis)

NuPAGE® LDS Sample Buffer (4X)

NuPAGE® REDUCING AGENT (10X)

Buffers:

TBS (Tris-buffered saline): NaCl 8g, KCl 0.2g, Tris base 3g, in 800ml distilled water, adjust pH to 8.0 with 1M HCl, adjust volume to 1000ml, sterilise by autoclaving.

TBST (Tris-buffered saline with Tween): TBS + 0.1% Tween

LDS sample buffer and reducing agent were added to the sample and the mix was heated for 10 minutes at 70 °C in a heat block. Samples were then resolved on 10% Bis-Tris polyacrylamide or 3-8% Tris-Acetate or 4-12% Bis-Tris precast polyacrylamide

gradient gels (NuPAGE). Protein sizes were marked using the Rainbow molecular weight marker (Amersham).

Proteins were subsequently transferred to a nitrocellulose membrane using the iBlot system (Invitrogen). After transfer, membranes were processed according to the following protocol (incubations on a rotating table):

1. Block for 1 hour in block solution (TBST+5% dried milk powder)
2. Incubation in primary antibody at the appropriate dilution in block solution for 2 hrs at room temperature or overnight at 4°C followed by 3 brief rinses and 3x 5 min washes in TBST.
3. Secondary antibody incubation (1/10 000 dilution) in block solution for 1 hr at room temperature followed by 3 brief rinses and 3x 5 min washes in TBST.
4. Incubation with Super Signal West Pico Chemiluminescent Substrate (Pierce), according to the manufacturer's instructions.

Reblot

Blots were stripped and rebloted using the Millipore re-blot kit.

2.6.9 Luciferase assay in human cells

siRNAs

3 different pools of siRNAs were used at a final concentration of 300 nM (75nM of each individual siRNA):

ON-TARGETplus Set of 4 Mask1/ANKHD1 (Dharmacon)

ON-TARGETplus Set of 4 Mask2/ANKRD17(Dharmacon)

ON-TARGETplus Non targeting pool (Dharmacon)

The luciferase assay was performed in sextuplicates in a 96 well plate. 48 hours after transfection, cells were lysed and tested for Luciferase and Renilla activity using the Dual-luciferase reporter assay system kit (Promega) and a luminometer.

The night before transfection, HEK293T cells were plated in a white 96 well plate (BD falcon 353288) at a density of 15.000 cells/well, and a volume of 100 µl/well. Antibiotic-free growth medium was used to avoid cell lethality because of toxicity enhancement between antibiotics and Lipofectamine.

Cells were transfected using the Lipofectamine 2000 reagent (Invitrogen) with siRNAs and 20 ng of each DNA plasmid (pCMV-Flat YAP2 5SA, pCMX-GAL4 TEAD4 and UAS.Luciferase) per well (with the exception of the pRL-TK *Renilla* vector: 3ng per well) with the following protocol:

1. Set up a DNA/siRNA mix and a Lipofectamine mix:

- DNA/RNA mix: plasmids and siRNA were mixed with optiMEM medium (Invitrogen) in a final volume of 30 µl/well

- Lipofectamine mix: 0,2 µl Lipofectamine + 30 µl OptiMEM/well

vortex 5s, incubate 5min (max=25 min)

2. Add the Lipofectamine/OptiMEM mix to the DNA/RNA-Mix, vortex and incubate 20 min at RT.

3. Remove medium from the cell culture plate down to 30 µl growth medium per well

4. Apply the 60 µl LF/DNA complexes to the wells. (Volume=90 µl /well)

5. Incubate cells at 37°C for 48 hrs

Cell Lysis

Remove medium and apply 25 µl of Passive Lysis Buffer (Promega); incubate at RT for 15 to 20 min on a rocking platform (250 rpm). *(Cells can be frozen after that step and luciferase assay performed later)*

Luciferase assay (using the Promega dual Luciferase kit)

1. Add Fluc Buffer, 28 µl/well, incubate 2-3 min, read the plate
2. Add Rluc buffer, 28 µl/well, incubate 2-3 min, read the plate

Chapter 3. An in vivo RNAi screen for novel growth regulators

The control of tissue growth during development is essential to generate organs of the correct size and shape. Although genetic pathways involved in this process have been uncovered, how organs reach their final size and their correct proportions is still poorly understood. With the development of RNA interference (RNAi) as a tool to systematically knock-down genes from sequenced genomes, reverse genetics have proven to be a very efficient strategy to identify novel genes involved in cellular processes (Mohr et al., 2010). Until recently, genomic RNAi screens in *Drosophila* were limited to cell culture, and had not been used to study developmental processes. The creation of a *Drosophila* transgenic RNAi library (Dietzl et al., 2007) has extended the use of this technique, allowing tissue specific knock-down of any known or predicted *Drosophila* gene. Making use of this newly available tool, an in vivo RNAi screen was carried out in the laboratory in order to find new players in the regulation of organ size. My PhD project was to validate candidates from the screen and to focus on one for characterisation.

3.1 The screen

3.1.1 Principle

The screen was carried out using a collection of transgenic *Drosophila* lines from the VDRC library (Dietzl et al., 2007). Each transgenic line contains a fragment of 300 base pairs from a given gene *X* cloned as an inverted repeat. This inverted repeat *X-IR* is under the control of the *UAS* promoter, which can be activated by the yeast GAL4 transcription factor. Expression of *X-IR* leads to the production of RNA hairpins that are recognised and degraded by the cell RNA interference machinery (Fig 3.1). The small interfering RNAs (siRNAs) produced target the RNA Induced Silencing Complex (RISC) to complementary *X* mRNA, thereby triggering *X* mRNA degradation (Fig 3.1). In total, 11,512 *UAS.IR* lines, targeting a subset of *Drosophila* genes conserved in human, were crossed individually to a *hedgehog.GAL4* line, so that progeny expressed the transgene throughout development in the posterior compartment of the wing (Fig 3.1). To avoid

losing progeny due to increased apoptosis, an inhibitor of apoptosis (DIAP1) was co-expressed with the transgenes. Progeny was then screened for differences in wing size compared to a control. This work was carried out by B. J. Thompson. As the *UAS.IR* transgene is specifically expressed in the posterior compartment, it does not affect the anterior compartment of the wing, which can therefore be used as an internal control for size.

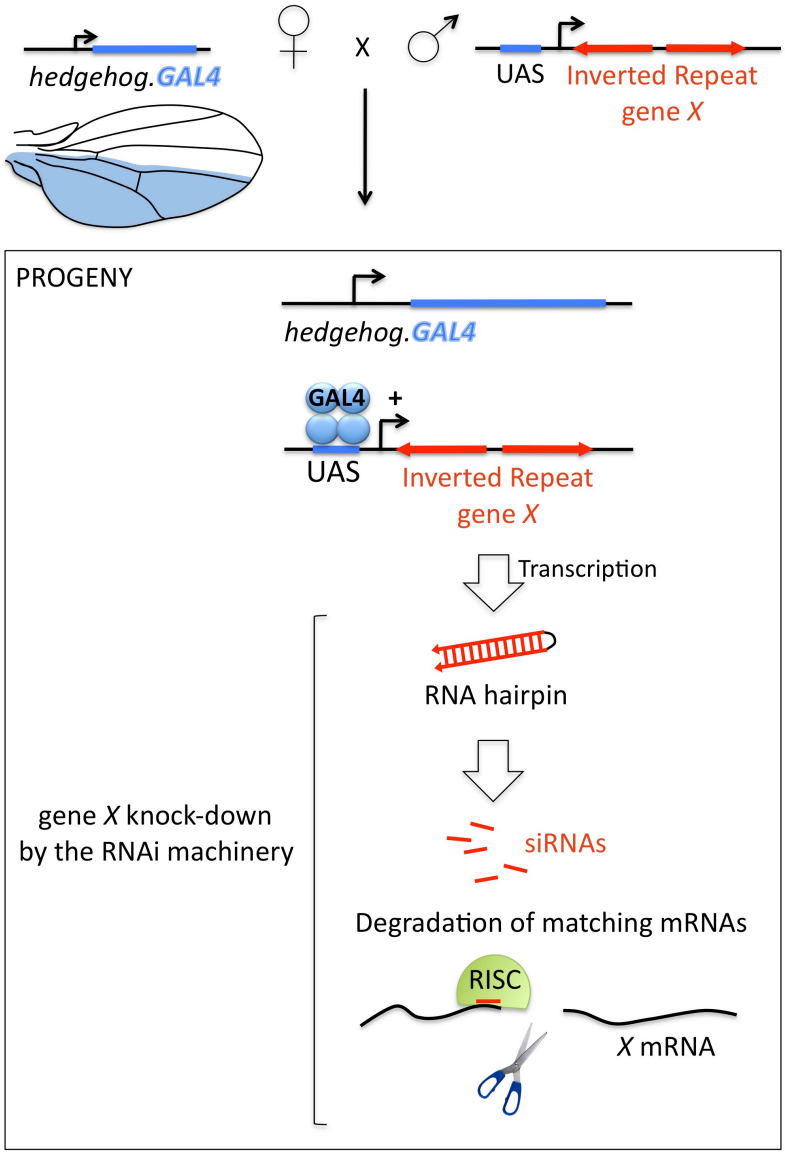

Figure 3.1: Principle of the screen
GAL4 expression (in blue) is driven by the *hedgehog* promoter in the posterior compartment of the wing. GAL4-induced-expression of an inverted repeat from gene *X* triggers degradation of *X mRNA* by RNA interference.

3.1.2 Results

Phenotypes were classified in different categories according to their effects on tissue size and cell size. In addition, the *Drosophila* wing is an excellent model to detect morphology and patterning defects such as wing hair mis-orientation, shape defects, vein defects, or wing margin defects, allowing the association of candidate genes with signaling pathways known to cause these phenotypes (Pearson et al, in preparation). I am not going to detail these classes of phenotypes, as my project focus was on the growth phenotypes categories. Of the 11512 lines screened, 8108 lines (70.4%) produced no observable phenotype and 1406 (12.2%) lines produced viable flies with phenotypes. Despite the co-expression of DIAP1, 17.4% of *UAS.IR* transgenes caused lethality prior to eclosion (1998 lines). The screen efficiency was estimated by looking at the recovery rate of genes from the Insulin signaling pathway: approximately half of the known pathway components were recovered in the screen. Thus, by extrapolation, approximately half the *UAS.IR* transgenes from the VDRC library trigger a sufficient gene silencing to generate a phenotype.

Undergrowth phenotypes

RNAi knock down of genes promoting cell cycle progression, such as *cdc25/string*, lead to an undergrowth phenotype accompanied by an increase in cell size, apparent by the reduced density of wing hairs, as each wing cell produces a single hair (Fig 3.2 A). This increase in cell size is due to the fact that the cell cycle is slowed down but the rate of cell growth is not affected [(Neufeld et al., 1998), Chapter 1]. Therefore, cells grow at the same rate but for longer periods between divisions. In this category, a number of known cell cycle regulator were recovered as well as some novel genes.

By contrast, downregulation of cell growth promoting genes, such as the Insulin pathway component *akt*, leads to an undergrowth phenotype accompanied by a reduction in cell size, apparent by an increase in wing hair density (Fig 3.2 A). In this category were recovered members of the Insulin/TOR pathway, ribosomal proteins, general transcription and translation factors, other essential genes such as mitochondrial genes, and a number of novel genes.

Genes promoting cell proliferation control both cell growth and cell cycle progression. Hence, downregulation of genes promoting cell proliferation lead to tissue undergrowth without strong effects on cell size (Fig 3.2 B). In this category were recovered *ajuba* and *zyxin*, from the Hippo signaling pathway, as well as components of the Ras signaling pathway, such as *raf* and *sos*, that presented vein loss in addition to their undergrowth phenotype, consistent with the role of Ras signaling in regulating both cell proliferation and vein patterning in the wing. Yki was not recovered in this category, as expression of *yki-IR* in the wing was lethal. In addition, a number of novel genes were identified.

Overgrowth phenotypes

Several genes producing overgrowth phenotypes were uncovered in the screen. Among those are known members of growth control signaling pathways such as the Hippo pathway, the Ras pathway, the Insulin/TOR pathway, as well as some apico-basal polarity proteins such as Crumbs and a number of novel genes (Fig 3.2 C). Apart from genes from the Insulin/TOR pathway, most lines in this category did not significantly alter hair density.

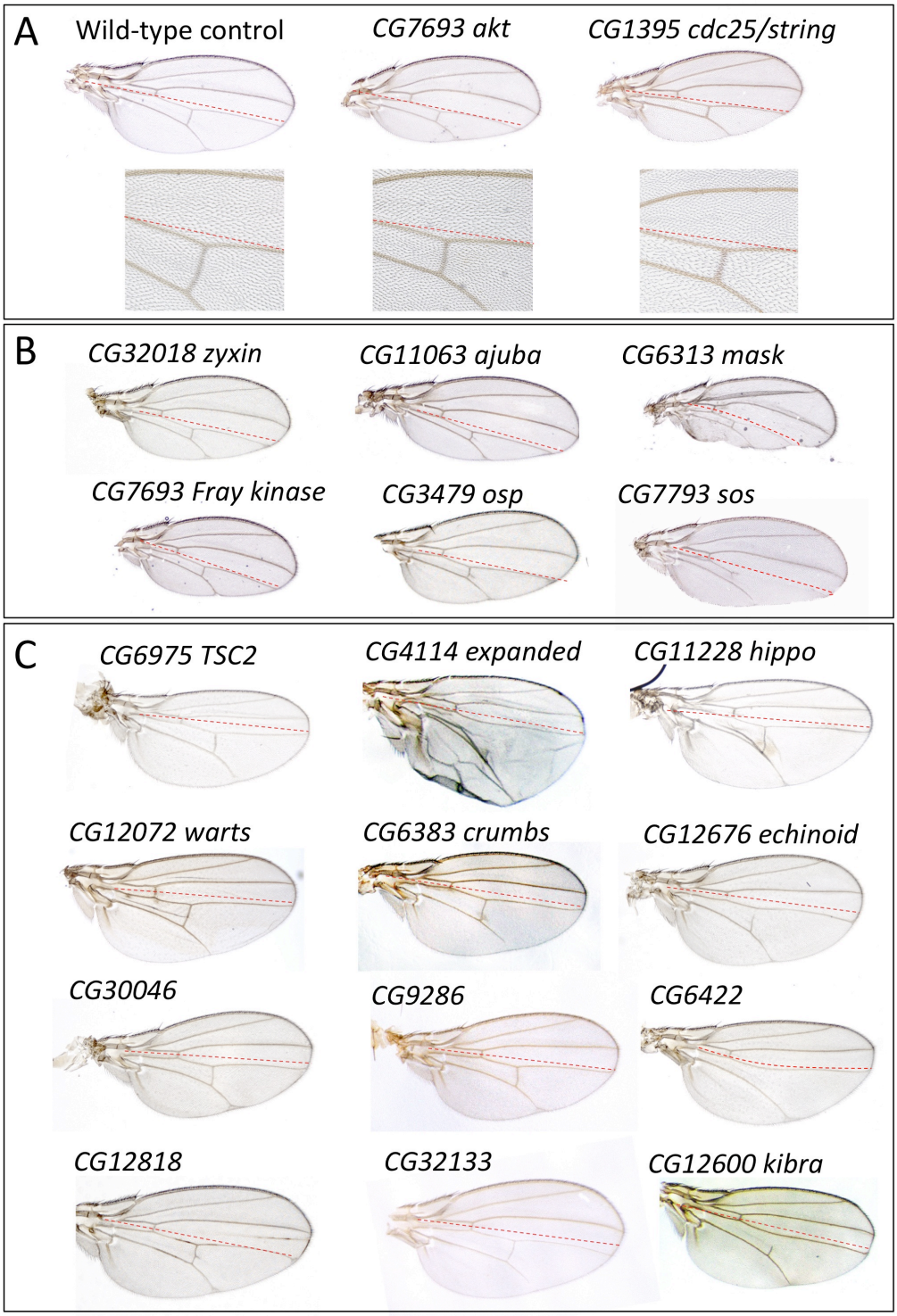

Figure 3.2: Growth phenotypes from the screen
Transgenic RNAi lines are expressed in the posterior compartment of the wing with the hh.GAL4 driver. (A) Undergrowth phenotypes strongly affecting cell size: knock-down of the Insulin pathway component *akt* results in an undergrowth phenotype accompanied by a reduction in cell size that can be observed from the higher density of wing hairs. Knock-down of the cell cycle regulator cdc25 results in an undergrowth phenotype accompanied by an increase in cell size that can be observed from the lower density of wing hairs. (B) undergrowth phenotypes of genes affecting cell proliferation. (C) Overgrowth phenotypes.

3.2 A systematic approach to validate the candidate genes identified in the screen

3.2.1 Strategy of validation

One possible source of false-positive artefacts in the screen is the off-targeting effect of siRNAs. Indeed, although transgenes were specifically designed to avoid non-specific gene targeting, some siRNAs may present complementarities with more mRNAs than the one they were designed to target. In order to rule out this artefact, we validated screen hits by testing second *UAS.IR* lines, targeting a different sequence of the candidate gene than the one targeted by the first hairpin. When they were available, we used RNAi lines from the NIG-FLY library, an independent library of transgenic RNAi lines (http://www.shigen.nig.ac.jp/fly/nigfly/; Table 1). We also generated second *UAS.IR* lines for some of the interesting candidates when they were not available from NIG-FLY.

3.2.2 Results

We started by testing candidates from the overgrowth phenotype category. A total of 12 novel genes were tested. 6 genes had multiple *UAS.IR* transgenic lines available from NIG-FLY (Table 1). For the 6 remaining genes, we cloned inverted-repeat constructs and generated transgenic *UAS.IR* lines. 2nd hairpins for CG6422, CG30046, CG9286 and CG33967 were cloned by Ruth Brain, while 2nd hairpins for CG32133 and CG12818 were cloned by myself. Transgenic lines were individually crossed to the *hh.GAL4* driver line and the progeny was screened for overgrowth phenotypes. Among the 12 overgrowth phenotype candidates tested, only 1 was confirmed by the second hairpin: CG33967 or Kibra, which was subsequently characterised by A. Genevet in a collaboration with the Tapon laboratory (Genevet et al., 2010). This rate of validation appears much lower than expected and remained unexplained until Ruth Brain investigated the genomic location of *UAS.IR* transgene insertions by inverse PCR and found that more than 50% of overgrowth phenotype were associated with insertions of the *UAS.IR* transgenes near the *miR278* locus, a micro RNA known to cause overproliferation when mis-expressed (Nairz et al., 2006), indicating that the UAS promoter is able to activate *miR278* when it is inserted nearby. CG6422, CG30046 and CG9286 phenotypes were due to this mis-expression artefact.

In the undergrowth category, candidates were selected according to their conserved domains and predicted functions, to avoid selecting housekeeping genes whose downregulation causes growth defects due to lower cell survival rather than specific mis-regulation of tissue growth. 32 of the selected genes had multiple available *UAS.IR* lines in the NIG-FLY library and were therefore tested with the *hh.GAL4* driver (Table1 ; a detailed list with the individual transgenic lines ID and phenotypes can be found in Appendix, Table 2). The rate of confirmation was much higher than in the overgrowth category. Undergrowth phenotypes of 17 out of the 32 selected genes were confirmed by expression of the second *UAS.IR* line (Table 1; Fig 3.3). 2 of them were lethal, so their growth phenotype could not be investigated. One of the candidate genes confirmed by a strong undergrowth phenotype with the second hairpin is the *mask* gene, which characterisation will be described in the next chapters. We chose this gene for its very strong and specific effect on tissue size without effects on patterning, a phenotype similar to that of Hippo signaling components such as *zyxin* and *ajuba*.

3.2.3 Conclusions

Following the finding that, in addition to the off-target effect, false-positives could be generated by mis-expression of genes neighbouring the *UAS.IR* transgene, validation of hits by a second independent *UAS.IR* line appears crucial. This strategy of validation has allowed confirmation of phenotypes for about half of the candidates tested. One of them, the *mask* gene, presented a particularly striking tissue size reduction without effects on tissue patterning, a phenotype similar to that of Hippo signaling negative regulators recovered in the screen. I chose to focus on that gene for further characterisation.

In 2009, a second generation library (KK library) was constructed by the VDRC using an engineered transgene landing site inserted on chromosome 2, carefully chosen to guarantee an optimal level of *UAS.IR* transgene expression upon GAL4 induction. Thus, all transgenes from the new library are inserted in the same unique genomic site and are expressed at the same level, thereby limiting the number of false-positive hits, by preventing mis-expression artefacts, and false-negatives, by ensuring optimised levels of *UAS.IR* transgene expression. In order to consolidate results from the first screen, the screen was repeated with all available KK library transgenic lines targeting

conserved genes (5802 lines). This second screen has allowed the identification of novel growth regulators with a high degree of confidence (Pearson et al, manuscript in preparation).

CG number	gene	# of NIG-FLY RNAi lines tested	x *hh.gal4*: PHENOTYPES
OVERGROWTH CATEGORY			
CG17245	PlexinB	6	5: no phenotype, 1: lethal
CG17342	Lk6 receptor kinase	2	no phenotype
CG14023		2	no phenotype
CG11567	cyp450	2	no phenotype
CG30078	(novel kinase)	1	no phenotype
CG1216	mrityu	2	no phenotype
UNDERGROWTH CATEGORY			
CG12217	PpV	2	1 line semi-lethal, undergrowth, blisters; 1 line lethal
CG10289	SAP	2	no phenotype
CG12139	LRP	2	undergrowth
CG7225	Wbl	2	no phenotype
CG6963	Casein kinase	2	undergrowth
CG6355	fab1	1	pigmentation defect?
CG3479	osp (PH)	2	undergrowth
CG5003		2	folded wings, crossvein defects semi lethal, folded wings, undergrowth
CG4792		1	no phenotype
CG7693	Fray	2	no phenotype ; mild undergrowth
CG18671	Mask	4	lethal, semi-lethal, undergrowth
CG17293	(wd40 domain)	1	undergrowth
CG9063		2	no phenotype ; lethal
CG17599		2	no phenotype
CG32018	zyx102F	2	Undergrowth
CG3825	PP1 15A	2	mild undergrowth ; undergrowth, rounded
CG9732	midnolin	1	mild undergrowth, few blisters
CG7111	rack1	2	undergrowth
CG32685	zap3	1	undergrowth
CG11722	(novel kinase)	2	undergrowth
CG10579	Pftaire	2	shape defects
CG11137		2	semilethal, undergrowth
CG8721	Odc1	2	no phenotype
CG18005		2	lethal
CG13139	Lix1	2	shape defects
CG11006	mucin	2	undergrowth, a few nicks
CG15143		2	no phenotype
CG7085		1	no phenotype
CG11130		2	lethal
CG2736		2	no phenotype
CG30092	jbug	2	undergrowth
CG30334		2	no phenotype

Table 1: List of candidate genes tested for validation with 2nd hairpin lines from the NIG-fly library
Validated candidates are highlighted in yellow, lethal phenotypes are highlighted in grey.

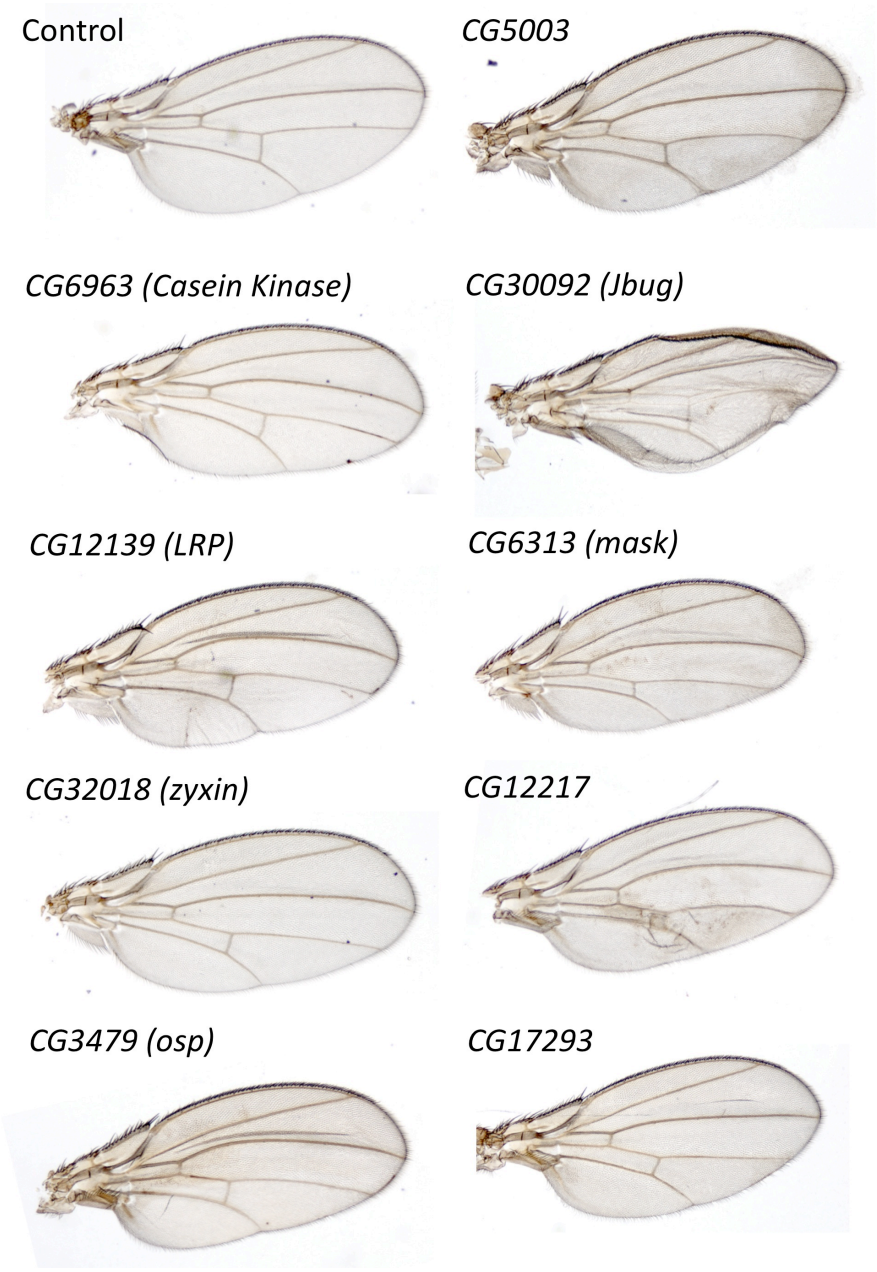

Figure 3.3: Validated candidate genes from the screen
2nd hairpins are expressed in the posterior compartment under the control of the *hh.GAL4* driver.

Chapter 4. Identification of *Drosophila* Mask as an essential co-factor of Yki in the Hippo signaling pathway

4.1 Identification of Mask as an essential regulator of growth

4.1.1 *Mask*: Multiple Ankyrin and Single KH domain protein

One of the candidate genes uncovered in the screen is the *mask* gene (*CG6313*). Expression of *mask-IR* in the whole wing (with the *MS1096.GAL4* driver) or in the eye (with the *ey.GAL4, GMR.GAL4* driver) causes a strong undergrowth phenotype compared to control (Fig 4.1). *mask* is an essential gene encoding a large protein of 4001 amino acids, which is composed of two blocks of ankyrin repeats and a single KH domain (Fig 4.2). Ankyrin repeats are motifs of 33 amino acids repeated from 2 to 24 times. In the case of Mask, the first block of ankyrin repeats contains 15 repeats, and the second block contains 10 repeats. These motifs are known to mediate protein-protein interactions but do not bind to a consensus protein sequence. They are present in a large number of proteins, involved in a variety of processes, including cyclin dependent kinase inhibitors, transcriptional regulators, cytoskeletal organizers and developmental regulators (Michaely and Bennett, 1992). The KH domain is a nucleic acid binding domain that can bind to RNA or single stranded DNA and is found in various proteins including RNA splicing factors, translational and transcriptional regulators (reviewed by (Valverde et al., 2008)). Mask sequence also contains 2 putative coiled-coil regions, a predicted nuclear export signal (NES) and a predicted nuclear localisation signal (NLS). Mask protein is well conserved among metazoans and it has 2 homologues in human that I will describe in Chapter 5: ANKHD1, which I will refer to as Mask1, and ANKRD17, which I will refer to as Mask2. Despite a low conservation in some regions of the protein, the ankyrin repeat blocks and the KH domain, as well as the predicted NES and NLS, are highly conserved (Fig 4.2).

Drosophila mask was originally identified in a modifier screen for new components of receptor tyrosine kinase signaling. It was found to genetically interact with the protein tyrosine phosphatase Corkscrew (Csw) (Smith et al., 2002). Csw participates in

signaling by the Receptor tyrosine kinases (RTKs) Torso, Sevenless (Sev) and *Drosophila* Epidermal growth factor Receptor (EGFR) (Allard et al., 1996; Herbst et al., 1996; Perkins et al., 1992) (Perkins et al., 1996). RTKs transduce signals through a common set of signaling molecules that lead to the activation of the Ras/MAPK pathway. Although its exact role is not clear, Csw binds to RTKs through scaffolding proteins and is required for RTK signaling and MAPK activation. In the wing, mutation of *csw* causes undergrowth and partial vein loss (Perkins et al., 1996). Furthermore, expression of a dominant negative form of Csw in the eye causes strong undergrowth and loss of photoreceptors R3, R4 and R7 (Allard et al., 1996). These effects on growth and patterning are characteristic phenotypes of genes affecting Receptor Tyrosine kinase signaling: patterning of the wing veins is also dependent on EGFR signaling (Martín-Blanco et al., 1999) and photoreceptor specification relies on EGFR and Sev signaling (Doroquez and Rebay, 2006; Freeman, 1996; Hafen et al., 1987). Smith *et al*. found that in the eye, mutation of one copy of *mask* enhances the undergrowth and loss of photoreceptor phenotype induced by the expression of a dominant negative form of Corkscrew (csw^{cs}). *Mask* mutants are also able to suppress the ectopic R7 photoreceptor phenotype induced by hyper-activation of Sev, Csw, or Ras. However, loss of *mask* does not affect MAPK activation, indicating that Mask acts either downstream of MAPK signaling, or in parallel.

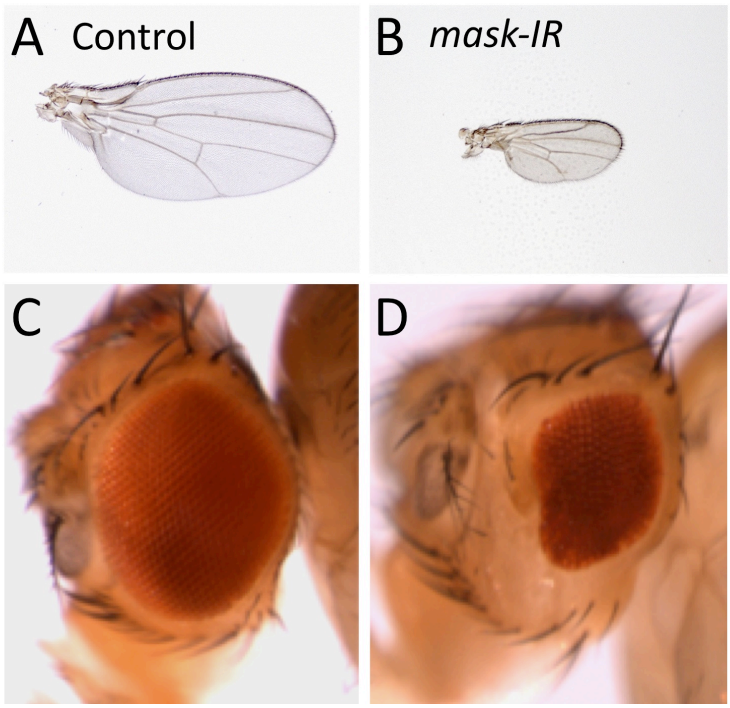

Figure 4.1: *mask* RNAi causes tissue undergrowth in the wing and in the eye.
(A) Wild-type adult *Drosphila* wing.
(B) RNAi knockdown of the *mask* gene during wing development results in an abnormally small wing.
(C) Wild-type adult *Drosophila* eye.
(D) RNAi knockdown of the *mask* gene during eye development results in an abnormally small eye.

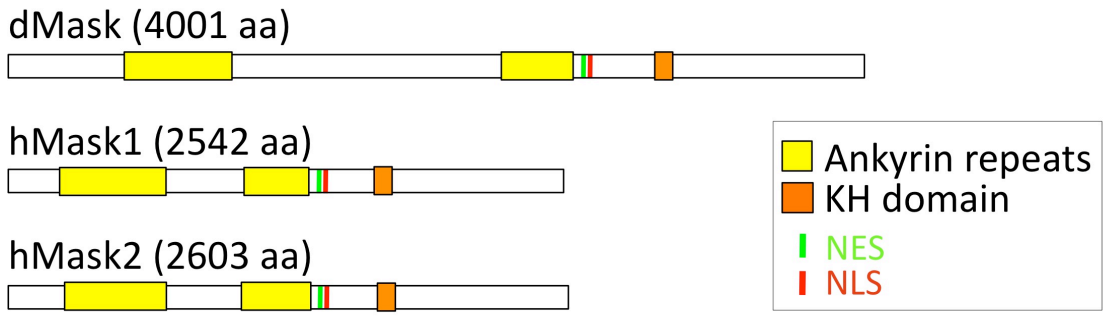

Figure 4.2: Mask protein is conserved in humans
Drosophila Mask, human Mask1 and human Mask2 schematic representation.

4.1.2 Mask is essential for tissue growth in *Drosophila*

We further analysed *mask* phenotype by making use of the embryonic lethal *mask*$^{10.22}$ mutant allele generated by Smith et al., which contains a nonsense mutation and produces a protein truncated of 80% of its sequence (Smith et al., 2002). The *ey.flp FRT Minute* system was used to generate *mask*$^{10.22}$ homozygous mutant eyes. *mask*$^{10.22}$ homozygous mutant clones of cells carrying a wild-type *Minute* allele, marked by the absence of a *white*$^{+}$ marker, were generated in a tissue heterozygous mutant for the homozygous lethal *Minute* gene, marked by the presence of a *w*$^{+}$ marker. *Minute* mutant cells are outcompeted by cells carrying the wild type Minute allele, resulting in an eye mostly composed of non-pigmented *mask*$^{10.22}$ homozygous mutant cells. This was confirmed by the small number of ommatidia expressing the *w*$^{+}$ marker (Fig 4.3 A-B'). *mask*$^{10.22}$ mutant eyes were much smaller than controls (Fig 4.3 A-B'), similar to *mask-IR* eyes, indicating that the RNAi line strongly down-regulates *mask*. We also generated *mask*$^{10.22}$ mutant clones in the developing larval wing imaginal disc using the *FLP/FRT* system. This genetic tool allows the generation of a homozygous mutant clone of cells marked by the absence of GFP, and a twin clone of wild type cells (or twin-spot) expressing a double dose of GFP, in a heterozygous mutant tissue expressing GFP. *mask*$^{10.22}$ mutant clones proliferated poorly, growing to only 10% of the size of their wild type twin-spots (Fig 4.3 C-E).

In order to investigate the effect of Mask over-expression, we used the P-element *P{EPgy2}EY01848*. This transposon is inserted 0.8 kb before the *mask* start codon and contains a *UAS* sequence in the same orientation as the *mask* gene. To test this insertion we used a Mask antibody from M. Simon (Smith et al., 2002). The specificity of Mask antibody was verified by immunostainings in wing discs containing *mask*$^{10.22}$ mutant clones. Although some mild background noise could be detected, the antibody staining was mostly lost in the mutant clones compared to the surrounding wild type tissue (Fig 4.4). When crossed to the *hh.GAL4* driver, *P{EPgy2}EY01848* was able to drive the over-expression of Mask in the wing disc, detected by an increase in Mask antibody staining in the posterior compartment (Fig 4.5 A,B). In some rare cases adult wings presented nicks in the posterior wing margin but in most cases growth of the wing was not affected (Fig 4.5 C,D). The lack of phenotype could be due to the fact that EP lines usually do not strongly activate gene expression. Expression of a *mask*

transgenic construct under the control of a *UAS* promoter may cause a more obvious phenotype. To date, *mask* gene has not been cloned due to its large size. These data show that *mask* is essential for cell proliferation and tissue growth but its overexpression does not seem to be sufficient to induce tissue overgrowth.

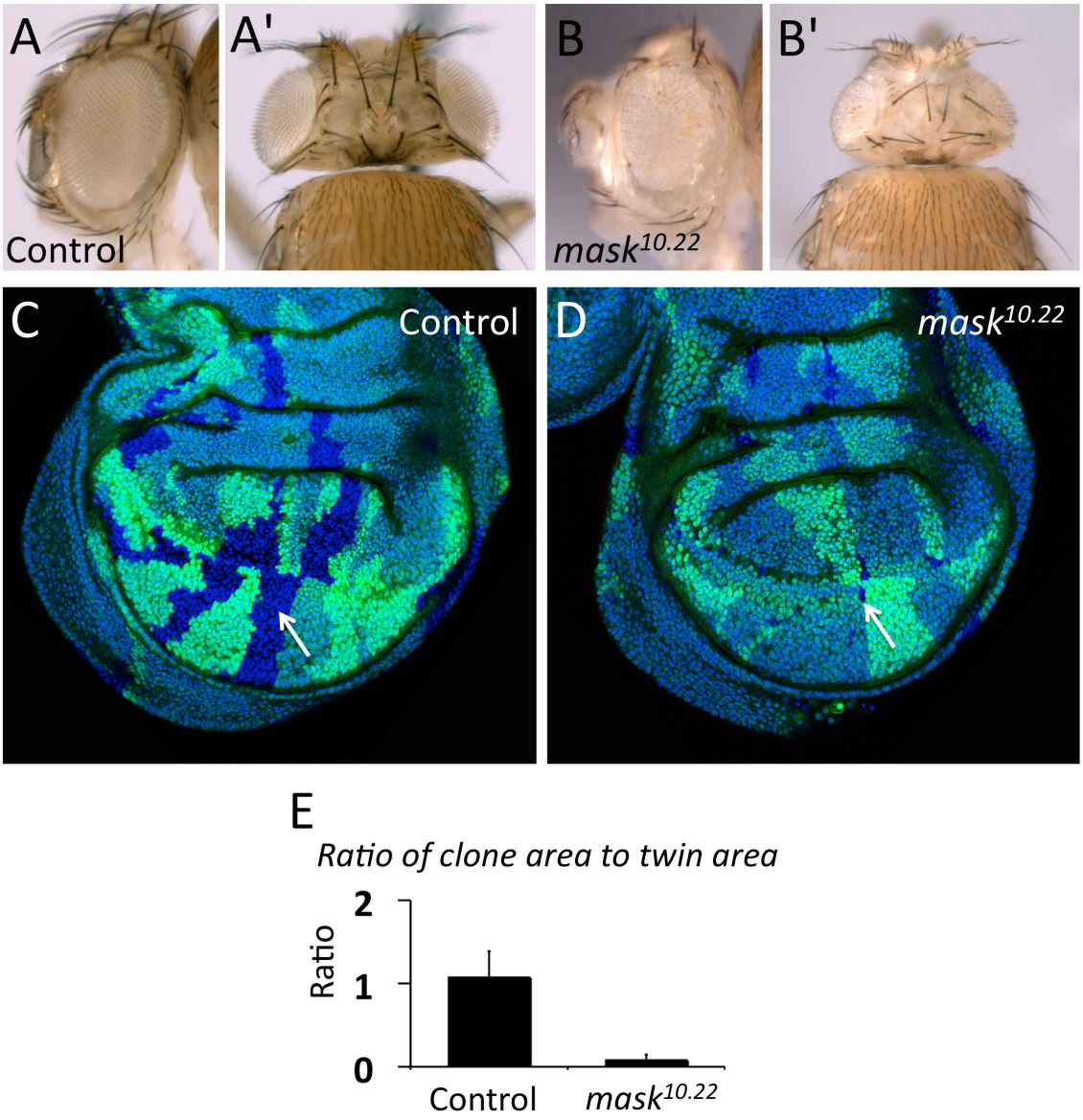

Figure 4.3: *mask* mutant confirms *mask* RNAi phenotype
(A) Control (*white*) adult eye. Top view in (A').
(B) A *mask*$^{10.22}$ homozygous mutant eye generated with the *eyFlp Minute* sytem is small and rough. Top view in (B').
(C-E) Third instar wing imaginal discs containing mitotic recombination clones. Clones were induced by heat shocking larvae at 84 hr (± 12 hr) of development.
(C) Third instar wing imaginal disc containing control (GFP negative) mitotic recombination clones and sister twin-spot clones (2x GFP) of similar size. DAPI (blue) marks nuclei.
(D) Third instar wing imaginal disc containing *mask*$^{10.22}$ homozygous mutant clones (GFP negative) that are drastically smaller than their sister twin spots (2x GFP). DAPI (blue) marks nuclei.
(E) Quantification of the ratio between clone and twin sizes in (C) and (D).

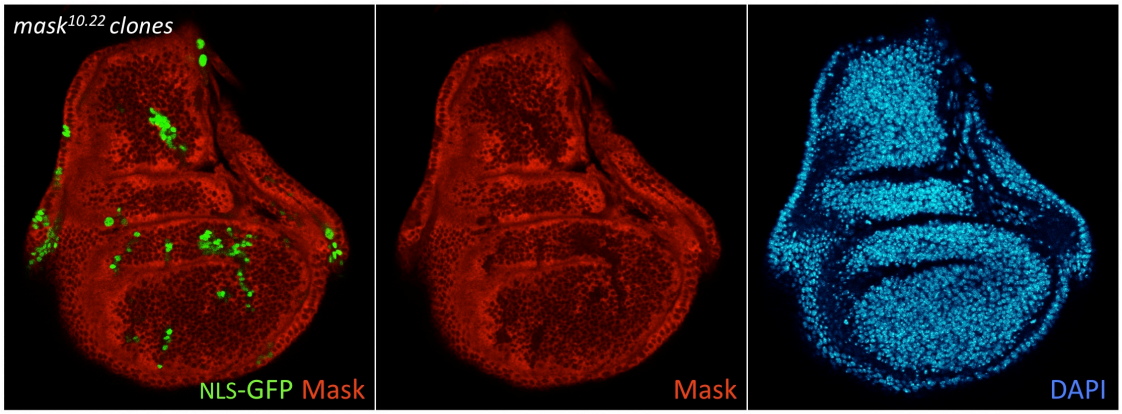

Figure 4.4: Mask antibody staining is lost in *mask*$^{10.22}$ mutant clones
Third instar wing imaginal disc stained with Mask antibody (red). *mask*$^{10.22}$ mutant clones were generated using the MARCM system and are marked by the expression of NLS-GFP (green). DAPI stains nuclei (blue).

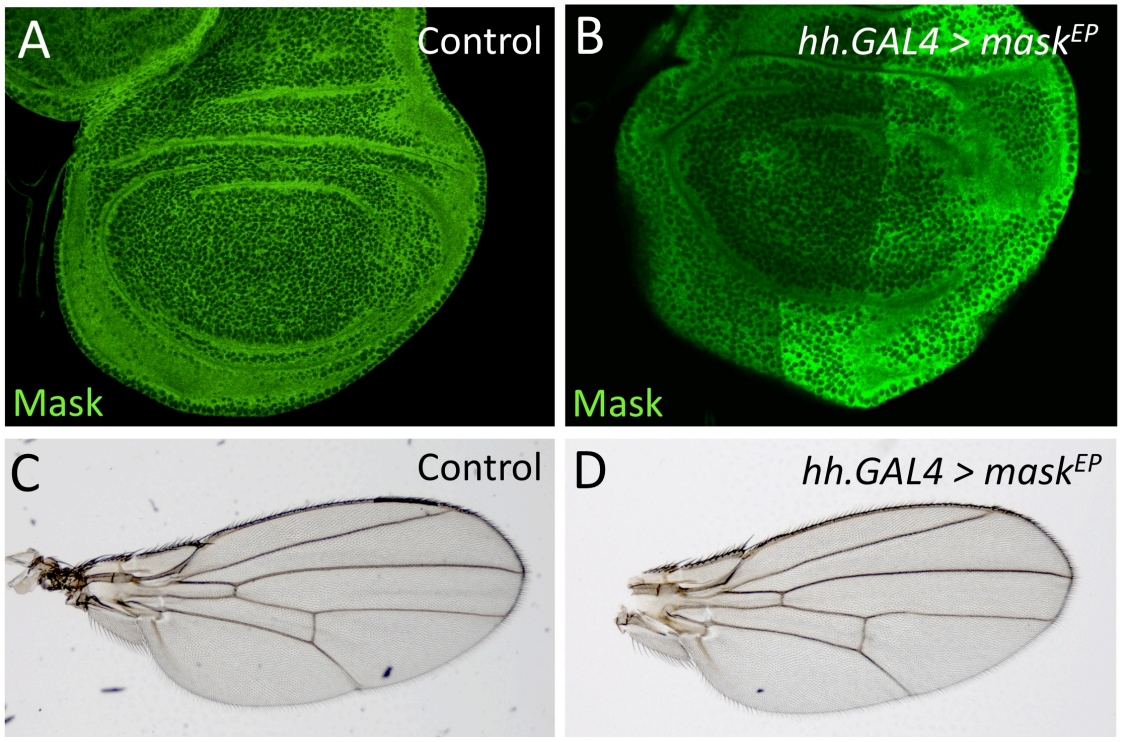

Figure 4.5: Mask overexpression does not drive tissue overgrowth.
(A) Third instar wing imaginal disc stained with anti-Mask (green)
(B) Third instar imaginal disc expressing Mask in the posterior compartment under the control of *P{EPgy2}EY01848* driven by *hh.GAL4*, stained with anti-Mask (green)
(C) Adult control wing
(D) Adult wing overexpressing Mask in the posterior compartment under the control of *P{EPgy2}EY01848* driven by *hh.GAL4*

4.1.3 *Mask* mutant does not affect patterning

Despite the strikingly small size of *mask-IR* expressing wings, the pattern of differentiated features, such as veins and bristles, is not affected (Fig 4.1 A,B). This phenotype is different from that of genes affecting Ras/MAPK kinase signaling. For instance, downregulation of the Ras activated kinase Raf by expression of *raf-IR* in the posterior half of the wing results in an undergrowth phenotype similar to that caused by expression of *mask-IR*. However, by contrast with *mask-IR*, *raf-IR* undergrowth phenotype is also accompanied by a severe loss of veins (Fig 4.6 A-C). Thus, mask does not regulate vein patterning in the wing.

The wild type adult eye is composed of about 800 clusters of cells, called ommatidia, organised in a regular pattern across the eye. Each ommatidium contains 8 photoreceptor cells, R1 to R8, surrounded by a fixed number of accessory (interommatidial) cells. R1 to R6 are arranged in a precise order around the inner photoreceptor cells R7 and R8 and disruptions in EGFR or Sevenless signaling result in loss of photoreceptor cells. In order to examine *mask* role in eye patterning, control flies carrying the *eyGMR.GAL4* driver and flies expressing *mask-IR* with the *eyGMR.GAL4* driver were prepared for eye sectioning. In the control eye sections, each ommatidium presented the same organised pattern of photoreceptor cells R1 to R7 (Fig 4.6 D,D'). R8 cell is not visible as it is stacked under R7. Despite the strong undergrowth caused by down regulation of the *mask* gene, sectioning of *mask-IR* eyes revealed that the number of photoreceptors per ommatidium was not affected compared to wild type (Fig 4.6 E,E'). However, the number of interommatidial cells appeared slightly reduced compared to the control. This could be due to a patterning defect, or a defect in cell proliferation/survival. For instance, the Hippo signaling pathway is known to affect the number of interommatidial cells by controlling cell survival and proliferation in these cells. Our finding that *mask* mutant does not affect the number of photoreceptors is in contradiction with the results of Smith *et al* who found some loss of photoreceptors in $mask^{10.22}$ mutant eye. This may be due to the fact that the RNAi knockdown is not as strong as the mutant. Loss of photoreceptors in $mask^{10.22}$ mutant eyes could be due to a defect in cell viability, stronger in the mutant than in the RNAi knock-down. Consistently, our results and those of Smith *et al* show that *mask* mutant cells under-proliferate and have a lower survival than wild type cells. In order to confirm our result,

we generated mutant clones of mask in the eye imaginal disc and stained with an ELAV antibody, a marker of neuronal differentiation used to mark differentiated photoreceptor cells. No loss of ELAV staining was observed in the *mask* mutant cells compared to the surrounding wild type cells (Fig 4.6 F). Thus, *mask* does not control photoreceptor cell specification. Together these data show that *mask* downregulation does not strongly affect Ras/MAPK signaling.

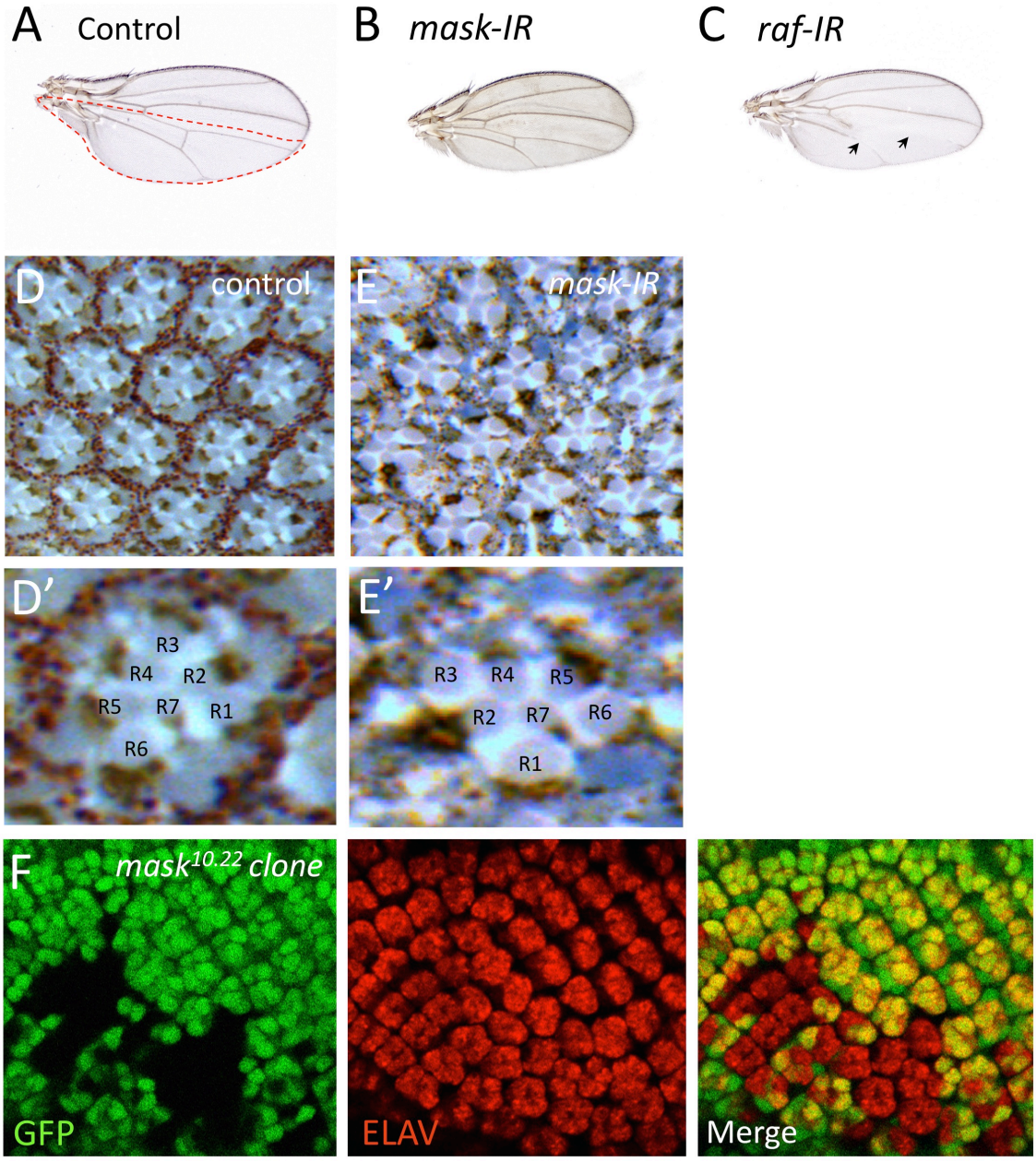

Figure 4.6: *mask* RNAi or mutant does not affect patterning in the wing or in the eye

(A) Wild-type adult *Drosophila* wing. Red dotted line indicates the posterior compartment. (B) RNAi knockdown of *mask* specifically in the posterior compartment causes undergrowth (C) RNAi knockdown of *raf* specifically in the posterior compartment causes undergrowth and loss of vein differentiation (arrows). Picture from BJ Thompson. (D) Section through an adult eye showing multiple ommatidia in which red pigment cells surround photoreceptor cells. (D') Zoom from section D, single wild type ommatidium with photoreceptor cells annotated from R1 to R7. (E) RNAi knockdown of the *mask* gene causes occasional loss of pigment cells and moderate disorganisation of the ommatidia, but does not cause loss of photoreceptor cells. (E') Zoom from section E, single ommatidium from a *mask-IR* expressing eye with photoreceptor cells annotated from R1 to R7. (F) A homozygous $mask^{10.22}$ mutant clone (GFP-negative) does not block differentiation of ELAV-positive photoreceptor neurons in the 3rd instar eye imaginal disc, indicating that Ras-signalling is functional in *mask* mutants.

4.2 Mask acts in the Hippo pathway

Mutations affecting tissue growth without affecting patterning are uncommon. Known examples include mutations affecting genes of the Hippo signaling pathway. For instance, inhibition of the Warts (Wts) kinase by expression of a *wts-IR* transgene in the wing causes tissue overgrowth without altering veins or bristles (Fig 4.7 A,B). In the eye, expression of *wts-IR* causes tissue overgrowth and increased number of interommatidial cells but it does not alter the number of photoreceptors per ommatidium (Fig 4.7 C-E). Thus, *mask-IR* and *wts-IR* cause opposite phenotypes in the wing and in the eye. In addition, the *mask* mutant phenotype – increased apoptosis and reduced cell proliferation – is highly similar to that caused by mutations in the Hippo pathway component *yki* (Huang et al., 2005). Together, these data suggest that *mask* may be involved in the Hippo signaling pathway.

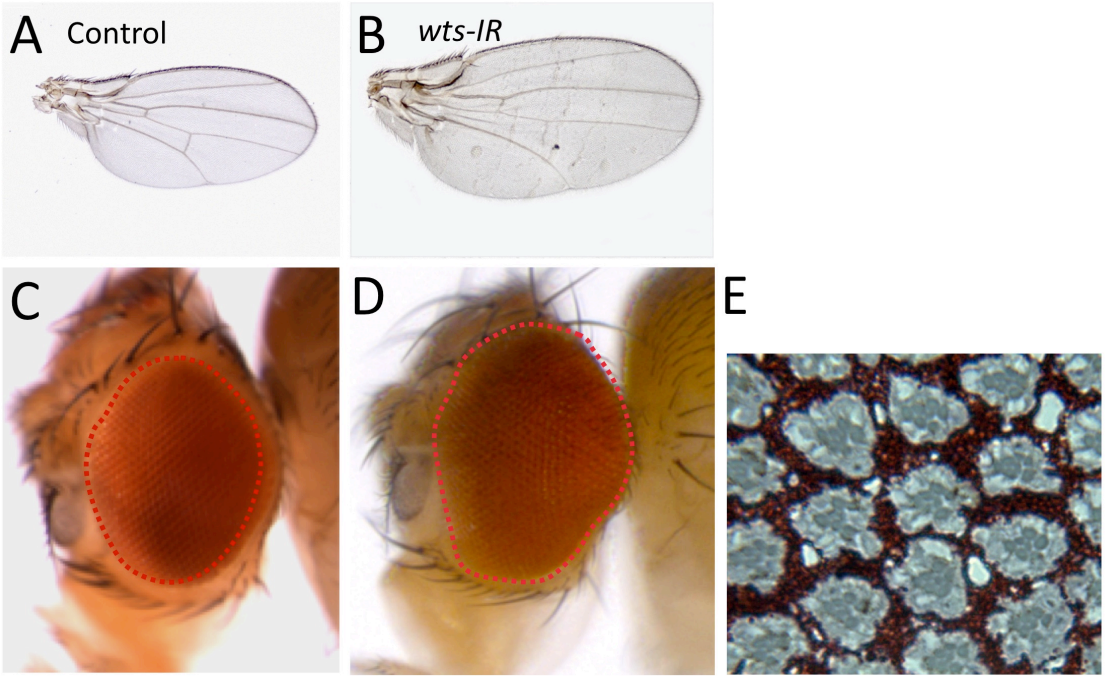

Figure 4.7: Wts RNAi downregulation affects tissue growth but not patterning
RNAi knockdown of the *wts* gene during wing development results in an abnormally large wing (A) compared to control (B) with no obvious defects in patterning. RNAi knockdown of the *wts* gene during eye development results in an abnormally large eye (C) compared to control (D). (E) RNAi knockdown of the *wts* gene causes a strong increase in pigment cell number, but does not cause a gain of photoreceptor cells. Pictures from BJ Thomspon.

4.2.1 *Mask* is required for Yki target gene expression

Hippo pathway signaling restricts cell proliferation by inhibiting the transcriptional co-activator Yki. We used *LacZ* reporters for the Yki target genes *four-jointed (fj)*, *expanded (ex)* and *DIAP1* as a read out to test if *mask* was affecting Hippo signaling. The *LacZ* gene encodes the β-galactosidase bacterial protein, easily detectable by antibody staining. Down-regulation of *mask* in the posterior compartment of the wing by expression of *mask-IR* with the *hh.GAL4* or the *en.GAL4* driver led to a significant reduction in the expression of *fj.LacZ*, *ex.LacZ* and *DIAP1.LacZ* reporters compared to control (Fig 4.8). To confirm these results, we generated $mask^{10.22}$ mutant clones in flies carrying either of the three reporters. In *mask* mutant cells, the level of expression of Yki reporter genes was reduced compared to their level in wild type surrounding cells (Fig 4.9). These results show that *mask* is required for the expression of Yki target genes.

4.2.2 Mask binds to and colocalises with Yki

In order to determine how Mask is involved in the Hippo pathway, we cloned tagged versions of Mask conserved domains to test their interaction with proteins of the Hippo pathway in co-immunoprecipitation assays. We generated 3 different Flag-tagged constructs (Fig 4.10 A):

- ANKRI: region containing the first block of Ankyrin repeats

- ANKRII: region containing the second block of Ankyrin repeats

- ANKRII+KH: region containing the second block of Ankyrin repeats and the KH domain.

Interestingly, when expressed in cultured *Drosophila* S2R+ cells, ANKRI-Flag was found very often in the nucleus whereas Flag-ANKRII and Flag-ANKRII+KH were predominantly cytoplasmic (Fig 4.10 B-D). This indicates that although no consensus NLS sequence was found in that region, Mask may contain an NLS in ANKRI sequence. Alternatively, ANKRI may bind a nuclear protein. ANKRI-Flag, ANKRII-Flag and ANKRII+KH-Flag were all able to co-immunoprecipitate with an EGFP-tagged form of Yki (Fig 4.10 E). The presence or absence of the KH domain next to the second ankyrin repeats domain did not affect the binding to Yki. These results show that Mask can bind to Yki via its ankyrin repeat domains. We also tested the interaction of Mask conserved domains

with an HA tagged form of Yki partner Scalloped (Sd) but no interaction was detected between Mask constructs and Sd (Appendix, Fig A.1).

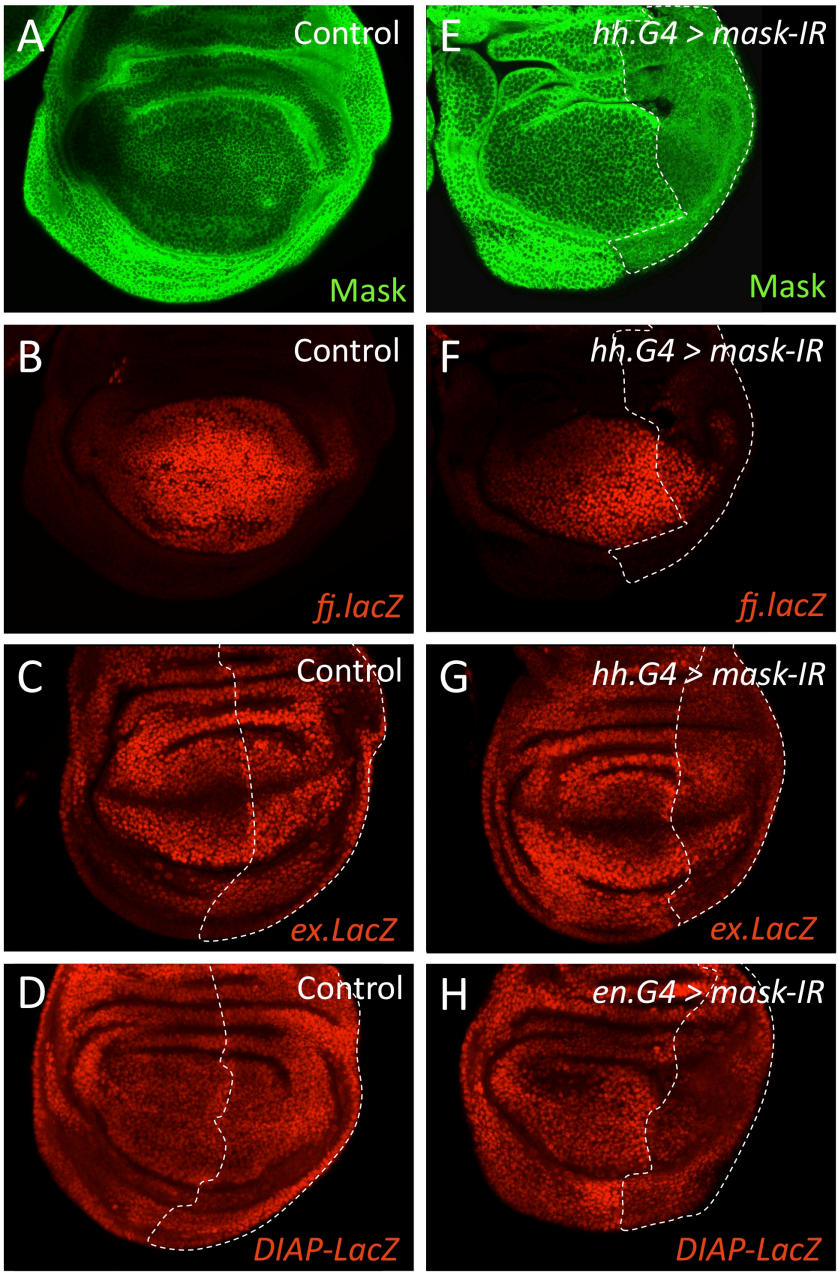

Figure 4.8: *mask* is required for Yki target gene expression (1)
Third instar wing imaginal discs immunostained for Mask (green) or for β-galactosidase (red). Control or expressing *mask-IR* with the *hh.GAL4* or *en.GAL4* driver.
(A) Control third instar wing imaginal disc stained with an anti-Mask antibody.
(B) Expression pattern of the *fj.lacZ* reporter gene in a control wing disc. A and B are pictures from the same imaginal disc. (C) Expression pattern of the *ex.lacZ* reporter gene in a control wing disc. (D) Expression pattern of the *DIAP1.lacZ* reporter gene in a control wing disc. (E) RNAi knockdown of *mask* in the posterior compartment (dotted line) reduces the level of Mask protein expression. (F) RNAi knockdown of *mask* in the posterior compartment (dotted line) reduces the level of *fj.lacZ* expression. E and F are pictures from the same disc. (G) RNAi knockdown of *mask* in the posterior compartment (dotted line) reduces the level of *ex.lacZ* expression. (H) RNAi knockdown of *mask* in the posterior compartment (dotted line) reduces the level of *DIAP1.lacZ* expression. The dotted lines in C, D, G and H outline the posterior compartment marked by the expression of a *UAS.GFP* transgene (not shown).

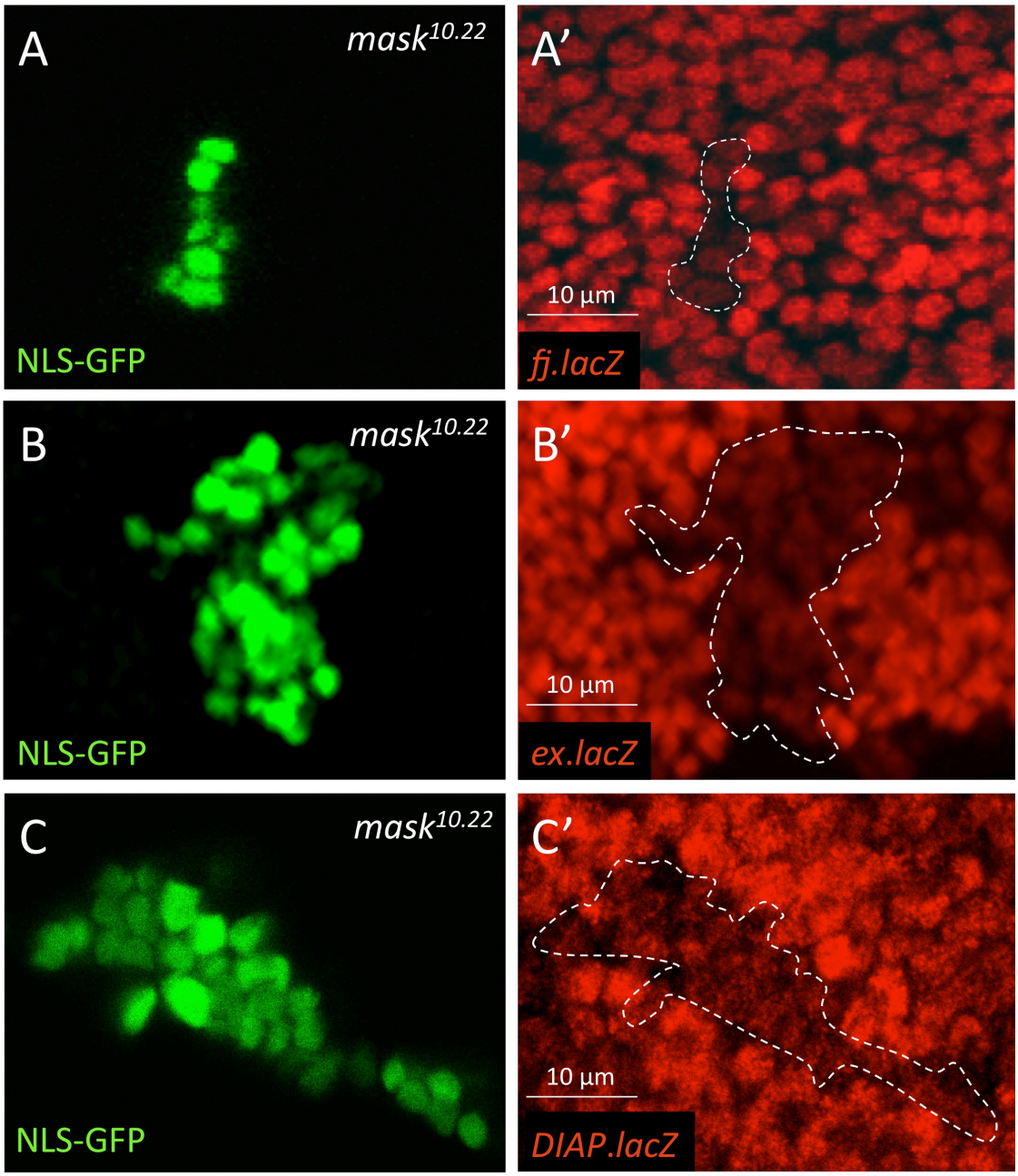

Figure 4.9: *mask* is required for Yki target gene expression (2)
MARCM clones in the pouch of third instar wing imaginal discs (distal region). (A) A *mask*$^{10.22}$ homozygous mutant clone (GFP-positive) shows reduced expression of *fj.lacZ* detected by the β-galactosidase antibody (red) compared to control neighbouring cells (A').
(B) A *mask*$^{10.22}$ homozygous mutant clone (GFP-positive) shows reduced expression of *ex.lacZ* detected by the β-galactosidase antibody (red) compared to control neighbouring cells (B').
(C) A *mask*$^{10.22}$ homozygous mutant clone (GFP-positive) shows reduced expression of *DIAP1.lacZ* detected by the β-galactosidase antibody (red) compared to control neighbouring cells (C').

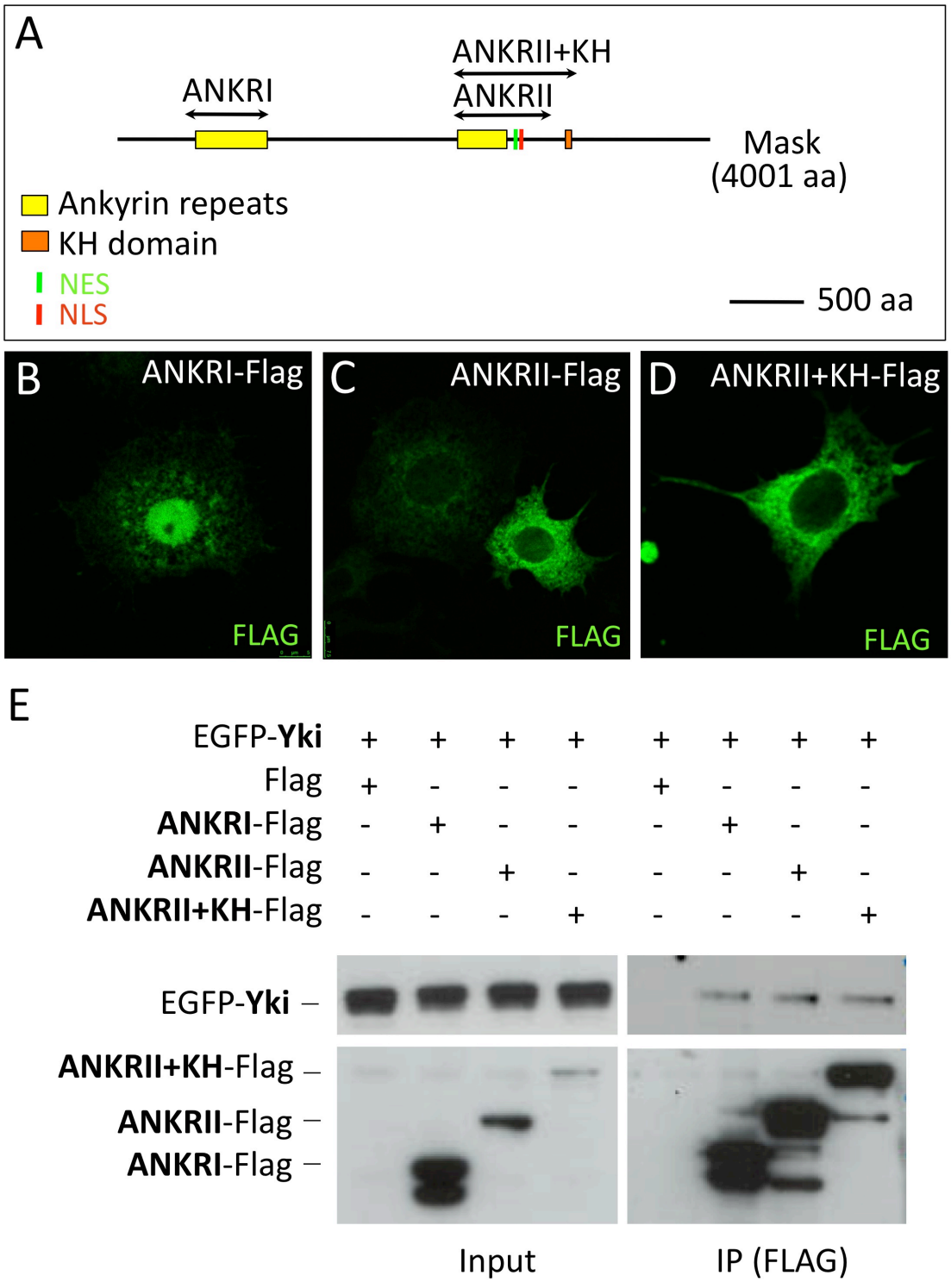

Figure 4.10: Mask binds to Yki
(A) Schematic diagram of the Mask protein domain structure and the cloned domains
(B-D) Localisation of ANKRI-Flag (B), ANKRII-Flag (C) and ANKRII+KH-Flag (D) constructs upon expression in *Drosophila* S2R+ cells (anti-Flag immunostaining).
(E) Co-immunoprecipitation of GFP-tagged Yki with Flag-tagged Mask ankyrin repeat domains (ANKRI, ANKRII, or ANKRII+KH). S2 cells were transfected with an EGFP-Yki plasmid and a FLAG vector either empty or containing Mask conserved domains ANKRI or ANKRII or ANKRII+KH.

To further investigate the relationship between Mask and Yki, we examined their subcellular localisation by immunostaining in *Drosophila* tissues and cultured cells (Fig 4.11). Both proteins localised in a very similar pattern, predominantly cytoplasmic in the developing wing disc epithelium and more nuclear in cultured S2R+ cells, where the two proteins also localise in perinuclear dots (Fig 4.11 A-C). In the *Drosophila* adult gut, Yki has been shown to be upregulated and to translocate into the nucleus upon stress – such as infection or activation of JNK signaling – to promote gut regeneration (Shaw et al., 2010) (Staley and Irvine, 2010). We examined Mask and Yki localisation in the gut and found that the 2 proteins also co-localise and appear to move together into the nucleus in some regions of the gut (Fig 4.11 D-E). The *Drosophila* adult gut epithelium is mostly composed of large enterocytes (ECs), which ensure the absorptive function of the intestine (Fig 4.12 A). The maintenance of the epithelium is ensured by small diploid intestinal stem cells (ISCs), which are localised basally in the epithelium. The ISC divides to produce an ISC and a progenitor cell, the enteroblast (EB), which then divides to produce ECs and occasionally small entero-endocrine cells (ee) (Fig 4.12 B). In flies expressing a *UAS.GFP* construct under the control of the EC specific driver *MyoIA.GAL4*, we found that both Mask and Yki were upregulated together in some isolated ECs, and in small GFP negative cells (presumably ISCs and EBs, as Yki was shown to be upregulated in those cells upon stress) (Fig 4.12 C-F). Thus, Mask colocalises with Yki and may be subject to the same regulation in response to stress.

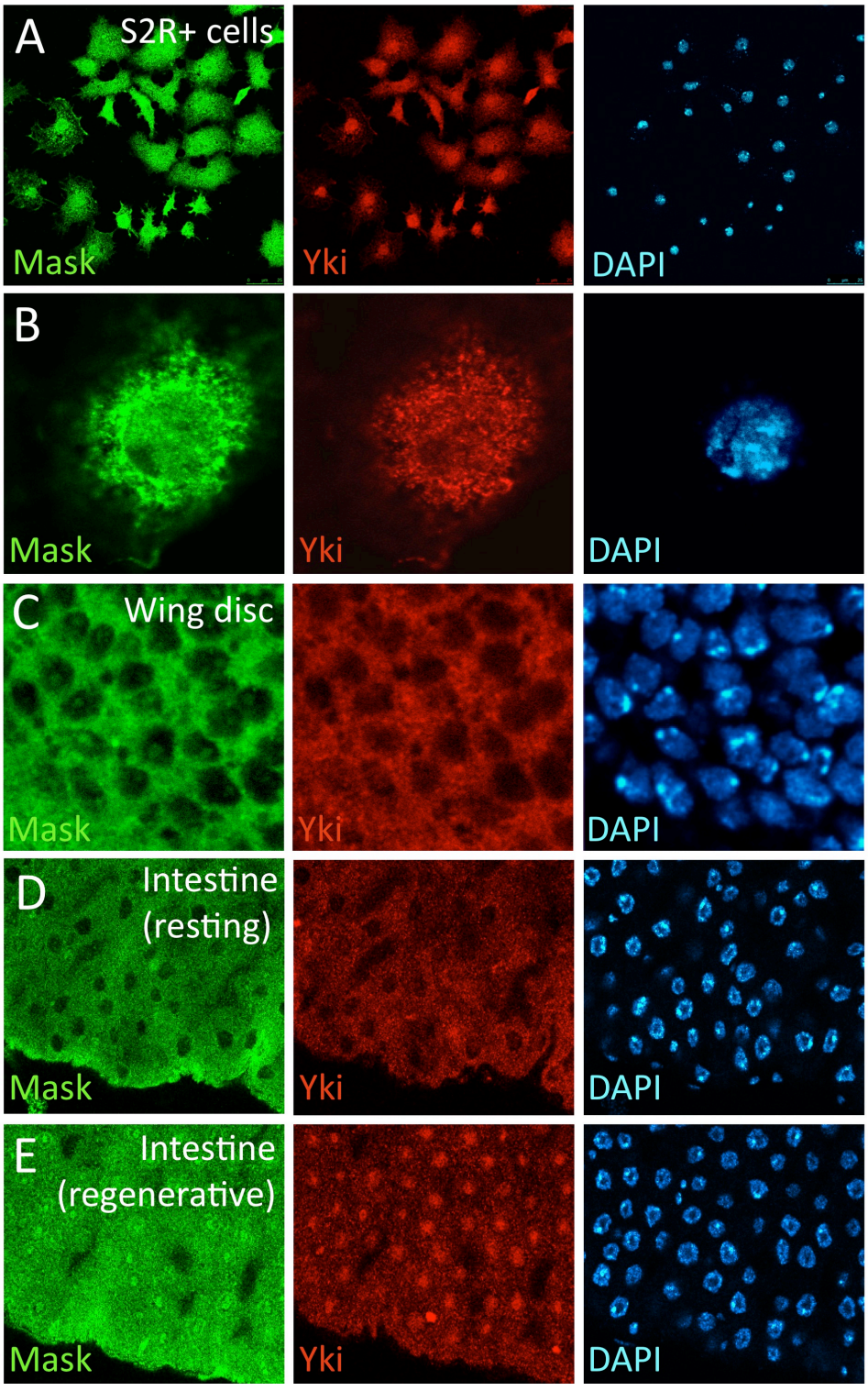

Figure 4.11: Mask colocalises with yki in *Drosophila* cells and tissues
Immunostainings for Mask (in green) and Yki (in red), nuclei are stained with DAPI (blue)
(A-B) Mask and Yki co-localise in both nucleus and cytoplasm of cultured S2R+ cells. (C) Mask and Yki co-localise in the cytoplasm of wing imaginal disc epithelial cells. (D) Mask and Yki co-localise in the cytoplasm of resting adult midgut intestinal cells. (E) Mask and Yki co-localise in both nucleus and cytoplasm of regenerating adult midgut intestinal cells.

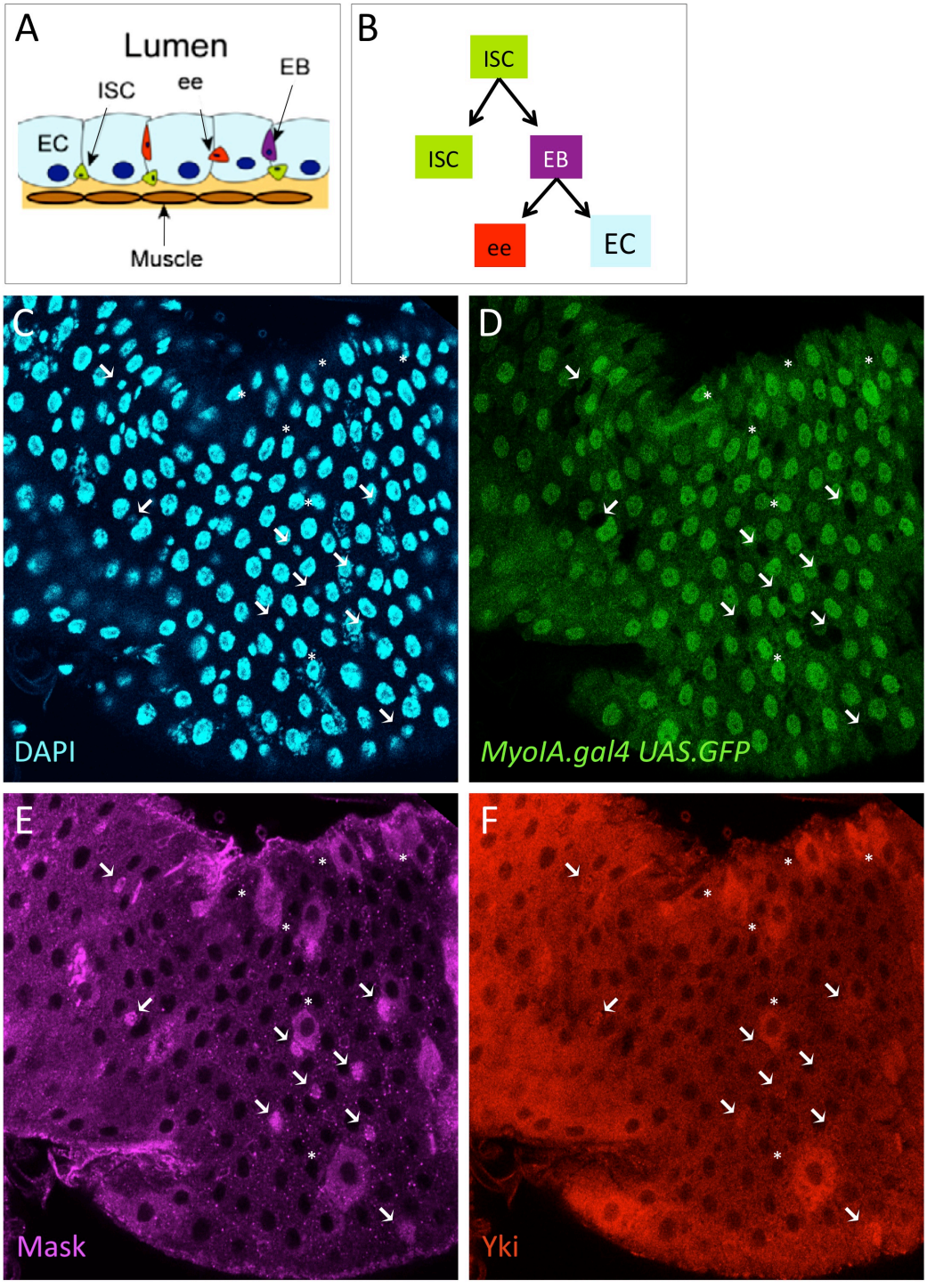

Figure 4.12: Mask is co-expressed with Yki in isolated enterocytes and progenitor cells in the adult midgut.
(A) Schematics of the intestinal epithelium from (Shaw et al., 2010). EC: enterocyte. ISC: intestinal stem cell. ee: entero-endocrine cell. EB: enteroblast. The gut is covered by a muscle layer. (B) Diagram of an ISC progeny
(C) Portion of an adult midgut with nuclei stained with DAPI (blue), ECs are marked by the expression of GFP (green) (D). Immunostaining for Mask (pink, E) and Yki (red, F) reveals that the two proteins are upregulated together in isolated enterocytes (asterisks) and progenitor cells (arrows).

4.2.3 Mask is required for Yki activity

Taken together, our results strongly suggest that Mask acts at the level of Yki in the Hippo pathway. To analyse the role of Mask in Yki regulation, we performed a genetic epistasis experiment in the wing imaginal disc. The MARCM system was used to over-express a V5-tagged Yki construct in clones of cells either control or mutant for *mask*. Over-expression of V5-tagged Yki in clones of cells is sufficient to cause a strong over-proliferation phenotype compared to wild type clones (Fig 4.13 A,B). In contrast, when V5-tagged Yki is over-expressed in $mask^{10.22}$ mutant clones, it is no longer able to induce over-proliferation (Fig 4.13 C-E). Thus, *mask* is required for over-expressed Yki to drive cell proliferation. This effect could be indirect: *mask* may be essential for cell survival independently of Yki. However, considering the binding of Mask to Yki, their cytoplasmic/nuclear co-translocation, and *mask* specific effects on Yki target gene expression, $mask^{10.22}$ effect on Yki-dependent cell over-proliferation is more likely to be specifically through Yki regulation.

4.2.4 Mask affects the level of Yki phosphorylation

A major regulator of Yki activity is the Warts kinase (Wts), which negatively regulates Yki by phosphorylating it on three conserved Serine residues (S111, S168, S250), one of which – S168 – is most crucial to regulate Yki activity (Oh et al., 2009). Activation of Wts in the eye by overexpression of its activating kinase Hpo is sufficient to induce a strong undergrowth phenotype, similar to that of *mask* mutant phenotype (Wu et al., 2003). As Mask appears essential for Yki activity, it may be required to limit Yki phosphorylation by Wts. To test this hypothesis, we made use of an anti-phospho-S168 Yki antibody (N. Tapon) to compare Yki levels of phosphorylation in control and *mask* mutant larvae. As $mask^{10.22}$ homozygous mutant is embryonic lethal, we used a combination of two hypomorphic alleles, both homozygous lethal: $mask^{6.3}$ and $mask^{7.29}$ (Smith et al., 2002). $mask^{6.3}$/*TM3SerGFP* females were crossed to $mask^{7.29}$/*TM3SerGFP* males and GFP expression in the progeny was used to identify the genotypes. GFP negative $mask^{6.3}/mask^{7.29}$ transheterozygous larvae are viable but grow much smaller than wild type and die before pupariation. 20 GFP positive larvae ($mask^{6.3}$/ TM3SerGFP or $mask^{6.3}$/ *TM3SerGFP*: control) and 20 GFP negative *mask* mutant larvae ($mask^{6.3}/mask^{7.29}$) of similar sizes were collected. Proteins from each sample were extracted and analysed by Western blot with the anti-phospho-S168 Yki antibody. We

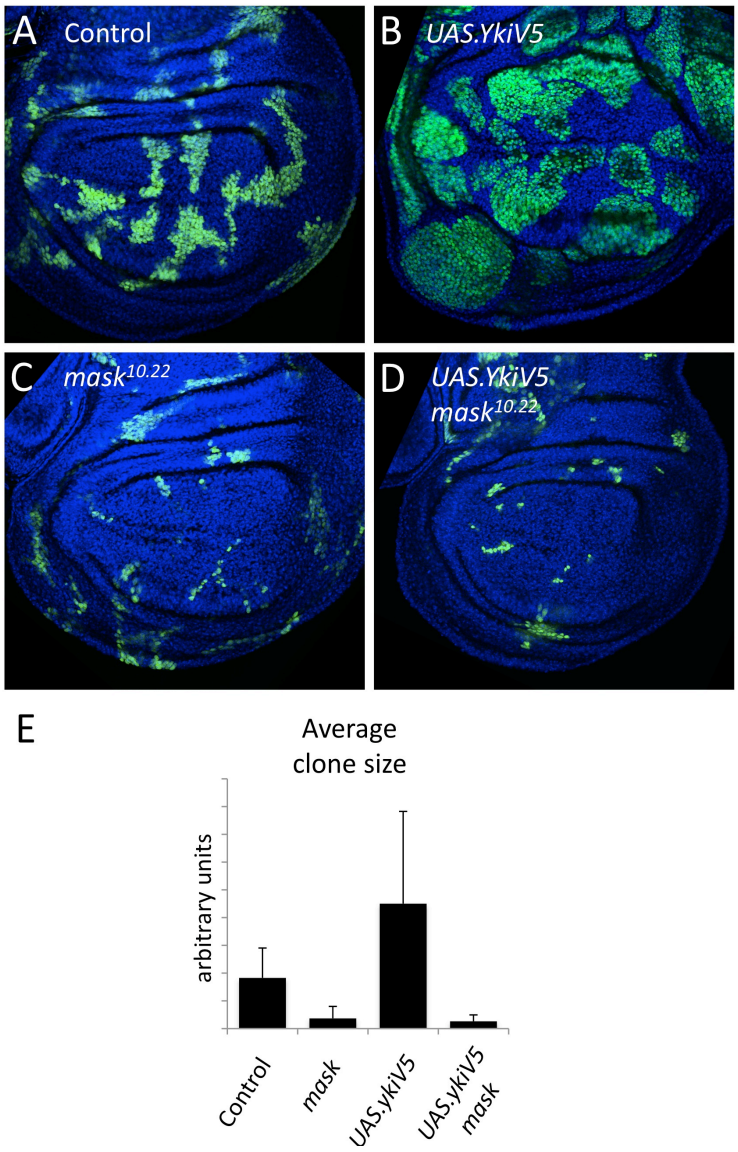

Figure 4.13: Overexpressed Yki requires Mask to drive cell proliferation
Third instar wing imaginal discs. Nuclei are marked with DAPI (blue). Clones, marked by the expression of NLS-GFP (green), were generated using the MARCM system and induced by heat shocking larvae at 84 hr (± 12 hr) of development.
(A) Control clones (GFP-positive)
(B) Overexpression of Yki-V5 in clones drives overproliferation of cells, leading to enlarged clone sizes.
(C) Mutation of *mask* inhibits cell proliferation, resulting in small clones.
(D) Overexpression of Yki-V5 in *mask* mutant cells fails to drive overproliferation, resulting in small clones.
(E) Quantification of clone sizes in (A-D).

found that phospho-Yki levels were elevated in *mask* mutant larvae compared to control larvae (Fig 4.14). This effect was repeated between different sets of experiments. However, its extent was variable and on average mild. Thus, Mask has a mild negative effect on the ability of Wts to phosphorylate Yki.

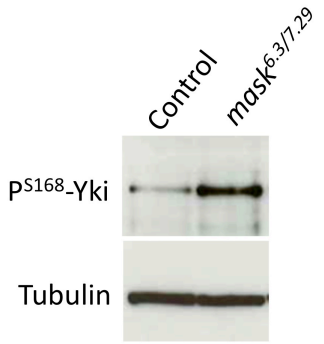

Figure 4.14: Mask affects Yki phosphorylation.
Homozygous *mask* mutant larvae exhibit elevated levels of phosphorylated Yki, as detected by a western blot using an anti-phospho-Ser168-Yki antibody.

4.3 Mask promotes Yki function in the nucleus

4.3.1 Mask is essential for activated Yki function downstream of Warts

If *mask* unique role was to antagonise Yki phosphorylation by Wts, then mutation of *wts* should fully rescue *mask* mutant. *Mask* and *wts* are both located on the right arm of chromosome 3, allowing the recombination of *mask* and *wts* alleles for epistasis experiments. $mask^{10.22}$ allele was recombined with 2 different alleles of *wts*: wts^{M541} (hypomorph) and wts^{X1} (null). We used the *eyFlp FRT minute* system to generate whole mutant and double mutant eyes for $mask^{10.22}$ and wts^{M541} alleles. wts^{M541} mutant eyes were strongly overgrown, but wts^{M541} mutation was not able to rescue the growth of $mask^{10.22}$ wts^{M541} double mutant eye (Fig 4.15 A-D). We also tested *mask* and *wts* epistasis in clones in the wing disc using wts^{X1} null allele, which was pupal lethal with the *eyFlp FRT M* system. We find that, compared with wts^{X1} mutant clones, which strongly overproliferate, $mask^{10.22}$ wts^{X1} double-mutant clones still show impaired proliferation (Fig 4.15 E-I). Thus, Mask is required for active, non-phosphorylated Yki to drive overproliferation.

To confirm these results, we used the MARCM system to test the ability of 2 non-phosphorylatable (activated) forms of Yki to rescue *mask* mutant phenotype compared to the wild-type Yki-V5 construct mentioned previously (paragraph 4.2.3). The 3 Yki-V5 transgenes are all inserted in the same location in the genome and only differ in point mutations affecting Wts phosphorylation sites (Oh and Irvine, 2009). The strength of their phenotypes can thus be compared:

- Yki-V5, V5 tagged wild-type Yki
- Yki^{S168A}-V5, V5 tagged mutant Yki that contains a substitution of Serine 168 to Alanine
- Yki$^{S111A-S168A-S250A}$-V5 (Yki^{3SA}-V5), V5 tagged mutant Yki that contains substitutions of Serine111, Serine168 and Serine250 to Alanines.

Clones expressing either of these constructs overproliferate compared to control wild type clones (Fig 4.16). As expected, expression of activated forms of Yki induce a stronger overgrowth than expression of the wild type Yki, the strongest phenotype being that of the triple mutant: overgrown clones of cells overexpressing Yki-V5^{S168A} or Yki-V5$^{S111A-S168A-S250A}$ cause folds in the tissue and start extruding from the wing disc epithelium. Expression of these activated forms of Yki could partially rescue *mask$^{10.22}$* mutant clones in the hinge region of the wing disc but the clones were still much smaller than control clones expressing activated Yki. Moreover, mutant clones in the centre of the pouch were not rescued. Thus, none of the constructs was able to fully rescue *mask$^{10.22}$* mutant: Mask is essential for activated Yki to drive cell proliferation.

Taken together, these results show that Mask acts downstream or at the level of Wts and is essential for activated Yki function.

Two hypotheses could explain Mask requirement for activated Yki function:

1) Mask may be involved in Yki nuclear translocation
2) Mask may be involved in transactivation of Yki target genes in the nucleus

4.3.2 Mask does not regulate Yki nuclear localisation

To determine if Mask was involved in Yki nuclear translocation, we examined Yki localisation in mask mutant clones in the wing disc using a Yki antibody (Yki69, N. Tapon). No change in Yki localisation was detectable in those clones (Fig 4.17 A-D). However, detection of endogenous Yki in the nucleus is difficult with current available antibodies. In order to confirm this result, we examined the localisation of Yki-V5 in *mask* mutant clones compared to control clones (Fig 4.17 E-F'). In control cells, Yki-V5 localises mostly in the cytoplasm but is also detectable in the nucleus. Despite the strong undergrowth of *mask* mutant cells overexpressing Yki-V5, no detectable difference in Yki-V5 localisation was observed in those mutant cells compared to controls. Similar results were obtained when looking at the localisation of Yki ^{S168A} -V5 and Yki $^{S111A\text{-}S168A\text{-}S250A}$-V5 (Appendix, Fig A.2). Thus, the undergrowth phenotype of *mask* mutant clones expressing Yki-V5 is not due to a defect in Yki-V5 translocation into the nucleus. These results show that Mask does not regulate Yki nuclear localisation.

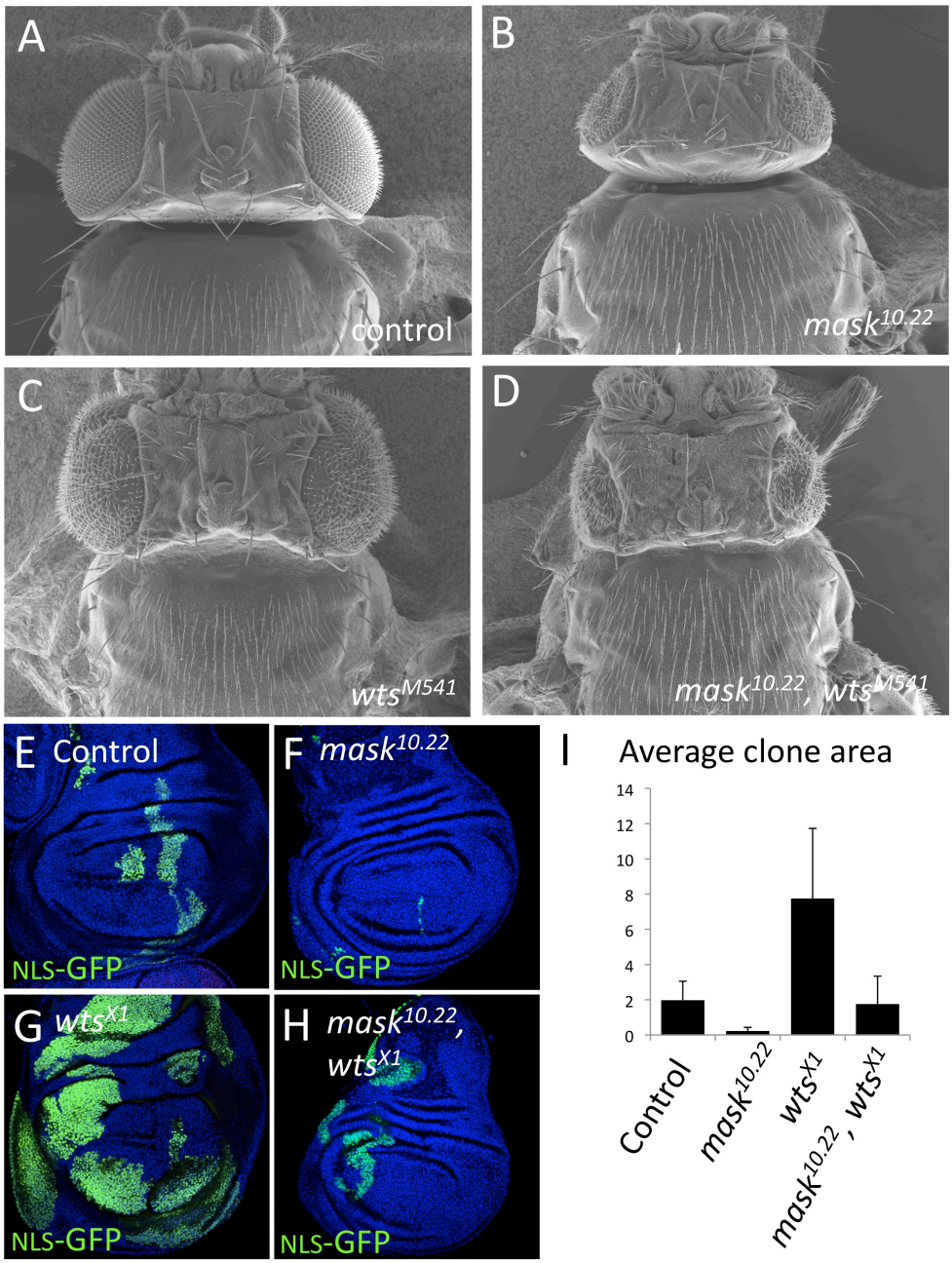

Figure 4.15: Mask acts downstream or at the same level as Wts
(A-D) Scanning electron Micrographs of *Drosophila* heads processed by CRUK Electronic Microscopy Unit. (A) Control *Drosophila* head, top view. (B) *mask*$^{10.22}$ mutation in the eye results in abnormally small eyes. (C) *wts*^{M541} hypomorphic mutation in the eye results in an abnormally large eye. (D) *wts*^{M541}mutation in the eye cannot rescue the undergrowth phenotype of *mask*$^{10.22}$ mutation. (E-H) Third instar wing imaginal discs. Nuclei are marked with DAPI (blue). Clones, marked by the expression of NLS-GFP (green), were generated using the MARCM system and induced by heat shocking larvae at 84 hr (± 12 hr) of development. (E) Control clones (GFP-positive) in a third instar wing imaginal disc. (F) *mask*$^{10.22}$ mutant clones proliferate slowly, leading to small clone sizes. (G) *wts*^{X1} mutant clones overproliferate, leading to enlarged clone sizes. (H) *mask*$^{10.22}$ *wts*^{X1} double mutants grow to larger sizes than *mask*$^{10.22}$ mutants, but are still much smaller than *wts*^{X1} mutants, indicating that even fully activated Yki requires Mask to drive cell proliferation.(I) Quantification of clone sizes in (E-H).

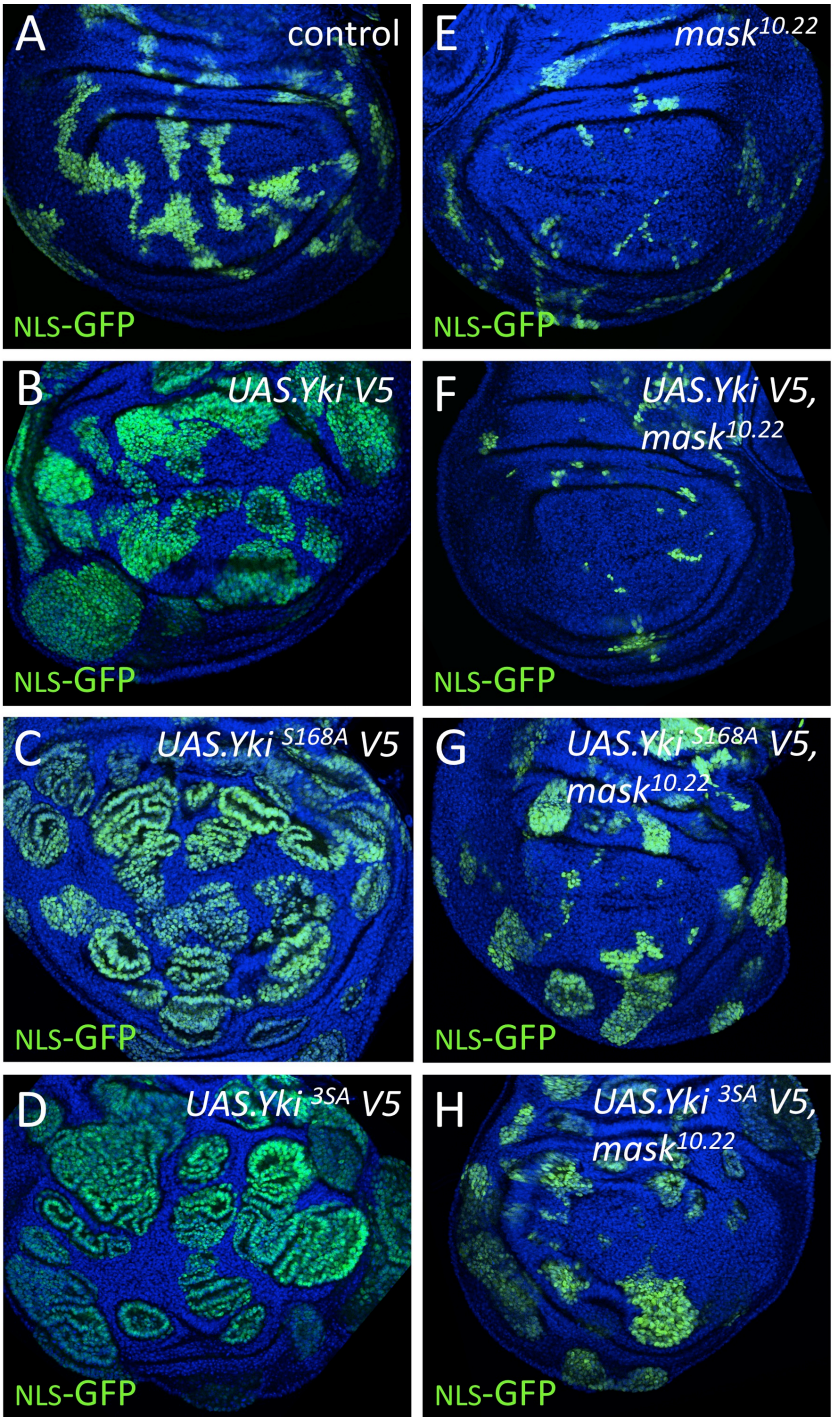

Figure 4.16: Activated Yki expression does not fully rescue the growth of *mask* mutant clones

Third instar wing imaginal discs. Nuclei are marked with DAPI (blue). Clones, marked by the expression of NLS-GFP (green), were generated using the MARCM system and induced by heat shocking larvae at 84 hr (± 12 hr) of development. (A) Control clones (GFP-positive).
Clones overexpressing Yki-V5 (B), Yki^{S168A}-V5 (C) and Yki^{3SA}-V5 (D) overproliferate, leading to enlarged clone sizes. Activated forms of Yki present stronger phenotypes. (E) *mask*$^{10.22}$ mutant clones proliferate slowly, leading to small clone sizes. (F-H) *mask*$^{10.22}$ mutant clones are not recued by *Yki-V5* overexpression (F) and are only partially rescued by *Yki*^{S168A}*-V5* (G) and *Yki*^{3SA}*-V5* (H) overexpression.

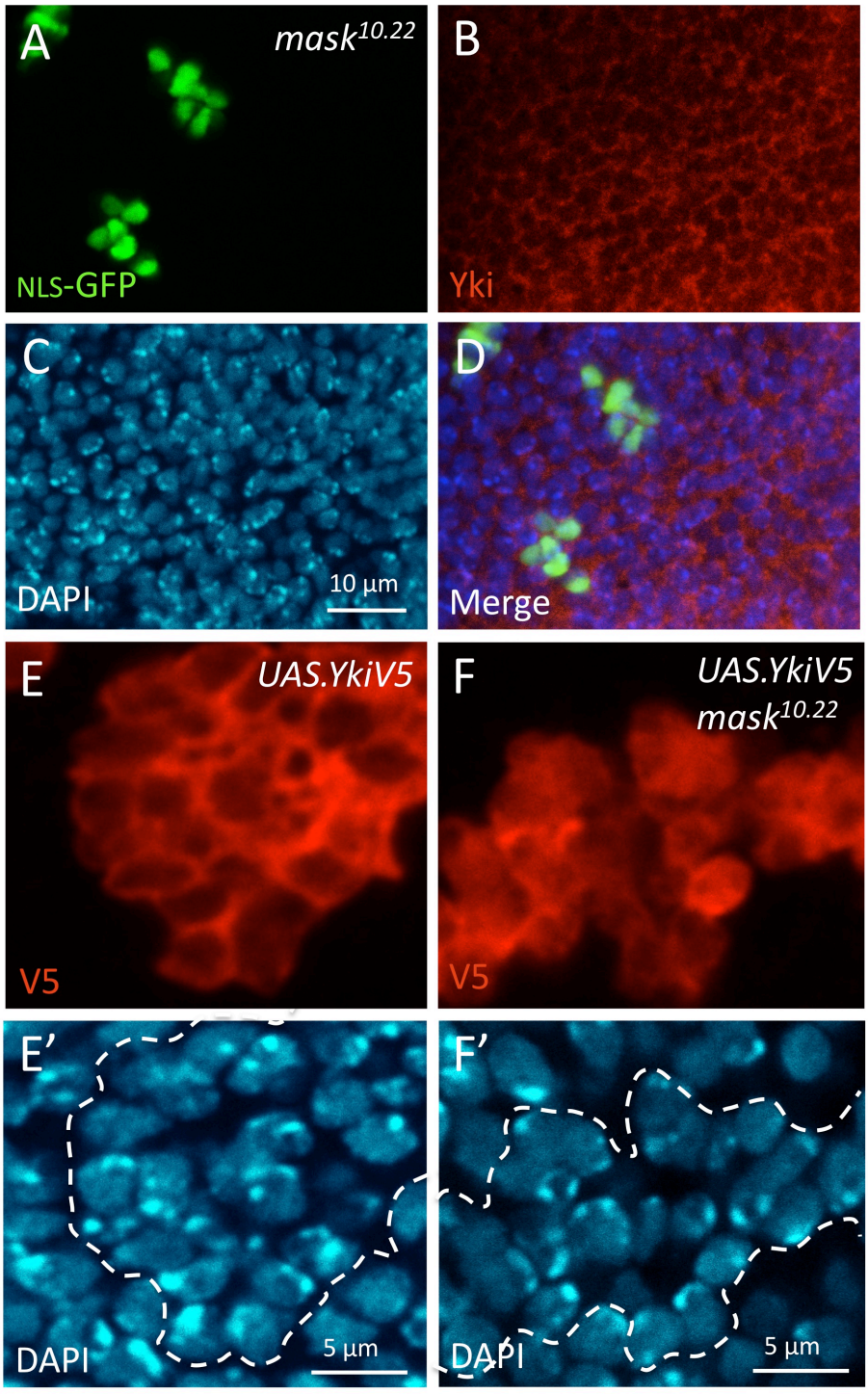

Figure 4.17: *mask* mutant does not affect Yki nuclear localisation
(A-D) Clones mutant for *mask*$^{10.22}$ induced with the MARCM system (A, green) do not alter the subcellular localisation of Yki (B, red) in the wing imaginal disc. (C) DAPI (blue) marks nuclei.
(E) Yki-V5 expressed in a clone with the MARCM system localises in the cytoplasm and the nucleus (anti-V5, red). Nuclei are marked by DAPI (blue) and a dotted line outlines the clone (E'). (F) Yki-V5 expressed in a *mask*$^{10.22}$ mutant clone with the MARCM system is still able to localise in the nucleus (anti-V5, red). Nuclei are marked by DAPI (blue), and a dotted line outlines the clone (F').

4.3.3 Mask acts with Yki in the nucleus to activate its target genes

As Mask is essential for Yki function but *mask* mutant does not affect Yki nuclear translocation, Mask may be involved in regulating Yki transactivation in the nucleus. To test this hypothesis, we examined activated Yki capacity to activate its target genes in the absence of Mask. We generated single and double mutant clones for *mask* and *wts* in wing discs carrying the *ex.lacZ* or *fj.lacZ* reporters. In wts^{X1} mutant clones, Yki is more active and this can be measured by an increase in *ex.lacZ* expression (Fig 4.18 A). By contrast, induction of *ex.lacZ* is impaired in wts^{X1} $mask^{10.22}$ double-mutant clones in the wing pouch (Fig 4.18 B). Similarly, *fj.lacZ* expression remains low in wts^{X1} $mask^{10.22}$ double-mutant clones in the wing pouch (Fig 4.18 C). Induction of *fj.lacZ* was not detectable in wts^{X1} mutant clones in the wing pouch, but it could be detected in some clones in the hinge region. This may be due to the fact that in the distal region of the wing disc, *fj* expression is already very strong. In addition, it is controlled by other unknown signals. Thus, Mask is required for Yki target gene up-regulation in *wts* mutant clones, supporting the hypothesis that Mask acts by promoting transactivation of Yki target genes in the nucleus.

A more detailed examination of *mask wts* double mutant clones revealed a difference in the requirement for Mask in Yki reporter gene expression. While double mutant clones in the inner (distal) region of the wing disc present no change in target gene expression or sometimes a downregulation, some clones in the outer region present a mild upregulation of these reporter genes (Fig 4.19). Yki target gene upregulation correlates with a partial rescue of cell proliferation. Thus, Mask is less required for Yki activity in the hinge region of the wing disc, indicating that Yki may be more active in this region. This may explain why *mask* mutant clones are also partially rescued by activated forms of Yki specifically in the proximal region of the wing disc (Fig 4.16 G,H).

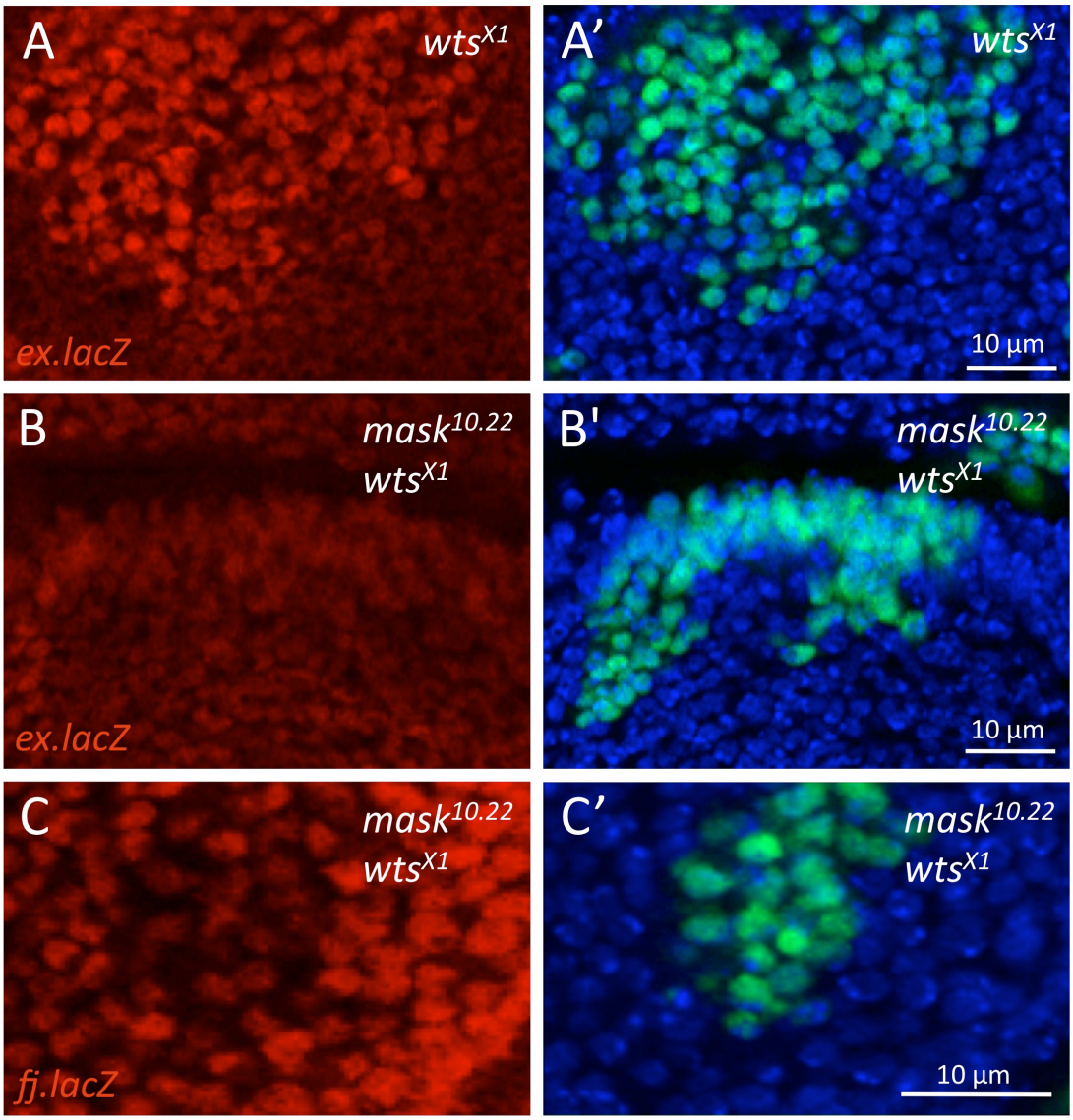

Figure 4.18: Mask regulates Yki target gene activation
MARCM clones marked by the expression of NLS-GFP (green) in third instar imaginal discs immunostained for β-galactosidase (red). DAPI marks nuclei (blue)
(A-A') *ex.lacZ* is up-regulated in *wts*^{X1} mutant clones (wing pouch)
(B-B') *mask*$^{10.22}$ *wts*^{X1} double mutant clones fail to upregulate *ex.lacZ* expression (wing pouch, proximal edge)
(C-C') *mask*$^{10.22}$ *wts*^{X1} double mutant clones fail to maintain *fj.lacZ* expression (wing pouch)

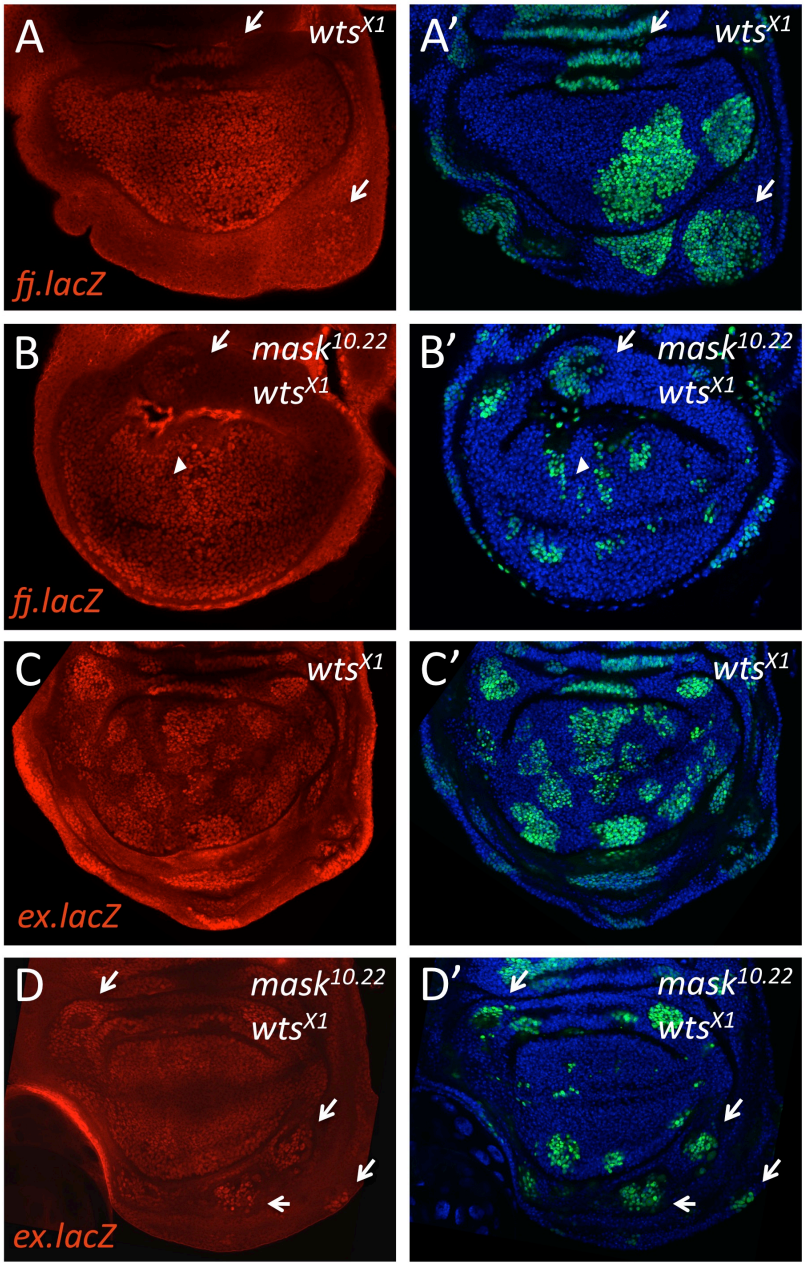

Figure 4.19: Different requirement for Mask in distal region versus hinge region in the wing imaginal disc

MARCM clones marked by the expression of NLS-GFP (green) in third instar imaginal discs immunostained for β-galactosidase (red). DAPI marks nuclei (blue)

(A-A') *wts*^{X1} mutant clones show mild upregulation of *fj.lacZ* expression in the hinge region (arrows) (B-B') *fj.lacZ* expression is down-regulated in *mask*$^{10.22}$ *wts*^{X1} double mutant clones in the wing pouch (arrow head) but is slightly upregulated in clones in the hinge region (arrow).

(C) *wts*^{X1} mutant clones show upregulation of *ex.lacZ* expression (D) *mask*$^{10.22}$ *wts*^{X1} double mutants fail to maintain *ex.lacZ* expression in the wing pouch but *ex.lacZ* is slightly upregulated in clones in the hinge region (arrows).

4.3.4 Wts does not regulate Mask

Altogether, these data strongly suggest that Mask is an essential co-activator of Yki in the nucleus. As Mask localises in a similar pattern to Yki and translocates with Yki in the nucleus, it may be regulated by Wts in the same way as Yki is. In order to test this hypothesis, we examined Mask localisation in wts^{X1} mutant clones using Mask antibody (Fig 4.20). Mask protein levels and localisation were not affected. Thus, Wts does not regulate Mask nuclear translocation or Mask stability. In addition, this result shows that *mask* is not a target gene of the Hippo signaling pathway.

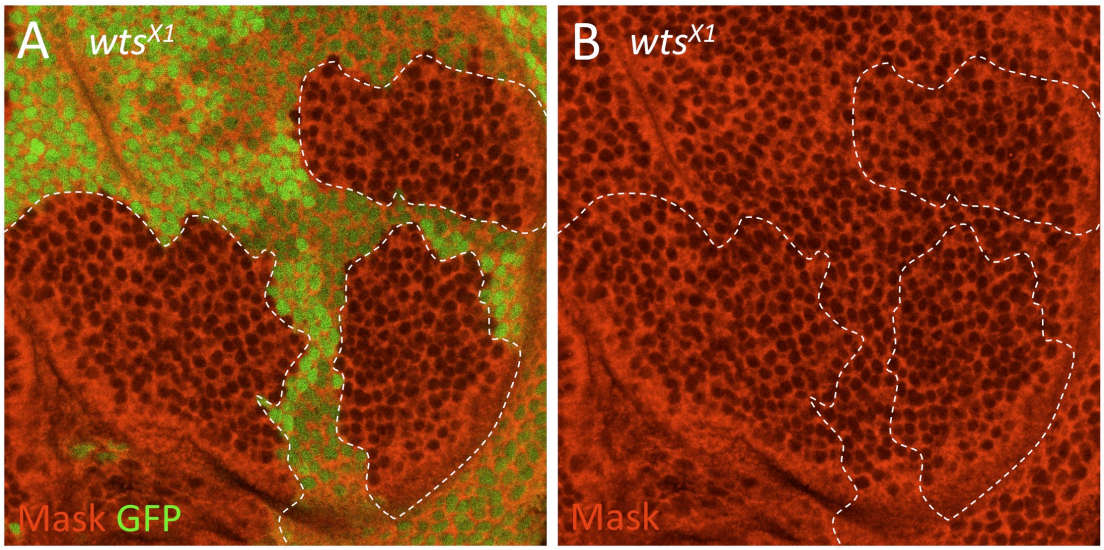

Figure 4.20: Wts does not regulate Mask localisation and level of expression
wts^{X1} FLP/FRT mutant clones (dotted line) in a third instar larva wing imaginal disc. The mutant clones are marked by the absence of GFP (A), and have no effect on Mask protein levels or localisation detected by immunostaining (B)

Chapter 5. Mask function in Yki/YAP regulation is conserved in humans

5.1 Mask proteins

Drosophila Mask is well conserved across metazoans and has two homologues in human: ANKHD1 or Mask1, and ANKRD17 or Mask2. The two human proteins are smaller than *Drosophila* Mask but both contain the 2 blocks of ankyrin repeats, the KH domain, and the putative NES and NLS, which are all highly conserved (Fig 5.1).

5.1.1 hMask1

Human Mask1 is a ubiquitously expressed protein of 2542 amino acids. One isoform of Mask1 (VBARP) has been shown to be important for cell survival and to prevent apoptosis (Miles et al., 2005). Other isoforms of Mask1 were found strongly upregulated during haematopoietic cell differentiation (Santos Duarte et al., 2005). A functional study of Mask1 was done following the track of *Drosophila* Mask genetic interaction with Corkscrew (Smith et al., 2002). Corkscrew homologue in human is the protein-tyrosine phosphatase SHP2 (Freeman et al., 1992). Like Csw, SHP2 promotes Ras/MAPK signaling. It regulates numerous processes like cell growth, differentiation, migration and death, and does not solely act through Ras/MAPK signaling (Feng, 1999). SHP2 has been implicated in human diseases, including 3 different types of leukemias and found overexpressed in leukemia cell lines (Grossmann et al., 2010; Neel et al., 2003). Traina *et al* investigated the potential link between Mask1 and SHP2 (Traina et al., 2006). They found that Mask1 was overexpressed in leukemia cell lines and samples from leukemia patients. Besides this, Mask1 co-immunoprecipitates with SHP2 in 2 different cell lines. However, this association was not found in 4 other leukemia cell lines with high levels of both proteins. Thus, there may be a link between Mask1 and SHP2 but it is not a clear one.

5.1.2 hMask2

Human Mask2, a protein of 2603 amino acids, was originally identified in a screen for genes that respond to retinoic acid (Forrester et al., 1996). It has two alternative

promoters, one of which is activated in the liver lineage, and one that drives Mask2 expression ubiquitously (Watt et al., 2001).

Mask2 was recently identified as a substrate of cyclinE/Cdk2, the cyclin/Cdk complex that promotes G1/S transition during the cell cycle (Deng et al., 2009). Deng *et al* show that Mask2 is essential to promote cell proliferation in cultured cells. Furthermore, Mask2 is found in the cytoplasm and associated with chromatin during all phases of the cell cycle except in mitosis, where it is still present but not chromatin associated. Deng *et al* find that Mask2 co-immunoprecipitates with DNA replication factors and conclude that Mask2 is a general cell cycle regulator of G1/S transition that may be directly involved in DNA replication. Another study published the same year describes Mask2 as an essential regulator of vascular development (Hou et al., 2009). Hou et al generated Mask2 deficient mice and found that homozygous mutant embryos die between embryonic day (E) 10.5 and E11.5. These Mask2 mutant embryos present growth retardation and defects in vasculogenesis, with a pale yolk sac due to poor blood circulation. Interestingly, this phenotype is similar, although less severe, to that of YAP, the human homologue of Yki: embryos mutant for YAP present severe defects in growth and yolk sac vasculogenesis (Morin-Kensicki et al., 2006). The fact that cells in Mask2 mutant embryos can proliferate until E11.5 is not consistent with a role of Mask2 as a general cell cycle regulator as proposed by Deng *et al*. However, the growth retardation phenotype is consistent with a role of Mask2 in controlling cell proliferation.

Ankyrin repeats
Nuclear Export Signal
Nuclear Localisation Signal
KH domain

* = identical residue
: = conserved substitution
. = semi-conserved substitution

A Ankyrin repeat block 1

```
hMask1  HNAGQV-DTRSLAEACSDGDVNAVRKLLDEG----RSVNEHTEEGESLLCLACSAGYYEL 253
hMask2  ANAGQS-DNRSLAEACSEGDVNAVRKLLIEG----RSVNEHTEEGESLLCLACSAGYYEL 282
dMask   PRDKNSGFSRSLVAACTDNDVNTVKRLLCKGNVNLNDAAASTDDGESLLSMACSAGYYEL 600
         .  :   .***. **:::.***:*::** :*    ...   *::*****.:*********

hMask1  AQVLLAMHAN-VEDRGNKGDITPLMAASSGGYLDIVKLLLLHDADVNSQSATGNTALTYA 312
hMask2  AQVLLAMHAN-VEDRGIKGDITPLMAAANGGHVKIVKLLLAHKADVNAQSSTGNTALTYA 341
dMask   AQVLLAMSAAQVEDKGQK-DSTPLMEAASAGHLDIVKLLLNHNADVNAHCATGNTPLMFA 659
        ******* *  ***:* * * **** *:..*::.****** *.****::.:****.* :*

hMask1  CAGGFVDIVKVLLNEGANIEDHNENGHTPLMEAASAGHVEVARVLLDHGAGINTHSNEFK 372
hMask2  CAGGYVDVVKVLLESGASIEDHNENGHTPLMEAGSAGHVEVARLLLENGAGINTHSNEFK 401
dMask   CAGGQVDVVKVLLKHGANVEEQNENGHTPLMEAASAGHVEVAKVLLEHGAGINTHSNEFK 719
        **** **:*****: **.:*::***********.********::**::************

hMask1  ESALTLACYKGHLDMVRFLLEAGADQEHKTDEMHTALMEACMDGHVEVARLLLDSGAQVN 432
hMask2  ESALTLACYKGHLEMVRFLLEAGADQEHKTDEMHTALMEACMDGHVEVARLLLDSGAQVN 461
dMask   ESALTLACYKGHLDMVRFLLQAGADQEHKTDEMHTALMEASMDGHVEVARLLLDSGAQVN 779
        *************:******:******************.******************

hMask1  MPADSFESPLTLAACGGHVELAALLIERGANLEEVNDEGYTPLMEAAREGHEEMVALLLA 492
hMask2  MPADSFESPLTLAACGGHVELAALLIERGASLEEVNDEGYTPLMEAAREGHEEMVALLLG 521
dMask   MPTDSFESPLTLAACGGHVELATLLIERGANIEEVNDEGYTPLMEAAREGHEEMVALLLS 839
        **:*******************:*******.:*************************.

hMask1  QGANINAQTEETQETALTLACCGGFSEVADFLIKAGADIELGCSTPLMEASQEGHLELVK 552
hMask2  QGANINAQTEETQETALTLACCGGFLEVADFLIKAGADIELGCSTPLMEAAQEGHLELVK 581
dMask   KGANINATTEETQETALTLACCGGFMEVAAFLIKEGANLELGASTPLMEASQEGHTDLVS 899
        :****** ***************** *** **** **::***.*******:**** :**.

hMask1  YLLASGANVHATTATGDTALTYACENGHTDVADVLLQAGADLEHESEGGRTPLMKAARAG 612
hMask2  YLLAAGANVHATTATGDTALTYACENGHTDVADVLLQAGADLEHESEGGRTPLMKAARAG 641
dMask   FLLKKKANVHAETQTGDTALTHACENGHTDAAGVLLSYGAELEHESEGGRTPLMKACRAG 959
        :**   ***** * *******:********.*.***. **:***************.***

hMask1  HLCTVQFLISKGANVNRATANNDHTVVSLACAGGHLAVVELLLAHGADPTHRLKDGSTML 672
hMask2  HVCTVQFLISKGANVNRTTANNDHTVLSLACAGGHLAVVELLLAHGADPTHRLKDGSTML 701
dMask   HLCTVKFLIQKGANVNKQTTSNDHTALSLACAGGHQSVVELLLKNNADPFHKLKDNSTML 1019
        *:***:***.******: *:.****.:******** :****** :.*** *:***.****

hMask1  IEAAKGGHTNVVSYLLDYPNN--VLSVPTTDVSQLPPPS---------------------- 709
hMask2  IEAAKGGHTSVVCYLLDYPNN--LLSAPPPDVTQLTPPS---------------------- 738
dMask   IEASKGGHTRVVELLFRYPNISPTENAASANVTQAAPTSNQPGPNQMRQKIMKQQLQHQL 1079
        ***:***** **  *: ***     .....:*:* .*.*

hMask1  ---------QDQSQVPRVPTH---------------------------------------- 721
hMask2  ---------HDLNRAPRVPVQ---------------------------------------- 750
dMask   QQLNAPPGLHELSEAARASNQQHFHQQQFSSAGNGSSNIVAMGTGDFLDAGELQLTATAG 1139
                :: ....*.. :
```

continued on next page →

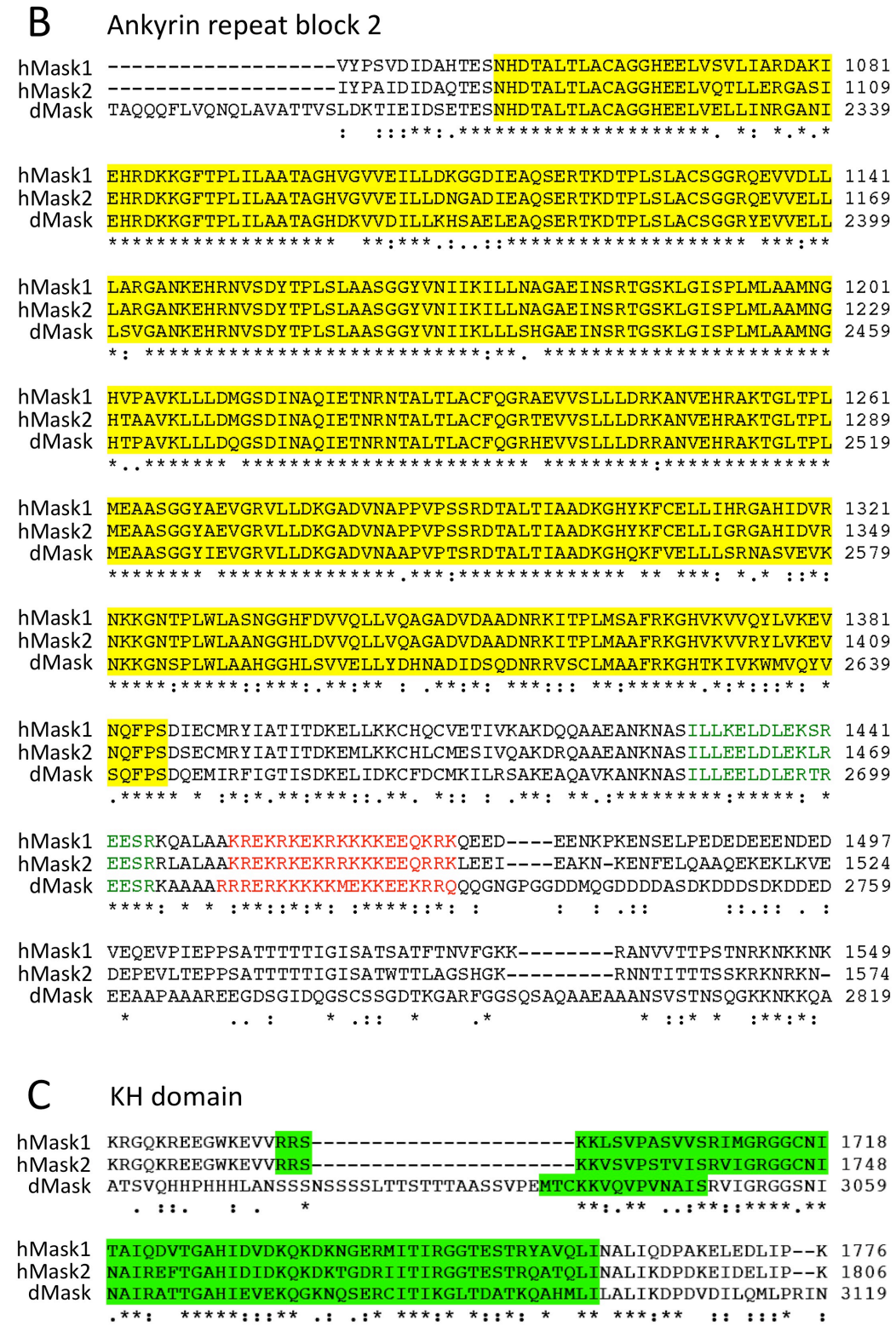

Figure 5.1: Mask protein is conserved in human
Sequence alignment of *Drosophila* Mask, human Mask1 and human Mask2 proteins, ClustalW2 program (Larkin et al., 2007). (A) Alignment of the first conserved block of ankyrin repeats (B) Alignment of the second conserved block of ankyrin repeats (C) Alignment of the KH domain region.

5.2 hMask proteins colocalise with YAP in human cells

In *Drosophila*, Mask colocalises and translocates with Yki into the nucleus. We examined Mask1 and Mask2 localisation in human cell cultures to determine if they behave the same as *Drosophila* Mask. YAP is known to become cytoplasmic upon cell-contact inhibition in certain human cancer cell lines, such as MCF10a cells (Zhao et al., 2007). We find that Mask1 and Mask2 co-localise with YAP in the cytoplasm of confluent MCF10a cells (Fig 5.2 A,B). By contrast, in malignant HEK293 cancer cells, which are resistant to contact inhibition, YAP is predominantly nuclear. In those cells, both Mask1 and Mask2 follow YAP pattern and localise in the nucleus (Fig 5.2 C,D). Note that Mask2 is more nuclear than Mask1. Translocation of Mask1, Mask2 and YAP from cytoplasm to nucleus is best observed in Caco2 cells, where the three proteins are cytoplasmic in confluent cells but strongly nuclear in less densely packed cells (Fig 5.2 E,E',E''). These results show that human Mask proteins, like their *Drosophila* counterpart, translocate with Yki/YAP between the cytoplasm and the nucleus in response to a stimulus, in this case cell-contact inhibition. Interestingly, hMask1 and hMask2 were sometimes observed with YAP at cell junctions (Fig 5.3)

Recent publications have shown that YAP is expressed in epithelial progenitor cells, where it is required and promotes cell proliferation (Camargo et al., 2007; Schlegelmilch et al., 2011; Zhang et al., 2011a). Epithelial tissue sections from human oesophagus were stained for Mask1, Mask2 and YAP by the Cancer Research UK Experimental HistoPathology laboratory. We find that the three proteins are strongly expressed in the basal cell layer of epithelial tissues – the zone of stem/progenitor cells (Fig 5.4). Note that in these tissue sections Mask2 appears more nuclear while Mask1 appears more cytoplasmic.

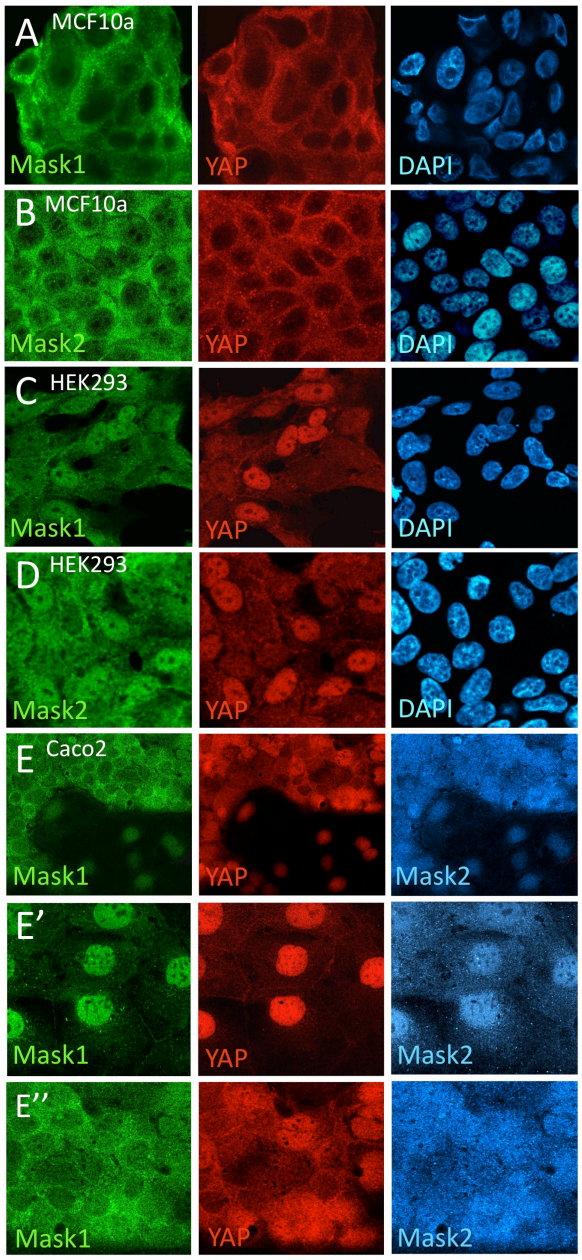

Figure 5.2: Human Mask proteins colocalise with YAP
Human cells immunostained for YAP, Mask1 and Mask2. Nuclei are stained with DAPI.
(A) Human Mask1 and YAP co-localise in the cytoplasm of MCF10A cells. (B) Human Mask2 and YAP co-localise in the cytoplasm of MCF10A cells. (C) Human Mask1 and YAP co-localise in the cytoplasm and nucleus of HEK293 cells. (D) Human Mask2 and YAP co-localise in the cytoplasm and nucleus of HEK293 cells, nuclei are stained with DAPI. (E) Human Mask1, Mask2 and YAP show similar redistribution from the nucleus to the cytoplasm upon contact inhibition in CACO2 cells (low magnification view). (E') Human Mask1, Mask2 and YAP co-localise in the nucleus in low-density Caco2 cells (high magnification view). (E'') Human Mask1, Mask2 and YAP co-localise in the cytoplasm in high-density Caco2 cells (high magnification view). Immunostainings in HEK293 and MCF10A cells were done in collaboration with Ruth Brain in the laboratory.

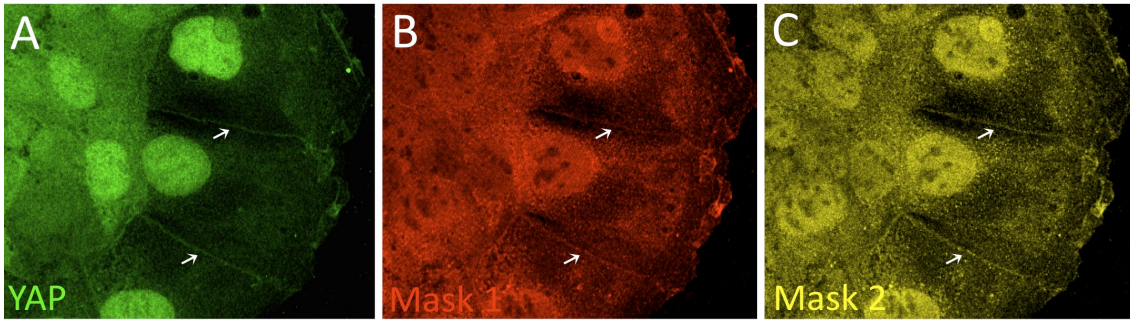

Figure 5.3: Mask protein are sometimes found with YAP at cell junctions
Caco2 cells immunostained for YAP (A), hMask1 (B), and hMask2 (C). Localisation of YAP and hMask proteins at cell junctions is indicated by arrows.

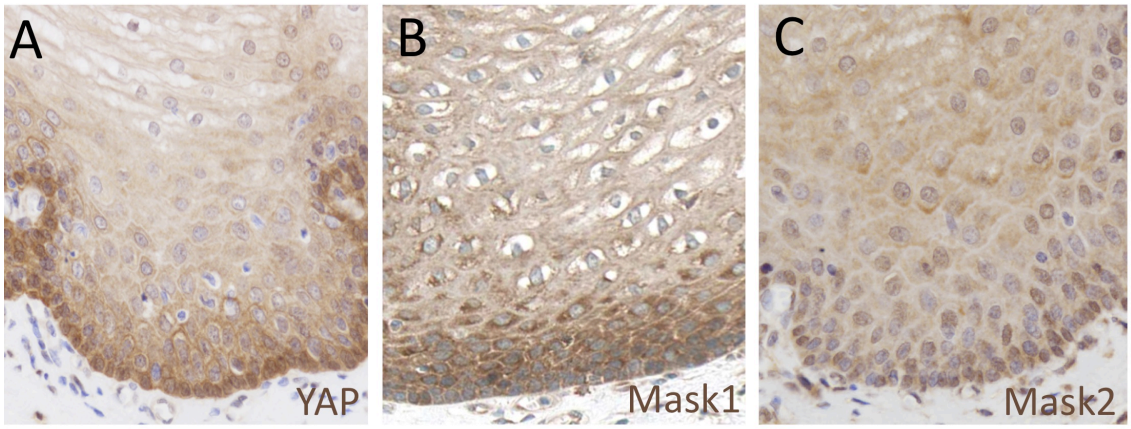

Figure 5.4: Human Mask proteins are coexpressed with YAP in epithelial stem cells
(A) YAP is mainly nuclear in the basal stem cell layer of human oesophageal epithelia.
(B) Mask1 is mainly cytoplasmic in the basal stem cell layer of human oesophageal epithelia.
(C) Mask2 is mainly nuclear in the basal stem cell layer of human oesophageal epithelia.

5.3 Mask 2 is essential for YAP transactivation activity

In order to test if human Mask proteins have a role in regulating Yki/YAP activity like their *Drosophila* homologue, we made use of a YAP-dependent transcription reporter assay (Zhao et al., 2008). HEK293T cells were transfected with a plasmid containing a *UAS.luciferase* reporter construct and a plasmid containing TEAD4 (Scalloped homologue) fused to the GAL4 DNA binding domain (G4-TEAD4). Transfection of G4-TEAD4 on its own was not able to drive significant expression of the *UAS.luciferase* reporter, but transfection of non-phosphorylatable Flag-tagged YAP^{5SA} together with G4-TEAD4 strongly induced expression of the reporter (Fig 5.5 A,B). We made use of siRNA pools targeting Mask1 and Mask2 to efficiently knock-down the two proteins (Fig 5.5 C) and found that knock-down of Mask1 had no effect on YAP-dependent transcription, but knockdown of Mask2 caused a significant decrease in reporter gene activity (Fig 5.5 B). This decrease is not due to an effect on YAP phosphorylation, as we used a non-phosphorylatable form of YAP. Hence, this result strongly suggests that hMask2 is required to promote YAP activity in the nucleus. Thus, *Drosophila* Mask function in controlling Yki/YAP activity is conserved in human and is ensured by Mask2.

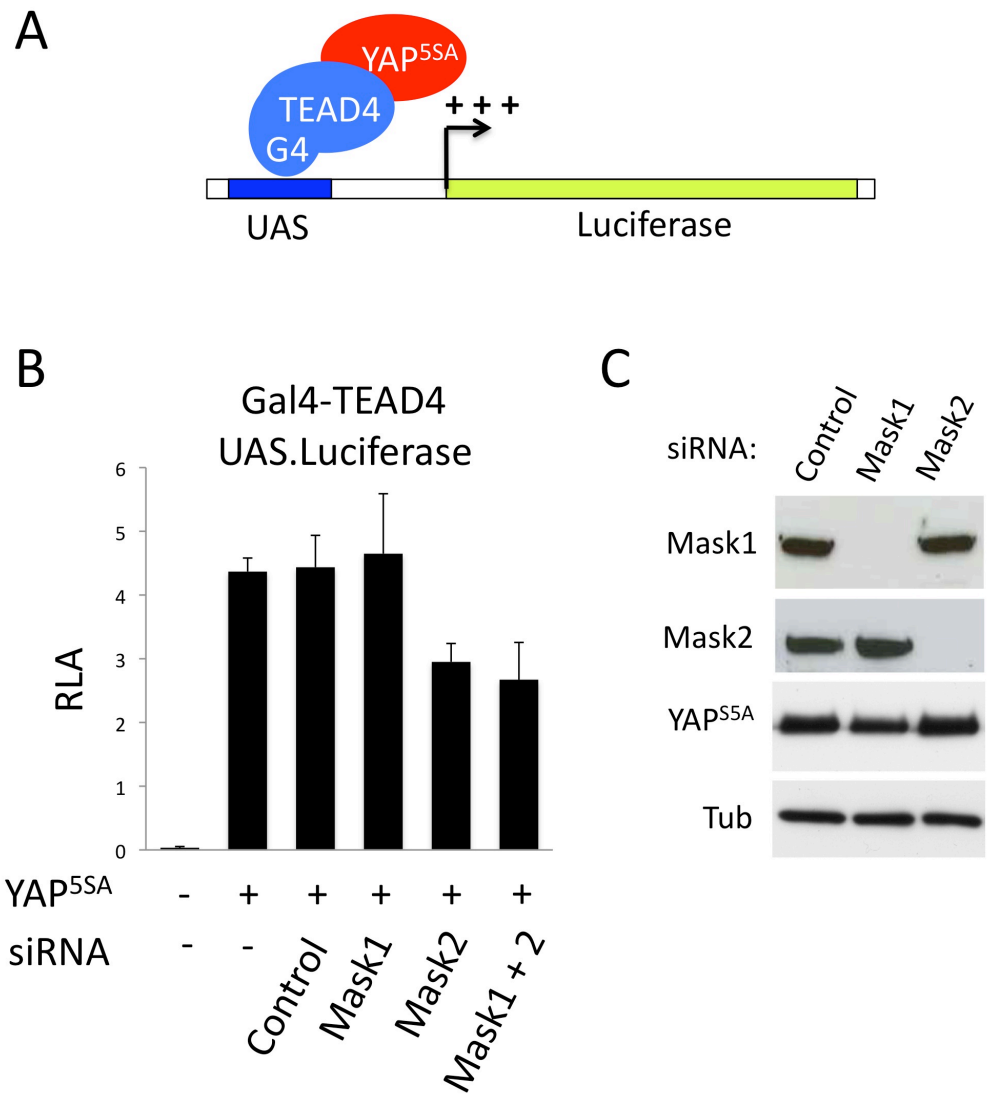

Figure 5.5: hMask2 regulates YAP transactivation activity
(A) Schematics of the TEAD/Luciferase reporter system: co-expression of YAP^{5SA} with G4-TEAD4 activates the transcription of the *UAS.Luciferase* reporter. (B) TEAD/Luciferase reporter assay results graph. Expression of YAP^{5SA} with the TEAD/Luciferase reporter produces a strong increase in Luciferase expression compared to G4-TEAD4 alone. siRNA mediated RNAi knock-down of hMask2, but not hMask1, significantly reduces YAP^{5SA} activity. (C) Control Western blot [from Ruth Brain] showing Mask1, Mask2 and YAP^{5SA} levels upon siRNA knock down of Mask1 or Mask2. Mask1 and 2 knock-down is efficient and it does not affect YAP^{5SA} stability.

Chapter 6. Discussion

Lessons from the screen

Our laboratory has carried out the first in vivo RNAi screen for novel regulators of tissue growth in *Drosophila*, making use of the newly developed VDRC transgenic RNAi library. This screen has successfully led to the discovery of conserved growth regulators including Mask and Kibra (Sidor et al, in preparation)(Genevet et al., 2010). The use of the wing, which is precisely patterned by several conserved signaling pathways, has allowed precise classification of candidate genes according to their growth phenotypes and other morphological defects. This classification has enabled us to link *mask* and *kibra* to the Hippo signaling pathway, as both genes presented cell proliferation phenotypes without patterning defects, like known genes from this pathway. Other candidate genes, some of which are being investigated in the laboratory, have been linked to all classes of phenotypes and may therefore lead to the identification of several new members of known signaling pathways.

We have estimated the efficiency of the RNAi screen at about 50%, meaning that 50% of the RNAi transgenic lines produce a knock-down sufficient to trigger a phenotype. In addition, our attempt to validate candidate genes by second RNAi transgenic lines has brought to light the importance of such confirmation to eliminate off-target and mis-expression artefacts. This validation process has not been done systematically by other laboratories who have carried out genome-wide RNAi screens using the VDRC library, and a significant proportion of their candidate genes may be false-positives (Mummery-Widmer et al., 2009; Neely et al., 2010a; Neely et al., 2010b; Schnorrer et al., 2010). Candidate gene validation will be made easier by the development of new libraries, such as the VDRC KK library, the NIG-fly library and the TRIP library (http://www.flyrnai.org). Thus, future in vivo RNAi screens should be carried out using multiple RNAi libraries in order to produce highly reliable lists of candidate genes free from false positives, and to reduce the number of false negatives by increasing the number of RNAi lines tested for each gene.

The *mask* gene acts in the Hippo signaling pathway

My results identify the *mask* gene as a novel component of the Hippo signaling pathway. Mask regulates Hippo pathway target gene expression and is required for Yki activity. It colocalises with Yki in both the cytoplasm and the nucleus and it binds to Yki through its conserved ankyrin repeats. In addition, Mask translocates simultaneously with Yki/YAP into the nucleus in *Drosophila* adult gut cells and upon cell contact inhibition in human cultured cells. Although Yki phosphorylation levels slightly increase in the absence of *mask*, suggesting a role for Mask in reducing Yki phosphorylation, the growth defects of *mask* mutant clones cannot be rescued either in *mask wts* double mutant clones, in which Yki is not phosphorylated by Wts, or by expression of non-phosphorylatable forms of Yki. Thus, *mask* function is required for non-phosphorylated Yki activity. Moreover, Mask is not required for Yki nuclear translocation as Yki is able to localise in the nucleus of *mask* mutant cells. Taken together, these data indicate that *mask* is required for Yki activity in the nucleus.

In support of this idea, we find that *mask* is required for activated Yki target gene upregulation in *wts* mutant clones. Furthermore, in human cells, RNAi knock-down of hMask2 reduces the activity of YAP in a transcriptional reporter assay, suggesting a conserved role for Mask proteins in the regulation of Yki/YAP transactivation activity. We have not yet detected any redundancy between hMask1 and hMask2 in the control of YAP dependent transcription activation, and we have not yet been able to demonstrate any role for hMask1 in YAP regulation. Nevertheless, both hMask1 and hMask2 are able to bind YAP in co-immunoprecipitation experiments (recent data from Ruth Brain), indicating that hMask1 is likely to regulate YAP. Moreover, both hMask1 and hMask2 are co-expressed with YAP in human epithelial progenitor cells. The Mask2 KO mouse phenotype resembles that of YAP KO but is less severe. It would be interesting to investigate the phenotype of Mask1/Mask2 double KO to see if it resembles more YAP phenotype.

Mask and RTK signaling

Mask was previously identified in a modifier screen for regulators of Receptor Tyrosine Kinase signaling but does not affect the activation of MAPK, suggesting a role in parallel or downstream of MAPK (Smith et al., 2002). Although our data show that

Mask acts in the Hippo signaling pathway, and although *mask* mutant phenotypes look distinctly different from Ras signaling mutant phenotypes, we cannot rule out some role for *mask* with the Ras signaling pathway, since *mask* does interact genetically with Ras signalling components in the fly eye. However, these results must be interpreted carefully as both Ras signaling and Hippo signaling are known to affect cell survival independently of each other. Indeed, genetic interactions between functionally unrelated genes affecting the same cellular processes are a known source of false positive artefacts in modifier screens (St Johnston, 2002).

Some 'crosstalk' between Hippo signaling and Ras signalling has been suggested from a study in human cultured cells, where YAP was found to induce the expression of the EGFR ligand amphiregulin (AREG) which mediates cell proliferation in a non-autonomous manner (Zhang et al., 2009b). In addition, Zhang et al show a genetic interaction between EGFR signaling and Hippo signaling in the *Drosophila* eye, where mutants of EGFR signaling components slightly enhance the undergrowth phenotype of Wts or Hpo overexpression. In the *Drosophila* midgut, loss of Hippo signaling in ECs leads to the production of EGFR ligands that activate EGFR signaling in neighbouring ISCs, shown by an increase in the levels of phosphorylation of the MAPK ERK (Ren et al., 2010). However, these non-autonomous effects of Hippo signaling on RTK signaling do not explain why Mask would affect RTK signaling without affecting MAPK activation.

Upstream regulation of Mask

Several lines of evidence suggest that Mask's subcellular localisation is regulated. The localisation of *Drosophila* Mask correlates with that of Yki, being more cytoplasmic in the wing disc, and more nuclear in S2R+ cells. In the *Drosophila* adult gut, Mask translocates with Yki to the nucleus in stressed guts and both proteins are upregulated in isolated enterocytes and progenitor cells in normal guts. As Mask seems to be co-regulated with Yki, we tested in the wing disc if Wts could regulate Mask. However, we found that Mask localisation was not affected in *wts* mutant clones, indicating that Mask is regulated in a Wts-independent manner. Nevertheless, Mask proteins relocalise in response to stress in *Drosophila* and in response to cell contact inhibition in human cells, indicating that they may be regulated by the same stimuli as Yki/YAP/TAZ.

In the *Drosophila* adult gut, increases in Yki levels and nuclear localisation are triggered by stress such as bacterial infection or toxic chemicals, to promote tissue regeneration. This response to stress involves the JNK signaling pathway, which was shown to promote Yki nuclear localisation in the adult gut but also in the larval wing disc, where Yki is also involved in regeneration upon tissue damage (Grusche et al., 2011; Shaw et al., 2010; Staley and Irvine, 2010). Indeed, damaging the wing disc by localised expression of pro-apoptotic genes such as *reaper* induces nuclear accumulation of Yki in cells neighbouring the wound. It will be interesting to examine Mask localisation in that context. Specifically, in order to test whether Mask can be regulated by JNK signaling, it will be interesting to investigate Mask localisation in clones of cells overexpressing an activated form of the JNK kinase Hemipterous (Hep) in the adult gut or in the larval wing disc where it has been shown to promote Yki nuclear translocation (Staley and Irvine, 2010; Sun and Irvine, 2011).

In human cultured cells, we have found that Mask proteins translocate like YAP and TAZ from the nucleus to the cytoplasm in response to cell contact inhibition. YAP/TAZ were shown to be sequestered in the cytoplasm upon cell contact inhibition via a Hippo signaling dependent mechanism, but also independently via binding to tight junction Angiomotin family proteins and to α-catenin (Schlegelmilch et al., 2011; Silvis et al., 2011; Zhao et al., 2011). It will be very interesting to investigate how Mask localisation is regulated upon cell contact inhibition, if it requires Hippo signaling, or if Mask proteins are regulated independently, maybe through interactions with adhesion or junction proteins such as E-Cadherin, catenins, or proteins from the Crumbs complex including Angiomotin. Indeed, hMask proteins were sometimes observed localised with YAP at cell junctions.

Mask is a novel transcriptional co-activator

Our data indicate that Mask is a transcriptional co-activator required for Yki/YAP to activate its target genes in the nucleus. These results are also supported by the fact that Mask proteins contain conserved NLS and NES sequences, and localise in the nucleus. Moreover, hMask2 was shown to associate with chromatin during all phases of the cell cycle except mitosis (Deng et al., 2009), which is consistent with a role for hMask2 in transcription regulation, as most transcription is stopped during mitosis and

transcription factors dissociate from chromatin during that phase (Gottesfeld and Forbes, 1997).

The presence of ankyrin repeats in Mask sequence does not suggest a specific function, as these protein-protein interaction domains are found in a wide variety of proteins of diverse localisations and functions (Michaely and Bennett, 1992). Interestingly however, ankyrin repeats can be found in nuclear proteins such as the yeast transcription factors SWI4 and SWI6 (Breeden and Nasmyth, 1987), and the mammalian GABPβ transcriptional co-activator (Batchelor et al., 1998).

More importantly, Mask contains a highly conserved KH domain. The KH domain is known to bind single-stranded RNA or DNA, and was first identified in the human heterogenous ribonucleoprotein K (hnRNP K) (Valverde et al., 2008). hnRNP K was initially described as an RNA/RNP associated protein, but was later shown to be a transcriptional activator able to bind single-stranded DNA (ssDNA) secondary structures in the *c-myc* and *VEGF* promoters via its KH domains (Michelotti et al., 1996; Takimoto et al., 1993; Tomonaga and Levens, 1996; Uribe et al., 2011). hnRNP K was also found to be activated upon DNA damage and required for p53 target gene expression, binding with p53 to target gene promoters in an interdependent manner (Moumen et al., 2005). Another example of transcriptional regulation involving a KH domain containing protein is the Ribosomal Protein S3 (RPS3), which is required for full activation of target genes by the NFκB transcription factor (Wan et al., 2007). RPS3 translocates into the nucleus upon stimuli known to activate NFκB signaling, and strongly stabilises NFκB binding to DNA. A parallel can be established between hnRNP K/p53, RPS3/ NFκB, and Mask/Yki pairs of proteins. In all three cases, a KH domain containing protein translocates into the nucleus upon the same stimuli as its transcription activation partner and is required for target gene expression. Wan et al propose the very attractive idea that the KH domain binds to certain actively transcribed genes, which have open ssDNA due to the action of RNA polymerase, and then help transcription factors to bind to ssDNA sequences. This is very speculative in the case of Mask and Yki/YAP, and more experiments should be carried out to understand the exact mechanism of Yki/YAP target gene activation by Mask proteins.

It will be interesting to test if *Drosophila* Mask associates in a complex with any of the known partners of Yki such as Sd, Hth and Wbp2. As Mask ankyrin-repeat-domain binding to Yki is weak, it may be difficult to detect interaction between Mask and other Yki partners if the interaction is not direct. Co-immunoprecipitation experiments could be carried out using a cross-linking technique to ensure that the whole complex is pulled down.

One key result that would confirm our hypothesis that Mask acts at the transcriptional level to activate Yki target genes would be to show the binding of Mask to a Yki/YAP target gene promoter. Thus, chromatin immunoprecipitation experiments should be carried out to test Mask binding to Yki/YAP target gene promoters both in *Drosophila* and human. For instance, it would be interesting to determine if *Drosophila* Mask binds the Hippo Responsive Element in *DIAP1* promoter. In human cells, microarray and Q-PCR analysis of gene expression upon YAP or hMask knock-down will shed more light on the regulation of gene expression by these proteins. Furthermore, chromatin immunoprecipitaion experiments in cells treated with Mask RNAi could also help determine if Yki/YAP binding to its target genes is dependent on Mask proteins or if Mask proteins have a different role in gene activation.

A new branch in Yki regulation?

The Hippo signaling pathway was initially thought of as a linear pathway, with upstream components regulation converging on Hpo, and a linear cascade of regulatory phosphorylations leading to Yki cytoplasmic retention. However, this view was progressively challenged with the discovery of new entry points in Yki regulation. The upstream component Ex was found to regulate Yki cytoplasmic retention downstream of Wts through direct binding, the proteins Dachs, Zyxin and Ajuba modulate Hippo signaling by regulating Wts stability and activity downstream of Hpo, and the protein Myopic represses Yki activity downstream of Wts. Mask also acts downstream of Wts and is regulated by different signals, independently from the Hippo signaling cascade. Thus, Mask could be another entry point in the regulation of Yki, on which would converge other signals (Fig 6.1). Considering the increasing evidence for roles of mammalian Hippo signaling in tissue growth control during embryonic development, but also tissue regeneration, control of stem-cell proliferation, and cancer development,

and considering that Mask proteins seem critical for Yki/YAP/TAZ function, Mask proteins may also be crucial in those processes, and understanding how Mask is regulated will give new insight into how Yki/YAP/TAZ activity is controlled.

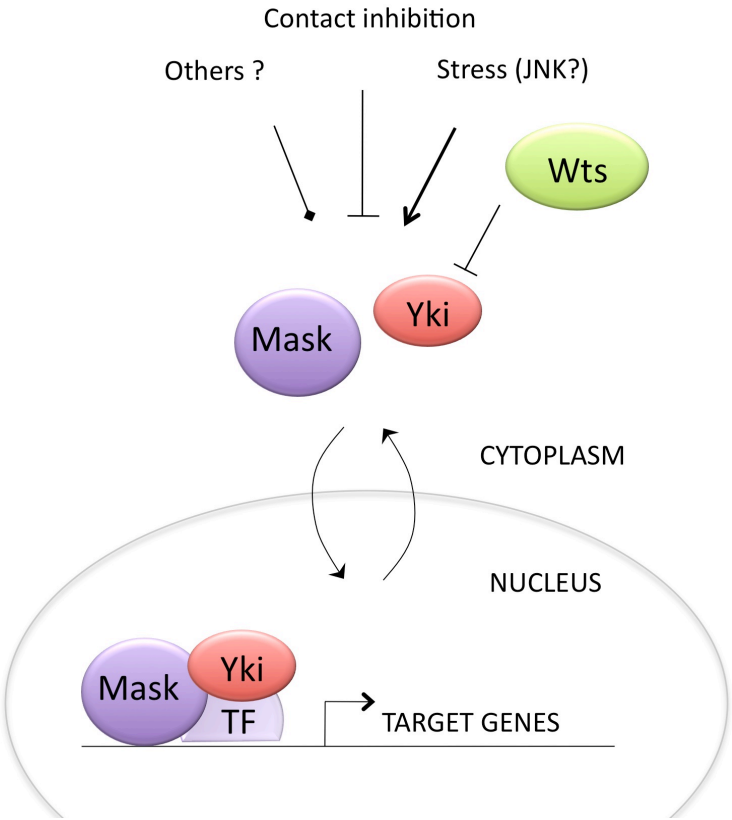

Figure 6.1: Model of Mask function in Yki regulation

Appendix

TABLE 2

OVERGROWTH CATEGORY			
CG number	gene	NIG-FLY RNAi lines x *hh.gal4*: PHENOTYPE	
CG17245	PlexinB	17245R-4(III)	no phenotype
		17245-2R-2(III)	no phenotype
		17245R-2 (II)	no phenotype
		17245-3R (III)	no phenotype
		17245-3R-2 (III)	lethal
		17245-2R-3 (III)	no phenotype
CG17342	Lk6	17342R-2 (II)	no phenotype
		17342R-1 (III)	no phenotype
CG14023		14023R-1 (II)	no phenotype
		14023R-3 (II)	no phenotype
CG11567	cyp450	11567R-4 (III)	no phenotype
		11567R-1 (III)	no phenotype
CG30078	(novel kinase)	16805R-4 (III)	no phenotype
CG1216	mrityu	1216R-2 (II)	no phenotype
		1216R-1 (III)	no phenotype
UNDERGROWTH CATEGORY			
CG12217	PpV	12217R-1 (II)	semi-lethal, undergrowth, blisters
		12217R-2 (II)	lethal
CG10289	SAP	10289R-1 (II)	no phenotype
		10289R-2 (II)	no phenotype
CG12139	LRP	12139R-2 (II)	undergrowth
		12139R-1 (II)	undergrowth
CG7225	Wbl	7225R-2 (III)	no phenotype
		7225R-1 (II)	no phenotype
CG6963	Casein kinase	6963R-1 (III)	undergrowth
		6963R-3 (III)	undergrowth
CG6355	fab1	6355R-2 (II)	pigmentation defect?
CG3479	osp (PH)	3479R-2 (II)	undergrowth
		3479R-1 (II)	undergrowth
CG5003		5003R-1 (III)	folded wings, crossvein defects
		5003R-3 (I)	semi lethal, folded wings, undergrowth
CG4792		4792R-2 (X)	no phenotype
CG7693	Fray	7693R-2 (III)	no phenotype
		7693R-3 (III)	mild undergrowth
CG6313	Mask	6313R-2 (II)	lethal
		6313R-3 (II)	semi-lethal, strong undergrowth
		6268R-2 (II)	mild undergrowth

continued on the next page

TABLE 2 - continued

CG17293	(wd40 domain)	17293R-4 (II)	undergrowth
CG9063		9063R2(II)	no phenotype
		9063R4(III)	lethal
CG17599		17599R-2 (II)	no phenotype
		17599R-1 (III)	no phenotype
CG32018	zyx102F	32018R-1 (II)	Undergrowth
		32018R-3 (III)	Undergrowth
CG3825	PP1 15A	3825R3(II)	mild undergrowth ?
		3825R2(III)	undergrowth, rounded and slightly Cy
CG9732	midnolin	9732R2(III)	mild undergrowth, few blisters
CG7111	rack1	7111R1(II)	undergrowth
		7111R2(X)	mild undergrowth ?
CG32685	zap3	2971R2(II)	undergrowth
CG11722		11722R1(III)	undergrowth
		11722R1(III)	undergrowth, less dense hair
CG10579	Pftaire	10579R2(III)	shape defects
		10579R3(II)	shape defects
CG11137		11137R2(III)	semilethal, undergrowth
		11137R3(III)	semilethal, undergrowth
CG8721	Odc1	8721R3(III)	no phenotype
		8721R1(III)	no phenotype
CG18005		18005R-3(III)	lethal
		18005R1(III)	lethal
CG13139	Lix1	13139R1	shape defects
		13139R3(III)	shape defects
CG11006	mucin	11006R1(III)	undergrowth, a few nicks
		11006R2(II)	mild undergrowth
CG15143		15143R-3 (III)	no phenotype
		15143R-2 (III)	no phenotype
CG7085		7085R-4 (II)	no phenotype
CG11130		11130R-1 (III)	lethal
		11130R-3 (III)	lethal
CG2736		2736R-2 (II)	no phenotype
		2736R-3 (III)	no phenotype
CG30092	jbug	11605R-1 (II)	undergrowth
		11605R-2 (III)	undergrowth
CG30334		30334R-1 (III)	no phenotype
		30334R-4 (X)	no phenotype

Table 2: List of candidates from the screen re-tested with NIG-FLY 2nd hairpin lines
Validated hits in yellow, lethal phenotypes in grey

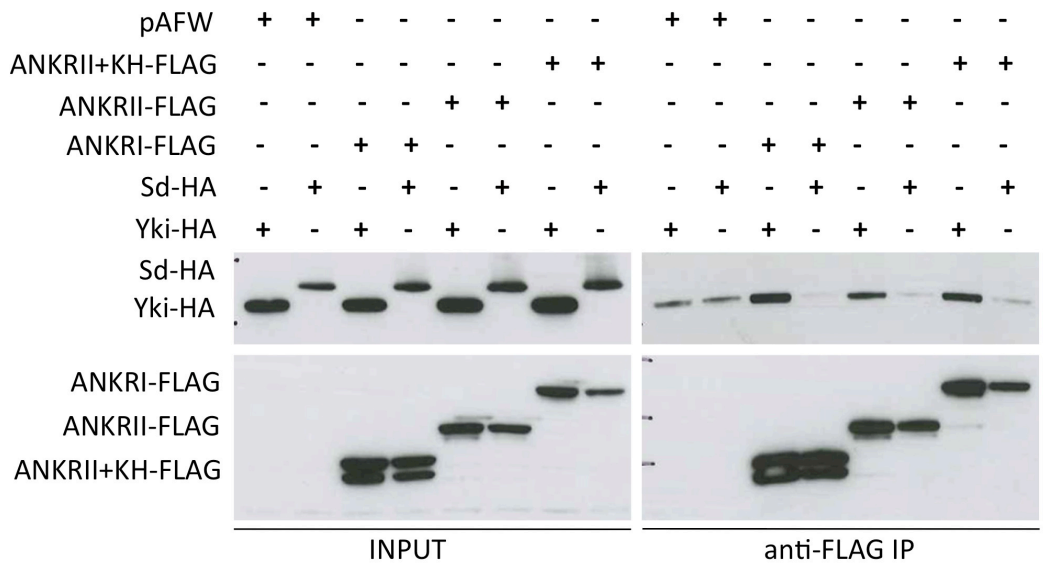

Figure A.1: Mask conserved domains do not bind Sd
Co-immunoprecipitation (Co-IP) of HA-tagged Sd or HA-tagged Yki with Flag-tagged Mask ankyrin repeat domains (ANKRI, ANKRII, or ANKRII+KH). Yki-HA but not Sd-HA binds to Mask ankyrin repeats.

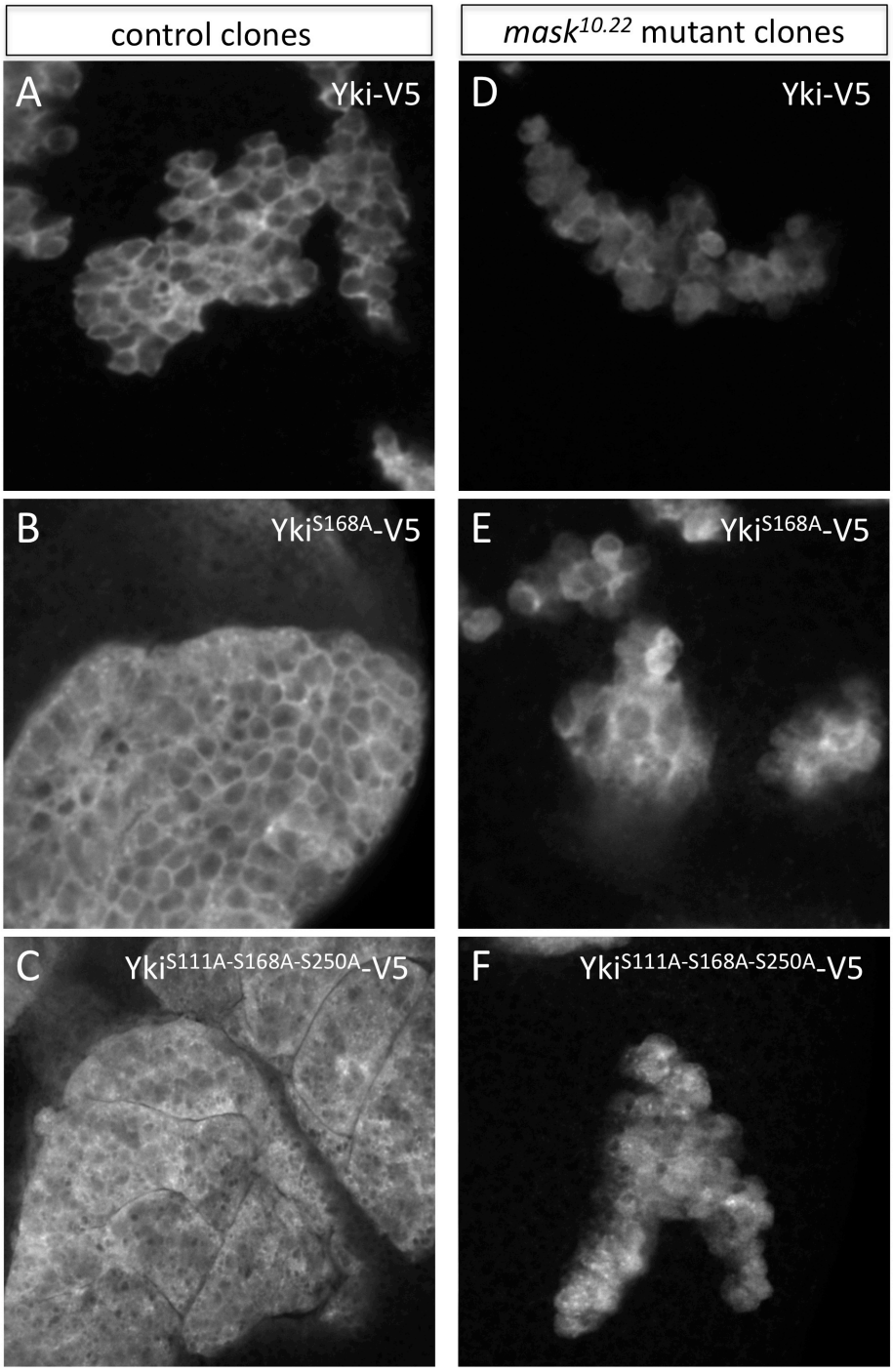

Figure A.2: Wild-type and mutant forms of Yki can still localise in the nucleus in the absence of Mask

MARCM clones expressing different V5-tagged forms of Yki in third instar larvae wing discs immunostained for V5.

(A) Yki-V5 localises in the cytoplasm and the nucleus

(B) Yki^{S168A}-V5 localises more strongly in the nucleus than Yki-V5

(C) Yki^{3SA}-V5 localises more strongly in the nucleus than Yki-V5 and Yki^{S168A}-V5

(D-F) In the absence of *mask*, the 3 forms of Yki are still able to localise in the nucleus

Reference List

Affolter, M. and Basler, K. (2007). The Decapentaplegic morphogen gradient: from pattern formation to growth regulation. In *Nature reviews Genetics*, vol. 8 (ed., pp. 663-74.

Alarcón, C., Zaromytidou, A.-I., Xi, Q., Gao, S., Yu, J., Fujisawa, S., Barlas, A., Miller, A. N., Manova-Todorova, K., Macias, M. J. et al. (2009). Nuclear CDKs drive Smad transcriptional activation and turnover in BMP and TGF-beta pathways. In *Cell*, vol. 139 (ed., pp. 757-69.

Allard, J. D., Chang, H. C., Herbst, R., McNeill, H. and Simon, M. A. (1996). The SH2-containing tyrosine phosphatase corkscrew is required during signaling by sevenless, Ras1 and Raf. In *Development*, vol. 122 (ed., pp. 1137-46.

Angus, L., Moleirinho, S., Herron, L., Sinha, A., Zhang, X., Niestrata, M., Dholakia, K., Prystowsky, M. B., Harvey, K. F., Reynolds, P. A. et al. (2011). Willin/FRMD6 expression activates the Hippo signaling pathway kinases in mammals and antagonizes oncogenic YAP. In *Oncogene*, (ed.

Axelrod, J. D. (2009). Progress and challenges in understanding planar cell polarity signaling. In *Semin Cell Dev Biol*, vol. 20 (ed., pp. 964-71.

Azpiazu, N. and Morata, G. (2000). Function and regulation of homothorax in the wing imaginal disc of Drosophila. In *Development*, vol. 127 (ed., pp. 2685-93.

Badouel, C., Gardano, L., Amin, N., Garg, A., Rosenfeld, R., Le Bihan, T. and McNeill, H. (2009). The FERM-domain protein Expanded regulates Hippo pathway activity via direct interactions with the transcriptional activator Yorkie. In *Dev Cell*, vol. 16 (ed., pp. 411-20.

Basler, K. and Struhl, G. (1994). Compartment boundaries and the control of Drosophila limb pattern by hedgehog protein. In *Nature*, vol. 368 (ed., pp. 208-14.

Batchelor, A. H., Piper, D. E., de la Brousse, F. C., McKnight, S. L. and Wolberger, C. (1998). The structure of GABPalpha/beta: an ETS domain- ankyrin repeat heterodimer bound to DNA. In *Science*, vol. 279 (ed., pp. 1037-41.

Baumgartner, R., Poernbacher, I., Buser, N., Hafen, E. and Stocker, H. (2010). The WW domain protein Kibra acts upstream of Hippo in Drosophila. In *Dev Cell*, vol. 18 (ed., pp. 309-16.

Bellosta, P. and Gallant, P. (2010). Myc Function in Drosophila. In *Genes Cancer*, vol. 1 (ed., pp. 542-546.

Bennett, F. C. and Harvey, K. F. (2006). Fat cadherin modulates organ size in Drosophila via the Salvador/Warts/Hippo signaling pathway. In *Current biology : CB*, vol. 16 (ed., pp. 2101-10.

Blair, S. S., Brower, D. L., Thomas, J. B. and Zavortink, M. (1994). The role of apterous in the control of dorsoventral compartmentalization and PS integrin gene expression in the developing wing of Drosophila. In *Development*, vol. 120 (ed., pp. 1805-15.

Bohn, H. (1967). Transplantations experimente mit interkalarer Regeneration zum Nachweis eines sich segmental wiederholenden Gradienten im Bein von Leucophaea (Blattaria). Zool. Anz. 30,499-508.

Brand, A. H. and Perrimon, N. (1993). Targeted gene expression as a means of altering cell fates and generating dominant phenotypes. In *Development*, vol. 118 (ed., pp. 401-15.

Breeden, L. and Nasmyth, K. (1987). Cell cycle control of the yeast HO gene: cis- and trans-acting regulators. In *Cell*, vol. 48 (ed., pp. 389-97.
Brennecke, J., Hipfner, D. R., Stark, A., Russell, R. B. and Cohen, S. M. (2003). bantam encodes a developmentally regulated microRNA that controls cell proliferation and regulates the proapoptotic gene hid in Drosophila. In *Cell*, vol. 113 (ed., pp. 25-36.
Brittle, A. L., Repiso, A., Casal, J., Lawrence, P. A. and Strutt, D. (2010). Four-jointed modulates growth and planar polarity by reducing the affinity of dachsous for fat. In *Current biology : CB*, vol. 20 (ed., pp. 803-10.
Brodsky, M. H. and Steller, H. (1996). Positional information along the dorsal-ventral axis of the Drosophila eye: graded expression of the four-jointed gene. In *Developmental Biology*, vol. 173 (ed., pp. 428-46.
Bryant, P. J., Huettner, B., Held, L. I., Ryerse, J. and Szidonya, J. (1988). Mutations at the fat locus interfere with cell proliferation control and epithelial morphogenesis in Drosophila. In *Developmental Biology*, vol. 129 (ed., pp. 541-54.
Bryant, P. J. and Simpson, P. (1984). Intrinsic and extrinsic control of growth in developing organs. In *Q Rev Biol*, vol. 59 (ed., pp. 387-415.
Camargo, F. D., Gokhale, S., Johnnidis, J. B., Fu, D., Bell, G. W., Jaenisch, R. and Brummelkamp, T. R. (2007). YAP1 increases organ size and expands undifferentiated progenitor cells. In *Current biology : CB*, vol. 17 (ed., pp. 2054-60.
Campbell, S., Inamdar, M., Rodrigues, V., Raghavan, V., Palazzolo, M. and Chovnick, A. (1992). The scalloped gene encodes a novel, evolutionarily conserved transcription factor required for sensory organ differentiation in Drosophila. In *Genes Dev*, vol. 6 (ed., pp. 367-79.
Casares, F. and Mann, R. S. (2000). A dual role for homothorax in inhibiting wing blade development and specifying proximal wing identities in Drosophila. In *Development*, vol. 127 (ed., pp. 1499-508.
Chan, S. W., Lim, C. J., Huang, C., Chong, Y. F., Gunaratne, H. J., Hogue, K. A., Blackstock, W. P., Harvey, K. F. and Hong, W. (2011). WW domain-mediated interaction with Wbp2 is important for the oncogenic property of TAZ. In *Oncogene*, vol. 30 (ed., pp. 600-10.
Chen, C.-L., Gajewski, K. M., Hamaratoglu, F., Bossuyt, W., Sansores-Garcia, L., Tao, C. and Halder, G. (2010). The apical-basal cell polarity determinant Crumbs regulates Hippo signaling in Drosophila. In *Proceedings of the National Academy of Sciences of the United States of America*, vol. 107 (ed., pp. 15810-5.
Chen, H. I., Einbond, A., Kwak, S. J., Linn, H., Koepf, E., Peterson, S., Kelly, J. W. and Sudol, M. (1997). Characterization of the WW domain of human yes-associated protein and its polyproline-containing ligands. In *J Biol Chem*, vol. 272 (ed., pp. 17070-7.
Chishti, A. H., Kim, A. C., Marfatia, S. M., Lutchman, M., Hanspal, M., Jindal, H., Liu, S. C., Low, P. S., Rouleau, G. A., Mohandas, N. et al. (1998). The FERM domain: a unique module involved in the linkage of cytoplasmic proteins to the membrane. In *Trends Biochem Sci*, vol. 23 (ed., pp. 281-2.
Cho, E., Feng, Y., Rauskolb, C., Maitra, S., Fehon, R. and Irvine, K. D. (2006). Delineation of a Fat tumor suppressor pathway. In *Nat Genet*, vol. 38 (ed., pp. 1142-50.
Cho, E. and Irvine, K. D. (2004). Action of fat, four-jointed, dachsous and dachs in distal-to-proximal wing signaling. In *Development*, vol. 131 (ed., pp. 4489-500.

Clark, H. F., Brentrup, D., Schneitz, K., Bieber, A., Goodman, C. and Noll, M. (1995). Dachsous encodes a member of the cadherin superfamily that controls imaginal disc morphogenesis in Drosophila. In *Genes Dev*, vol. 9 (ed., pp. 1530-42.
Colombani, J., Polesello, C., Josué, F. and Tapon, N. (2006). Dmp53 activates the Hippo pathway to promote cell death in response to DNA damage. In *Current biology : CB*, vol. 16 (ed., pp. 1453-8.
Crozatier, M., Glise, B. and Vincent, A. (2004). Patterns in evolution: veins of the Drosophila wing. In *Trends Genet*, vol. 20 (ed., pp. 498-505.
Das Thakur, M., Feng, Y., Jagannathan, R., Seppa, M. J., Skeath, J. B. and Longmore, G. D. (2010). Ajuba LIM proteins are negative regulators of the Hippo signaling pathway. *Curr Biol* **20**, 657-62.
Datar, S. A., Jacobs, H. W., de la Cruz, A. F., Lehner, C. F. and Edgar, B. A. (2000). The Drosophila cyclin D-Cdk4 complex promotes cellular growth. In *EMBO J*, vol. 19 (ed., pp. 4543-54.
Deng, M., Li, F., Ballif, B. A., Li, S., Chen, X., Guo, L. and Ye, X. (2009). Identification and functional analysis of a novel cyclin e/cdk2 substrate ankrd17. In *J Biol Chem*, vol. 284 (ed., pp. 7875-88.
Diaz-Benjumea, F. J. and Cohen, S. M. (1993). Interaction between dorsal and ventral cells in the imaginal disc directs wing development in Drosophila. In *Cell*, vol. 75 (ed., pp. 741-52.
Diaz-Benjumea, F. J. and Cohen, S. M. (1995). Serrate signals through Notch to establish a Wingless-dependent organizer at the dorsal/ventral compartment boundary of the Drosophila wing. In *Development*, vol. 121 (ed., pp. 4215-25.
Dietzl, G., Chen, D., Schnorrer, F., Su, K.-C., Barinova, Y., Fellner, M., Gasser, B., Kinsey, K., Oppel, S., Scheiblauer, S. et al. (2007). A genome-wide transgenic RNAi library for conditional gene inactivation in Drosophila. In *Nature*, vol. 448 (ed., pp. 151-6.
Dittmer, J. E., Goss, R. J. and Dinsmore, C. E. (1974). The growth of infant hearts grafted to young and adult rats. In *Am J Anat*, vol. 141 (ed., pp. 155-60.
Dong, J., Feldmann, G., Huang, J., Wu, S., Zhang, N., Comerford, S. A., Gayyed, M. F., Anders, R. A., Maitra, A. and Pan, D. (2007). Elucidation of a universal size-control mechanism in Drosophila and mammals. In *Cell*, vol. 130 (ed., pp. 1120-33.
Doroquez, D. B. and Rebay, I. (2006). Signal integration during development: mechanisms of EGFR and Notch pathway function and cross-talk. In *Critical Reviews in Biochemistry and Molecular Biology*, vol. 41 (ed., pp. 339-85.
Driever, W. and Nüsslein-Volhard, C. (1988). The bicoid protein determines position in the Drosophila embryo in a concentration-dependent manner. In *Cell*, vol. 54 (ed., pp. 95-104.
Dupont, S., Morsut, L., Aragona, M., Enzo, E., Giulitti, S., Cordenonsi, M., Zanconato, F., Le Digabel, J., Forcato, M., Bicciato, S. et al. (2011). Role of YAP/TAZ in mechanotransduction. In *Nature*, vol. 474 (ed., pp. 179-83.
Fagotto, F. and Gumbiner, B. M. (1996). Cell contact-dependent signaling. In *Developmental Biology*, vol. 180 (ed., pp. 445-54.
Fankhauser, G. (1941). The Frequency of Polyploidy and Other Spontaneous Aberrations of Chromosome Number among Larvae of the Newt, Triturus Viridescens. In *Proceedings of the National Academy of Sciences of the United States of America*, vol. 27 (ed., pp. 507-12.
Feng, G. S. (1999). Shp-2 tyrosine phosphatase: signaling one cell or many. In *Exp Cell Res*, vol. 253 (ed., pp. 47-54.

Feng, Y. and Irvine, K. D. (2007). Fat and expanded act in parallel to regulate growth through warts. In *Proceedings of the National Academy of Sciences of the United States of America*, vol. 104 (ed., pp. 20362-7.
Feng, Y. and Irvine, K. D. (2009). Processing and phosphorylation of the Fat receptor. In *Proceedings of the National Academy of Sciences of the United States of America*, vol. 106 (ed., pp. 11989-94.
Fernández, B. G., Gaspar, P., Brás-Pereira, C., Jezowska, B., Rebelo, S. R. and Janody, F. (2011). Actin-Capping Protein and the Hippo pathway regulate F-actin and tissue growth in Drosophila. In *Development*, vol. 138 (ed., pp. 2337-46.
Ferrigno, O., Lallemand, F., Verrecchia, F., L'Hoste, S., Camonis, J., Atfi, A. and Mauviel, A. (2002). Yes-associated protein (YAP65) interacts with Smad7 and potentiates its inhibitory activity against TGF-beta/Smad signaling. In *Oncogene*, vol. 21 (ed., pp. 4879-84.
Forrester, L. M., Nagy, A., Sam, M., Watt, A., Stevenson, L., Bernstein, A., Joyner, A. L. and Wurst, W. (1996). An induction gene trap screen in embryonic stem cells: Identification of genes that respond to retinoic acid in vitro. In *Proceedings of the National Academy of Sciences of the United States of America*, vol. 93 (ed., pp. 1677-82.
Freeman, M. (1996). Reiterative use of the EGF receptor triggers differentiation of all cell types in the Drosophila eye. In *Cell*, vol. 87 (ed., pp. 651-60.
Freeman, R. M., Plutzky, J. and Neel, B. G. (1992). Identification of a human src homology 2-containing protein-tyrosine-phosphatase: a putative homolog of Drosophila corkscrew. In *Proceedings of the National Academy of Sciences of the United States of America*, vol. 89 (ed., pp. 11239-43.
French, V., Bryant, P. J. and Bryant, S. V. (1976). Pattern regulation in epimorphic fields. In *Science*, vol. 193 (ed., pp. 969-81.
Genevet, A., Polesello, C., Blight, K., Robertson, F., Collinson, L. M., Pichaud, F. and Tapon, N. (2009). The Hippo pathway regulates apical-domain size independently of its growth-control function. In *Journal of Cell Science*, vol. 122 (ed., pp. 2360-70.
Genevet, A. and Tapon, N. (2011). The Hippo pathway and apico-basal cell polarity. In *Biochem J*, vol. 436 (ed., pp. 213-24.
Genevet, A., Wehr, M. C., Brain, R., Thompson, B. J. and Tapon, N. (2010). Kibra is a regulator of the Salvador/Warts/Hippo signaling network. In *Dev Cell*, vol. 18 (ed., pp. 300-8.
Gilbert, M. M., Tipping, M., Veraksa, A. and Moberg, K. H. (2011). A Screen for Conditional Growth Suppressor Genes Identifies the Drosophila Homolog of HD-PTP as a Regulator of the Oncoprotein Yorkie. In *Dev Cell*, vol. 20 (ed., pp. 700-12.
Gottesfeld, J. M. and Forbes, D. J. (1997). Mitotic repression of the transcriptional machinery. In *Trends Biochem Sci*, vol. 22 (ed., pp. 197-202.
Goulev, Y., Fauny, J. D., Gonzalez-Marti, B., Flagiello, D., Silber, J. and Zider, A. (2008). SCALLOPED interacts with YORKIE, the nuclear effector of the hippo tumor-suppressor pathway in Drosophila. In *Current biology : CB*, vol. 18 (ed., pp. 435-41.
Grossmann, K. S., Rosário, M., Birchmeier, C. and Birchmeier, W. (2010). The tyrosine phosphatase Shp2 in development and cancer. In *Adv Cancer Res*, vol. 106 (ed., pp. 53-89.
Grusche, F. A., Degoutin, J. L., Richardson, H. E. and Harvey, K. F. (2011). The Salvador/Warts/Hippo pathway controls regenerative tissue growth in Drosophila melanogaster. In *Developmental Biology*, vol. 350 (ed., pp. 255-66.

Grzeschik, N. A., Parsons, L. M., Allott, M. L., Harvey, K. F. and Richardson, H. E. (2010). Lgl, aPKC, and Crumbs Regulate the Salvador/Warts/Hippo Pathway through Two Distinct Mechanisms. In *Current biology : CB*, (ed.

Hafen, E., Basler, K., Edstroem, J. E. and Rubin, G. M. (1987). Sevenless, a cell-specific homeotic gene of Drosophila, encodes a putative transmembrane receptor with a tyrosine kinase domain. In *Science*, vol. 236 (ed., pp. 55-63.

Halder, G. and Johnson, R. L. (2011). Hippo signaling: growth control and beyond. In *Development*, vol. 138 (ed., pp. 9-22.

Halder, G., Polaczyk, P., Kraus, M. E., Hudson, A., Kim, J., Laughon, A. and Carroll, S. (1998). The Vestigial and Scalloped proteins act together to directly regulate wing-specific gene expression in Drosophila. In *Genes Dev*, vol. 12 (ed., pp. 3900-9.

Hamaratoglu, F., Willecke, M., Kango-Singh, M., Nolo, R., Hyun, E., Tao, C., Jafar-Nejad, H. and Halder, G. (2006). The tumour-suppressor genes NF2/Merlin and Expanded act through Hippo signalling to regulate cell proliferation and apoptosis. In *Nat Cell Biol*, vol. 8 (ed., pp. 27-36.

Harrison, D. A. and Perrimon, N. (1993). Simple and efficient generation of marked clones in Drosophila. In *Current biology : CB*, vol. 3 (ed., pp. 424-33.

Harvey, K. and Tapon, N. (2007). The Salvador-Warts-Hippo pathway - an emerging tumour-suppressor network. In *Nat Rev Cancer*, vol. 7 (ed., pp. 182-91.

Harvey, K. F., Pfleger, C. M. and Hariharan, I. K. (2003). The Drosophila Mst ortholog, hippo, restricts growth and cell proliferation and promotes apoptosis. In *Cell*, vol. 114 (ed., pp. 457-67.

Herbst, R., Carroll, P. M., Allard, J. D., Schilling, J., Raabe, T. and Simon, M. A. (1996). Daughter of sevenless is a substrate of the phosphotyrosine phosphatase Corkscrew and functions during sevenless signaling. In *Cell*, vol. 85 (ed., pp. 899-909.

Herranz, H., Hong, X., Pérez, L., Ferreira, A., Olivieri, D., Cohen, S. M. and Milán, M. (2010). The miRNA machinery targets Mei-P26 and regulates Myc protein levels in the Drosophila wing. In *EMBO J*, vol. 29 (ed., pp. 1688-98.

Hietakangas, V. and Cohen, S. M. (2009). Regulation of tissue growth through nutrient sensing. In *Annu Rev Genet*, vol. 43 (ed., pp. 389-410.

Hipfner, D. R., Weigmann, K. and Cohen, S. M. (2002). The bantam gene regulates Drosophila growth. In *Genetics*, vol. 161 (ed., pp. 1527-37.

Horn, T. and Boutros, M. (2010). E-RNAi: a web application for the multi-species design of RNAi reagents--2010 update. In *Nucleic Acids Res*, vol. 38 (ed., pp. W332-9.

Hou, S.-C., Chan, L.-W., Chou, Y.-C., Su, C.-Y., Chen, X., Shih, Y.-L., Tsai, P.-C., Shen, C.-K. J. and Yan, Y.-T. (2009). Ankrd17, an ubiquitously expressed ankyrin factor, is essential for the vascular integrity during embryogenesis. In *FEBS Lett*, vol. 583 (ed., pp. 2765-71.

Huang, J., Wu, S., Barrera, J., Matthews, K. and Pan, D. (2005). The Hippo signaling pathway coordinately regulates cell proliferation and apoptosis by inactivating Yorkie, the Drosophila Homolog of YAP. In *Cell*, vol. 122 (ed., pp. 421-34.

Ishikawa, H. O., Takeuchi, H., Haltiwanger, R. S. and Irvine, K. D. (2008). Four-jointed is a Golgi kinase that phosphorylates a subset of cadherin domains. In *Science*, vol. 321 (ed., pp. 401-4.

Jia, J., Zhang, W., Wang, B., Trinko, R. and Jiang, J. (2003). The Drosophila Ste20 family kinase dMST functions as a tumor suppressor by restricting cell proliferation and promoting apoptosis. In *Genes Dev*, vol. 17 (ed., pp. 2514-9.

Justice, R. W., Zilian, O., Woods, D. F., Noll, M. and Bryant, P. J. (1995). The Drosophila tumor suppressor gene warts encodes a homolog of human myotonic

dystrophy kinase and is required for the control of cell shape and proliferation. In *Genes Dev*, vol. 9 (ed., pp. 534-46.

Kango-Singh, M., Nolo, R., Tao, C., Verstreken, P., Hiesinger, P. R., Bellen, H. J. and Halder, G. (2002). Shar-pei mediates cell proliferation arrest during imaginal disc growth in Drosophila. In *Development*, vol. 129 (ed., pp. 5719-30.

Kim, N.-G., Koh, E., Chen, X. and Gumbiner, B. M. (2011). E-cadherin mediates contact inhibition of proliferation through Hippo signaling-pathway components. In *Proceedings of the National Academy of Sciences of the United States of America*, vol. 108 (ed., pp. 11930-5.

Klein, T. (2001). Wing disc development in the fly: the early stages. In *Current Opinion in Genetics & Development*, vol. 11 (ed., pp. 470-5.

Lai, Z.-C., Wei, X., Shimizu, T., Ramos, E., Rohrbaugh, M., Nikolaidis, N., Ho, L.-L. and Li, Y. (2005). Control of cell proliferation and apoptosis by mob as tumor suppressor, mats. In *Cell*, vol. 120 (ed., pp. 675-85.

Larkin, M. A., Blackshields, G., Brown, N. P., Chenna, R., McGettigan, P. A., McWilliam, H., Valentin, F., Wallace, I. M., Wilm, A., Lopez, R. et al. (2007). Clustal W and Clustal X version 2.0. In *Bioinformatics*, vol. 23 (ed., pp. 2947-8.

Lawrence, P. A. (2001). Morphogens: how big is the big picture? In *Nat Cell Biol*, vol. 3 (ed., pp. E151-4.

Lawrence, P. A., Struhl, G. and Casal, J. (2008). Do the protocadherins Fat and Dachsous link up to determine both planar cell polarity and the dimensions of organs? In *Nat Cell Biol*, vol. 10 (ed., pp. 1379-82.

Lee, T. and Luo, L. (1999). Mosaic analysis with a repressible cell marker for studies of gene function in neuronal morphogenesis. In *Neuron*, vol. 22 (ed., pp. 451-61.

Ling, C., Zheng, Y., Yin, F., Yu, J., Huang, J., Hong, Y., Wu, S. and Pan, D. (2010). The apical transmembrane protein Crumbs functions as a tumor suppressor that regulates Hippo signaling by binding to Expanded. In *Proceedings of the National Academy of Sciences of the United States of America*, vol. 107 (ed., pp. 10532-7.

Liu, C.-Y., Zha, Z.-Y., Zhou, X., Zhang, H., Huang, W., Zhao, D., Li, T., Chan, S. W., Lim, C. J., Hong, W. et al. (2010). The Hippo tumor pathway promotes TAZ degradation by phosphorylating a phosphodegron and recruiting the SCFbeta-TrCP E3 ligase. In *J Biol Chem*, (ed.

Mahoney, P. A., Weber, U., Onofrechuk, P., Biessmann, H., Bryant, P. J. and Goodman, C. S. (1991). The fat tumor suppressor gene in Drosophila encodes a novel member of the cadherin gene superfamily. In *Cell*, vol. 67 (ed., pp. 853-68.

Mao, Y., Kucuk, B. and Irvine, K. D. (2009). Drosophila lowfat, a novel modulator of Fat signaling. In *Development*, vol. 136 (ed., pp. 3223-33.

Mao, Y., Mulvaney, J., Zakaria, S., Yu, T., Morgan, K. M., Allen, S., Basson, M. A., Francis-West, P. and Irvine, K. D. (2011a). Characterization of a Dchs1 mutant mouse reveals requirements for Dchs1-Fat4 signaling during mammalian development. In *Development*, vol. 138 (ed., pp. 947-57.

Mao, Y., Rauskolb, C., Cho, E., Hu, W.-L., Hayter, H., Minihan, G., Katz, F. N. and Irvine, K. D. (2006). Dachs: an unconventional myosin that functions downstream of Fat to regulate growth, affinity and gene expression in Drosophila. In *Development*, vol. 133 (ed., pp. 2539-51.

Mao, Y., Tournier, A. L., Bates, P. A., Gale, J. E., Tapon, N. and Thompson, B. J. (2011b). Planar polarization of the atypical myosin Dachs orients cell divisions in Drosophila. In *Genes Dev*, vol. 25 (ed., pp. 131-6.

Martín-Blanco, E., Roch, F., Noll, E., Baonza, A., Duffy, J. B. and Perrimon, N. (1999). A temporal switch in DER signaling controls the specification and

differentiation of veins and interveins in the Drosophila wing. In *Development*, vol. 126 (ed., pp. 5739-47.
Matakatsu, H. and Blair, S. S. (2008). The DHHC palmitoyltransferase approximated regulates Fat signaling and Dachs localization and activity. In *Current biology : CB*, vol. 18 (ed., pp. 1390-5.
McCartney, B. M., Kulikauskas, R. M., LaJeunesse, D. R. and Fehon, R. G. (2000). The neurofibromatosis-2 homologue, Merlin, and the tumor suppressor expanded function together in Drosophila to regulate cell proliferation and differentiation. In *Development*, vol. 127 (ed., pp. 1315-24.
METCALF, D. (1963). THE AUTONOMOUS BEHAVIOUR OF NORMAL THYMUS GRAFTS. In *Aust J Exp Biol Med Sci*, vol. 41 (ed., pp. SUPPL437-47.
Michaely, P. and Bennett, V. (1992). The ANK repeat: a ubiquitous motif involved in macromolecular recognition. In *Trends Cell Biol*, vol. 2 (ed., pp. 127-9.
Michalopoulos, G. K. and DeFrances, M. C. (1997). Liver regeneration. In *Science*, vol. 276 (ed., pp. 60-6.
Michelotti, E. F., Michelotti, G. A., Aronsohn, A. I. and Levens, D. (1996). Heterogeneous nuclear ribonucleoprotein K is a transcription factor. In *Molecular and Cellular Biology*, vol. 16 (ed., pp. 2350-60.
Miles, M. C., Janket, M. L., Wheeler, E. D. A., Chattopadhyay, A., Majumder, B., Dericco, J., Schafer, E. A. and Ayyavoo, V. (2005). Molecular and functional characterization of a novel splice variant of ANKHD1 that lacks the KH domain and its role in cell survival and apoptosis. In *FEBS J*, vol. 272 (ed., pp. 4091-102.
Mohr, S., Bakal, C. and Perrimon, N. (2010). Genomic screening with RNAi: results and challenges. In *Annu Rev Biochem*, vol. 79 (ed., pp. 37-64.
Morin-Kensicki, E. M., Boone, B. N., Howell, M., Stonebraker, J. R., Teed, J., Alb, J. G., Magnuson, T. R., O'Neal, W. and Milgram, S. L. (2006). Defects in yolk sac vasculogenesis, chorioallantoic fusion, and embryonic axis elongation in mice with targeted disruption of Yap65. In *Molecular and Cellular Biology*, vol. 26 (ed., pp. 77-87.
Moumen, A., Masterson, P., O'Connor, M. J. and Jackson, S. P. (2005). hnRNP K: an HDM2 target and transcriptional coactivator of p53 in response to DNA damage. In *Cell*, vol. 123 (ed., pp. 1065-78.
Mummery-Widmer, J. L., Yamazaki, M., Stoeger, T., Novatchkova, M., Bhalerao, S., Chen, D., Dietzl, G., Dickson, B. J. and Knoblich, J. A. (2009). Genome-wide analysis of Notch signalling in Drosophila by transgenic RNAi. In *Nature*, vol. 458 (ed., pp. 987-92.
Nairz, K., Rottig, C., Rintelen, F., Zdobnov, E., Moser, M. and Hafen, E. (2006). Overgrowth caused by misexpression of a microRNA with dispensable wild-type function. In *Developmental Biology*, vol. 291 (ed., pp. 314-24.
Neel, B. G., Gu, H. and Pao, L. (2003). The 'Shp'ing news: SH2 domain-containing tyrosine phosphatases in cell signaling. In *Trends Biochem Sci*, vol. 28 (ed., pp. 284-93.
Neely, G. G., Hess, A., Costigan, M., Keene, A. C., Goulas, S., Langeslag, M., Griffin, R. S., Belfer, I., Dai, F., Smith, S. B. et al. (2010a). A genome-wide Drosophila screen for heat nociception identifies $\alpha 2\delta 3$ as an evolutionarily conserved pain gene. In *Cell*, vol. 143 (ed., pp. 628-38.
Neely, G. G., Kuba, K., Cammarato, A., Isobe, K., Amann, S., Zhang, L., Murata, M., Elmén, L., Gupta, V., Arora, S. et al. (2010b). A global in vivo Drosophila RNAi screen identifies NOT3 as a conserved regulator of heart function. In *Cell*, vol. 141 (ed., pp. 142-53.

Neto-Silva, R. M., de Beco, S. and Johnston, L. A. (2010). Evidence for a Growth-Stabilizing Regulatory Feedback Mechanism between Myc and Yorkie, the Drosophila Homolog of Yap. In *Dev Cell*, vol. 19 (ed., pp. 507-20.

Neufeld, T. P., de la Cruz, A. F., Johnston, L. A. and Edgar, B. A. (1998). Coordination of growth and cell division in the Drosophila wing. In *Cell*, vol. 93 (ed., pp. 1183-93.

Ng, M., Diaz-Benjumea, F. J., Vincent, J. P., Wu, J. and Cohen, S. M. (1996). Specification of the wing by localized expression of wingless protein. In *Nature*, vol. 381 (ed., pp. 316-8.

Nicolay, B. N., Bayarmagnai, B., Islam, A. B. M. M. K., Lopez-Bigas, N. and Frolov, M. V. (2011). Cooperation between dE2F1 and Yki/Sd defines a distinct transcriptional program necessary to bypass cell cycle exit. In *Genes Dev*, vol. 25 (ed., pp. 323-35.

Nolo, R., Morrison, C. M., Tao, C., Zhang, X. and Halder, G. (2006). The bantam microRNA is a target of the hippo tumor-suppressor pathway. In *Current biology : CB*, vol. 16 (ed., pp. 1895-904.

Oh, H. and Irvine, K. D. (2009). In vivo analysis of Yorkie phosphorylation sites. In *Oncogene*, vol. 28 (ed., pp. 1916-27.

Oh, H. and Irvine, K. D. (2011). Cooperative regulation of growth by Yorkie and Mad through bantam. In *Dev Cell*, vol. 20 (ed., pp. 109-22.

Oh, H., Reddy, B. V. V. G. and Irvine, K. D. (2009). Phosphorylation-independent repression of Yorkie in Fat-Hippo signaling. In *Developmental Biology*, vol. 335 (ed., pp. 188-97.

Ota, M. and Sasaki, H. (2008). Mammalian Tead proteins regulate cell proliferation and contact inhibition as transcriptional mediators of Hippo signaling. In *Development*, vol. 135 (ed., pp. 4059-69.

Pan, D. (2010). The hippo signaling pathway in development and cancer. In *Dev Cell*, vol. 19 (ed., pp. 491-505.

Pantalacci, S., Tapon, N. and Léopold, P. (2003). The Salvador partner Hippo promotes apoptosis and cell-cycle exit in Drosophila. In *Nat Cell Biol*, vol. 5 (ed., pp. 921-7.

Parker, J. (2011). Morphogens, nutrients, and the basis of organ scaling. In *Evol Dev*, vol. 13 (ed., pp. 304-14.

Pellock, B. J., Buff, E., White, K. and Hariharan, I. K. (2007). The Drosophila tumor suppressors Expanded and Merlin differentially regulate cell cycle exit, apoptosis, and Wingless signaling. In *Developmental Biology*, vol. 304 (ed., pp. 102-15.

Peng, H. W., Slattery, M. and Mann, R. S. (2009). Transcription factor choice in the Hippo signaling pathway: homothorax and yorkie regulation of the microRNA bantam in the progenitor domain of the Drosophila eye imaginal disc. In *Genes Dev*, vol. 23 (ed., pp. 2307-19.

Perkins, L. A., Johnson, M. R., Melnick, M. B. and Perrimon, N. (1996). The nonreceptor protein tyrosine phosphatase corkscrew functions in multiple receptor tyrosine kinase pathways in Drosophila. In *Developmental Biology*, vol. 180 (ed., pp. 63-81.

Perkins, L. A., Larsen, I. and Perrimon, N. (1992). corkscrew encodes a putative protein tyrosine phosphatase that functions to transduce the terminal signal from the receptor tyrosine kinase torso. In *Cell*, vol. 70 (ed., pp. 225-36.

Polesello, C., Huelsmann, S., Brown, N. H. and Tapon, N. (2006). The Drosophila RASSF homolog antagonizes the hippo pathway. In *Current biology : CB*, vol. 16 (ed., pp. 2459-65.

Rauskolb, C., Pan, G., Reddy, B. V. V. G., Oh, H. and Irvine, K. D. (2011). Zyxin links fat signaling to the hippo pathway. In *PLoS biology*, vol. 9 (ed., pp. e1000624.

Ren, F., Wang, B., Yue, T., Yun, E.-Y., Ip, Y. T. and Jiang, J. (2010). Hippo signaling regulates Drosophila intestine stem cell proliferation through multiple pathways. In *Proceedings of the National Academy of Sciences of the United States of America*, vol. 107 (ed., pp. 21064-9.

Ribeiro, P. S., Josué, F., Wepf, A., Wehr, M. C., Rinner, O., Kelly, G., Tapon, N. and Gstaiger, M. (2010). Combined functional genomic and proteomic approaches identify a PP2A complex as a negative regulator of Hippo signaling. In *Molecular Cell*, vol. 39 (ed., pp. 521-34.

Richardson, E. C. N. and Pichaud, F. (2010). Crumbs is required to achieve proper organ size control during Drosophila head development. In *Development*, vol. 137 (ed., pp. 641-50.

Robinson, B. S., Huang, J., Hong, Y. and Moberg, K. H. (2010). Crumbs Regulates Salvador/Warts/Hippo Signaling in Drosophila via the FERM-Domain Protein Expanded. In *Current biology : CB*, (ed.

Rogulja, D., Rauskolb, C. and Irvine, K. D. (2008). Morphogen control of wing growth through the Fat signaling pathway. In *Dev Cell*, vol. 15 (ed., pp. 309-21.

Saburi, S., Hester, I., Fischer, E., Pontoglio, M., Eremina, V., Gessler, M., Quaggin, S. E., Harrison, R., Mount, R. and McNeill, H. (2008). Loss of Fat4 disrupts PCP signaling and oriented cell division and leads to cystic kidney disease. In *Nat Genet*, vol. 40 (ed., pp. 1010-5.

Sansores-Garcia, L., Bossuyt, W., Wada, K.-I., Yonemura, S., Tao, C., Sasaki, H. and Halder, G. (2011). Modulating F-actin organization induces organ growth by affecting the Hippo pathway. In *EMBO J*, vol. 30 (ed., pp. 2325-35.

Santos Duarte, A. d. S., Traina, F., Favaro, P. M. B., Bassères, D. S., de Carvalho, I. C., Medina, S. d. S., Costa, F. F. and Saad, S. T. O. (2005). Characterisation of a new splice variant of MASK-BP3(ARF) and MASK human genes, and their expression patterns during haematopoietic cell differentiation. In *Gene*, vol. 363 (ed., pp. 113-22.

Schlegelmilch, K., Mohseni, M., Kirak, O., Pruszak, J., Rodriguez, J. R., Zhou, D., Kreger, B. T., Vasioukhin, V., Avruch, J., Brummelkamp, T. R. et al. (2011). Yap1 acts downstream of α-catenin to control epidermal proliferation. In *Cell*, vol. 144 (ed., pp. 782-95.

Schnorrer, F., Schönbauer, C., Langer, C. C. H., Dietzl, G., Novatchkova, M., Schernhuber, K., Fellner, M., Azaryan, A., Radolf, M., Stark, A. et al. (2010). Systematic genetic analysis of muscle morphogenesis and function in Drosophila. In *Nature*, vol. 464 (ed., pp. 287-91.

Schwank, G. and Basler, K. (2010). Regulation of organ growth by morphogen gradients. In *Cold Spring Harbor Perspectives in Biology*, vol. 2 (ed., pp. a001669.

Shaw, R. L., Kohlmaier, A., Polesello, C., Veelken, C., Edgar, B. A. and Tapon, N. (2010). The Hippo pathway regulates intestinal stem cell proliferation during Drosophila adult midgut regeneration. In *Development*, vol. 137 (ed., pp. 4147-58.

Silber, S. J. (1976). Growth of baby kidneys transplanted into adults. In *Arch Surg*, vol. 111 (ed., pp. 75-7.

Silva, E., Tsatskis, Y., Gardano, L., Tapon, N. and McNeill, H. (2006). The tumor-suppressor gene fat controls tissue growth upstream of expanded in the hippo signaling pathway. In *Current biology : CB*, vol. 16 (ed., pp. 2081-9.

Silvis, M. R., Kreger, B. T., Lien, W.-H., Klezovitch, O., Rudakova, G. M., Camargo, F. D., Lantz, D. M., Seykora, J. T. and Vasioukhin, V. (2011). α-catenin is a tumor suppressor that controls cell accumulation by regulating the localization and activity of the transcriptional coactivator Yap1. In *Sci Signal*, vol. 4 (ed., pp. ra33.

Simcox, A. A., Grumbling, G., Schnepp, B., Bennington-Mathias, C., Hersperger, E. and Shearn, A. (1996). Molecular, phenotypic, and expression analysis of vein, a gene required for growth of the Drosophila wing disc. In *Developmental Biology*, vol. 177 (ed., pp. 475-89.

Simon, M. A., Xu, A., Ishikawa, H. O. and Irvine, K. D. (2010). Modulation of Fat:Dachsous Binding by the Cadherin Domain Kinase Four-Jointed. In *Current biology : CB*, (ed.

Smith, R. K., Carroll, P. M., Allard, J. D. and Simon, M. A. (2002). MASK, a large ankyrin repeat and KH domain-containing protein involved in Drosophila receptor tyrosine kinase signaling. In *Development*, vol. 129 (ed., pp. 71-82.

Song, H., Mak, K. K., Topol, L., Yun, K., Hu, J., Garrett, L., Chen, Y., Park, O., Chang, J., Simpson, R. M. et al. (2010). Mammalian Mst1 and Mst2 kinases play essential roles in organ size control and tumor suppression. In *Proceedings of the National Academy of Sciences of the United States of America*, vol. 107 (ed., pp. 1431-1436.

Sopko, R., Silva, E., Clayton, L., Gardano, L., Barrios-Rodiles, M., Wrana, J., Varelas, X., Arbouzova, N. I., Shaw, S., Saburi, S. et al. (2009). Phosphorylation of the tumor suppressor fat is regulated by its ligand Dachsous and the kinase discs overgrown. In *Current biology : CB*, vol. 19 (ed., pp. 1112-7.

St Johnston, D. (2002). The art and design of genetic screens: Drosophila melanogaster. In *Nature reviews Genetics*, vol. 3 (ed., pp. 176-88.

Staley, B. K. and Irvine, K. D. (2010). Warts and Yorkie mediate intestinal regeneration by influencing stem cell proliferation. In *Current biology : CB*, vol. 20 (ed., pp. 1580-7.

Steinhardt, A. A., Gayyed, M. F., Klein, A. P., Dong, J., Maitra, A., Pan, D., Montgomery, E. A. and Anders, R. A. (2008). Expression of Yes-associated protein in common solid tumors. In *Hum Pathol*, vol. 39 (ed., pp. 1582-9.

Sturtevant, M. A. and Bier, E. (1995). Analysis of the genetic hierarchy guiding wing vein development in Drosophila. In *Development*, vol. 121 (ed., pp. 785-801.

Sun, G. and Irvine, K. D. (2011). Regulation of Hippo signaling by Jun kinase signaling during compensatory cell proliferation and regeneration, and in neoplastic tumors. In *Developmental Biology*, vol. 350 (ed., pp. 139-51.

Takimoto, M., Tomonaga, T., Matunis, M., Avigan, M., Krutzsch, H., Dreyfuss, G. and Levens, D. (1993). Specific binding of heterogeneous ribonucleoprotein particle protein K to the human c-myc promoter, in vitro. In *J Biol Chem*, vol. 268 (ed., pp. 18249-58.

Tapon, N., Harvey, K. F., Bell, D. W., Wahrer, D. C. R., Schiripo, T. A., Haber, D. A. and Hariharan, I. K. (2002). salvador Promotes both cell cycle exit and apoptosis in Drosophila and is mutated in human cancer cell lines. In *Cell*, vol. 110 (ed., pp. 467-78.

Thompson, B. J. and Cohen, S. M. (2006). The Hippo pathway regulates the bantam microRNA to control cell proliferation and apoptosis in Drosophila. In *Cell*, vol. 126 (ed., pp. 767-74.

Tomonaga, T. and Levens, D. (1996). Activating transcription from single stranded DNA. In *Proceedings of the National Academy of Sciences of the United States of America*, vol. 93 (ed., pp. 5830-5.

Traina, F., Favaro, P. M. B., Medina, S. d. S., Duarte, A. d. S. S., Winnischofer, S. M. B., Costa, F. F. and Saad, S. T. O. (2006). ANKHD1, ankyrin repeat and KH domain containing 1, is overexpressed in acute leukemias and is associated with SHP2 in K562 cells. In *Biochim Biophys Acta*, vol. 1762 (ed., pp. 828-34.

Tweedie, S., Ashburner, M., Falls, K., Leyland, P., McQuilton, P., Marygold, S., Millburn, G., Osumi-Sutherland, D., Schroeder, A., Seal, R. et al. (2009). FlyBase: enhancing Drosophila Gene Ontology annotations. In *Nucleic Acids Res*, vol. 37 (ed., pp. D555-9.

Udan, R. S., Kango-Singh, M., Nolo, R., Tao, C. and Halder, G. (2003). Hippo promotes proliferation arrest and apoptosis in the Salvador/Warts pathway. In *Nat Cell Biol*, vol. 5 (ed., pp. 914-20.

Uribe, D. J., Guo, K., Shin, Y.-J. and Sun, D. (2011). Heterogeneous nuclear ribonucleoprotein K and nucleolin as transcriptional activators of the vascular endothelial growth factor promoter through interaction with secondary DNA structures. In *Biochemistry*, vol. 50 (ed., pp. 3796-806.

Valverde, R., Edwards, L. and Regan, L. (2008). Structure and function of KH domains. In *FEBS J*, vol. 275 (ed., pp. 2712-26.

Varelas, X., Sakuma, R., Samavarchi-Tehrani, P., Peerani, R., Rao, B. M., Dembowy, J., Yaffe, M. B., Zandstra, P. W. and Wrana, J. L. (2008). TAZ controls Smad nucleocytoplasmic shuttling and regulates human embryonic stem-cell self-renewal. In *Nat Cell Biol*, vol. 10 (ed., pp. 837-48.

Varelas, X., Samavarchi-Tehrani, P., Narimatsu, M., Weiss, A., Cockburn, K., Larsen, B. G., Rossant, J. and Wrana, J. L. (2010). The Crumbs complex couples cell density sensing to Hippo-dependent control of the TGF-β-SMAD pathway. In *Dev Cell*, vol. 19 (ed., pp. 831-44.

Villano, J. L. and Katz, F. N. (1995). four-jointed is required for intermediate growth in the proximal-distal axis in Drosophila. In *Development*, vol. 121 (ed., pp. 2767-77.

Vincent, J. P. (1998). Compartment boundaries: where, why and how? In *Int J Dev Biol*, vol. 42 (ed., pp. 311-5.

Wada, K.-I., Itoga, K., Okano, T., Yonemura, S. and Sasaki, H. (2011). Hippo pathway regulation by cell morphology and stress fibers. In *Development*, vol. 138 (ed., pp. 3907-14.

Wan, F., Anderson, D. E., Barnitz, R. A., Snow, A., Bidere, N., Zheng, L., Hegde, V., Lam, L. T., Staudt, L. M., Levens, D. et al. (2007). Ribosomal protein S3: a KH domain subunit in NF-kappaB complexes that mediates selective gene regulation. In *Cell*, vol. 131 (ed., pp. 927-39.

Wang, S. H., Simcox, A. and Campbell, G. (2000). Dual role for Drosophila epidermal growth factor receptor signaling in early wing disc development. In *Genes Dev*, vol. 14 (ed., pp. 2271-6.

Watson, K. L., Justice, R. W. and Bryant, P. J. (1994). Drosophila in cancer research: the first fifty tumor suppressor genes. In *J Cell Sci Suppl*, vol. 18 (ed., pp. 19-33.

Watt, A. J., Jones, E. A., Ure, J. M., Peddie, D., Wilson, D. I. and Forrester, L. M. (2001). A gene trap integration provides an early in situ marker for hepatic specification of the foregut endoderm. In *Mech Dev*, vol. 100 (ed., pp. 205-15.

Weigmann, K., Cohen, S. M. and Lehner, C. F. (1997). Cell cycle progression, growth and patterning in imaginal discs despite inhibition of cell division after inactivation of Drosophila Cdc2 kinase. In *Development*, vol. 124 (ed., pp. 3555-63.
Willecke, M., Hamaratoglu, F., Kango-Singh, M., Udan, R., Chen, C.-L., Tao, C., Zhang, X. and Halder, G. (2006). The fat cadherin acts through the hippo tumor-suppressor pathway to regulate tissue size. In *Current biology : CB*, vol. 16 (ed., pp. 2090-100.
Willecke, M., Hamaratoglu, F., Sansores-Garcia, L., Tao, C. and Halder, G. (2008). Boundaries of Dachsous Cadherin activity modulate the Hippo signaling pathway to induce cell proliferation. In *Proceedings of the National Academy of Sciences of the United States of America*, vol. 105 (ed., pp. 14897-902.
Wu, S., Huang, J., Dong, J. and Pan, D. (2003). hippo encodes a Ste-20 family protein kinase that restricts cell proliferation and promotes apoptosis in conjunction with salvador and warts. In *Cell*, vol. 114 (ed., pp. 445-56.
Wu, S., Liu, Y., Zheng, Y., Dong, J. and Pan, D. (2008). The TEAD/TEF family protein Scalloped mediates transcriptional output of the Hippo growth-regulatory pathway. In *Dev Cell*, vol. 14 (ed., pp. 388-98.
Xiao, L., Chen, Y., Ji, M. and Dong, J. (2011). KIBRA regulates Hippo signaling activity via interactions with large tumor suppressor kinases. In *J Biol Chem*, vol. 286 (ed., pp. 7788-96.
Xu, T., Wang, W., Zhang, S., Stewart, R. A. and Yu, W. (1995). Identifying tumor suppressors in genetic mosaics: the Drosophila lats gene encodes a putative protein kinase. In *Development*, vol. 121 (ed., pp. 1053-63.
Yu, J., Zheng, Y., Dong, J., Klusza, S., Deng, W.-M. and Pan, D. (2010). Kibra functions as a tumor suppressor protein that regulates Hippo signaling in conjunction with Merlin and Expanded. In *Dev Cell*, vol. 18 (ed., pp. 288-99.
Zecca, M. and Struhl, G. (2007a). Control of Drosophila wing growth by the vestigial quadrant enhancer. In *Development*, vol. 134 (ed., pp. 3011-20.
Zecca, M. and Struhl, G. (2007b). Recruitment of cells into the Drosophila wing primordium by a feed-forward circuit of vestigial autoregulation. In *Development*, vol. 134 (ed., pp. 3001-10.
Zecca, M. and Struhl, G. (2010). A Feed-Forward Circuit Linking Wingless, Fat-Dachsous Signaling, and the Warts-Hippo Pathway to Drosophila Wing Growth. In *PLoS biology*, vol. 8 (ed., pp. e1000386.
Zeng, Q. and Hong, W. (2008). The emerging role of the hippo pathway in cell contact inhibition, organ size control, and cancer development in mammals. In *Cancer Cell*, vol. 13 (ed., pp. 188-92.
Zhang, H., Liu, C.-Y., Zha, Z.-Y., Zhao, B., Yao, J., Zhao, S., Xiong, Y., Lei, Q.-Y. and Guan, K.-L. (2009a). TEAD transcription factors mediate the function of TAZ in cell growth and epithelial-mesenchymal transition. In *J Biol Chem*, vol. 284 (ed., pp. 13355-62.
Zhang, H., Pasolli, H. A. and Fuchs, E. (2011a). Yes-associated protein (YAP) transcriptional coactivator functions in balancing growth and differentiation in skin. In *Proceedings of the National Academy of Sciences of the United States of America*, vol. 108 (ed., pp. 2270-5.
Zhang, J., Ji, J.-Y., Yu, M., Overholtzer, M., Smolen, G. A., Wang, R., Brugge, J. S., Dyson, N. J. and Haber, D. A. (2009b). YAP-dependent induction of amphiregulin identifies a non-cell-autonomous component of the Hippo pathway. In *Nat Cell Biol*, vol. 11 (ed., pp. 1444-50.

Zhang, L., Ren, F., Zhang, Q., Chen, Y., Wang, B. and Jiang, J. (2008). The TEAD/TEF family of transcription factor Scalloped mediates Hippo signaling in organ size control. In *Dev Cell*, vol. 14 (ed., pp. 377-87.

Zhang, N., Bai, H., David, K. K., Dong, J., Zheng, Y., Cai, J., Giovannini, M., Liu, P., Anders, R. A. and Pan, D. (2010). The Merlin/NF2 tumor suppressor functions through the YAP oncoprotein to regulate tissue homeostasis in mammals. In *Dev Cell*, vol. 19 (ed., pp. 27-38.

Zhang, X., Milton, C. C., Poon, C. L. C., Hong, W. and Harvey, K. F. (2011b). Wbp2 cooperates with Yorkie to drive tissue growth downstream of the Salvador-Warts-Hippo pathway. In *Cell death and differentiation*, (ed.

Zhao, B., Li, L., Lei, Q. and Guan, K.-L. (2010a). The Hippo-YAP pathway in organ size control and tumorigenesis: an updated version. In *Genes Dev*, vol. 24 (ed., pp. 862-74.

Zhao, B., Li, L., Lu, Q., Wang, L. H., Liu, C.-Y., Lei, Q. and Guan, K.-L. (2011). Angiomotin is a novel Hippo pathway component that inhibits YAP oncoprotein. In *Genes Dev*, vol. 25 (ed., pp. 51-63.

Zhao, B., Li, L., Tumaneng, K., Wang, C.-Y. and Guan, K.-L. (2010b). A coordinated phosphorylation by Lats and CK1 regulates YAP stability through SCF(beta-TRCP). In *Genes Dev*, vol. 24 (ed., pp. 72-85.

Zhao, B., Wei, X., Li, W., Udan, R. S., Yang, Q., Kim, J., Xie, J., Ikenoue, T., Yu, J., Li, L. et al. (2007). Inactivation of YAP oncoprotein by the Hippo pathway is involved in cell contact inhibition and tissue growth control. In *Genes Dev*, vol. 21 (ed., pp. 2747-61.

Zhao, B., Ye, X., Yu, J., Li, L., Li, W., Li, S., Yu, J., Lin, J. D., Wang, C.-Y., Chinnaiyan, A. M. et al. (2008). TEAD mediates YAP-dependent gene induction and growth control. In *Genes Dev*, vol. 22 (ed., pp. 1962-71.